



universität  
wien

# DIPLOMARBEIT

Titel der Diplomarbeit

RNA transfer of Human Rhinovirus through model membranes

angestrebter akademischer Grad

Magistra der Naturwissenschaften (Mag. rer.nat.)

Verfasserin / Verfasser: Nena M. Matscheko

Studienrichtung /Studienzweig Molekulare Biologie  
(lt. Studienblatt):

Betreuerin / Betreuer: Ao. Univ.-Prof. Dipl.-Ing. Dr. Dieter Blaas

Wien, im September 2010



## Table of contents

1.1	Abstract .....	- 3 -
1.2	Zusammenfassung (german abstract) .....	- 4 -
2	Introduction .....	- 5 -
2.1	Picornaviridae.....	- 5 -
2.1.1	Classification .....	- 5 -
2.1.2	Morphology .....	- 8 -
2.1.3	Replication pathway.....	- 9 -
2.2	Human Rhinovirus .....	- 12 -
2.2.1	Pathogenesis.....	- 12 -
2.2.2	Taxonomy .....	- 12 -
2.2.3	Virion structure and properties .....	- 13 -
2.2.4	Viral infection.....	- 15 -
2.2.5	Major Group Receptor: Human ICAM-1.....	- 16 -
2.2.6	Minor Group Receptor: LDLR family .....	- 18 -
2.3	Nanocontainers.....	- 19 -
2.3.1	Endosomal Membranes .....	- 20 -
2.3.2	Liposomal membrane .....	- 21 -
2.3.3	Proof of RNA transfer .....	- 22 -
2.4	Aim of the project .....	- 22 -
3	Materials and methods .....	- 23 -
3.1	Liposome Preparation .....	- 24 -
3.2	Cloning of soluble ICAM-1 receptor.....	- 32 -
3.3	V33333 receptor production .....	- 37 -
4	Results .....	- 40 -
4.1	Minor group receptor expression.....	- 40 -
4.2	Major group receptor cloning .....	- 42 -
4.3	RNA transfer through liposomal membranes .....	- 50 -

**Table of contents**

---

5	Discussion .....	- 70 -
5.1	Elimination of reactions potentially disturbing the nanocontainer system. ....	- 70 -
5.2	Generalizing the nanocontainer system for all HRV serotypes. ....	- 71 -
5.3	Determining the ideal sample composition. ....	- 72 -
5.4	Ratio total particles to infectious particles. ....	- 74 -
5.5	The influence of drugs and calcium on RNA transfer, determined by the nanocontainer system. ....	- 75 -
6	Conclusion.....	- 77 -
7	References .....	- 78 -
8	Appendices .....	- 81 -
8.1	Abbreviations.....	- 81 -
8.2	Primer index .....	- 82 -
8.3	Nucleotide sequences .....	- 83 -
8.3.1	Human Rhinovirus 2 with primer positions indicated.....	- 83 -
8.3.2	Sequence of pCDM8-ICAM1-D2 .....	- 84 -
8.3.3	Sequence of pCDM8-ICAM1-D5 .....	- 85 -
8.4	Acknowledgments .....	- 87 -
8.5	Curriculum Vitae .....	- 89 -

## 1.1 Abstract

As main cause of the common cold, Human Rhinoviruses are responsible for the expense of around \$40 billion each year alone in the US for lost working days and medical treatment. Prevention of the infection is difficult due to the more than 100 serotypes. Most employ either the major group receptor ICAM-1 or the minor group receptor from the LDLR family for attachment to the host cell. Upon binding to the receptor, the cell engulfs a vesicle containing the virus particle. These early endosomes mature to late endosome concomitant to decreasing the pH. At pH below 5.6 the capsid of HRV undergoes structural changes which trigger the (+)ss-RNA release and transfer across the endosomal membrane into the cytoplasm of the host cell. First, the viral protein (VP) 4, one of the four structural proteins of the icosahedral capsid, is lost and the N-terminus of VP1 is externalized to form the hydrophobic 135S subviral particle. Ejection of the RNA results in 80S subviral particle. The exact mechanism of the RNA release and transfer across the membrane is not known. For minor group viruses the implication of VP4 and the N-terminus of VP1 in pore formation is discussed, data for major group viruses rather point at disruption of the membrane. So far, neither was demonstrated visually. High resolution microscopic imaging of viral particles and their attachment site during the process of RNA transfer is difficult with cells, therefore liposomes were developed as model for endosomes.

To detect RNA transfer across the membrane, a reverse transcription kit was encapsulated for immediate transcription (RT) of RNA into cDNA which could subsequently be amplified by PCR. We termed these functional liposomes “nanocontainers” and decorated them with receptor and virus prior to triggering the RNA transfer via a pH of 5.4. For tight attachment of HRV2, a minor group virus, a recombinant VLDLR was bound via a His<sub>6</sub>-tag to the lipid Ni-DGS-NTA. The study of major group viruses requires a recombinant ICAM-1 receptor which was cloned for expression in eukaryotic cells in the course of the present diploma thesis. Disruption of the nanocontainer membrane either due to added detergent as a control or high virus concentration caused leakage and subsequently a decreased RNA transcription efficiency. This finding also points at RNA transfer through a pore in the membrane. The virus/lipid ratio yielding the highest cDNA transcription efficiency was determined at  $3.4 \times 10^{-6}$ . At this composition, the potentiating effect of calcium and the inhibiting effect of the antiviral drug amiloride on the RNA transfer efficiency could be elucidated.

The nanocontainer system is a fast and easily to manipulate model of viral infection and might be applicable to all minor and major group HRVs once the ICAM-1 receptor is expressed.

## **1.2 Zusammenfassung (german abstract)**

Obwohl das Humane Rhinovirus hauptsächlich gewöhnliche Erkältungen auslöst, verursacht es durch seine hohe Prävalenz alleine in den USA Kosten von \$40 Milliarden pro Jahr für Arbeitsentgang und medizinische Behandlung. Immunität ist kaum möglich, da mehr als 100 Serotypen zirkulieren, die man nach ihrem Bindungsprotein in major group und minor group HRV einteilt, die ICAM-1 bzw. ein Mitglied der LDLR superfamily als Rezeptor zur Bindung an die Wirtszelle benutzen. Bindet der Virus an seinen Rezeptor, wird der Komplex in einem Membranvesikel internalisiert, das während der Reifung zu einem späten Endosom den pH Werts unter 5.6 erniedrigt. Diese Azidifizierung löst im ikosaedrischen Capsid des HRV den Verlust des strukturellen viralen Proteins (VP) 4 und die Externalisierung des N-terminus von VP1 aus, was zu einem hydrophoben 135S subviralen Partikel führt. Diese Capsidbestandteile formen möglicherweise eine Pore in der Membran, durch die die (+)ss-RNA in das Cytoplasma der Wirtszelle geschleust werden kann; zurück bleibt das leere, nicht infektiöse 80S subvirale Partikel. Im Fall der major group HRVs wird auch ein Zerreißen der Membran diskutiert. Der genaue Hergang des RNA Transfers konnte in der Zelle bisher nicht visuell dargestellt werden. Deshalb wurden Liposomen als ein Modell der späten Endosomen hergestellt und mit einer Reaktionsmischung für reverse Transkription (RT) gefüllt um die Detektion der transferierten RNA zu ermöglichen.

Die dadurch entstehenden „Nanocontainer“ wurden mit einem rekombinanten VLDLR, der über ein His<sub>6</sub>-Tag an das Lipid Ni-DGS-NTA binden kann, dekoriert, die so eine feste Bindung zwischen Virus und Nanocontainer herstellen konnten. Durch einen pH-Wert von 5.4 wurde der Transfer der viralen RNA von HRV2, einem minor group Virus, in das Lumen der Nanocontainer ausgelöst und konnte vor Ort in cDNA umgekehrt transkribiert werden, die durch eine nachfolgende PCR vervielfacht und somit sichtbar gemacht werden konnte. Um auch major group HRVs untersuchen zu können, wurde im Laufe der vorliegenden Arbeit auch ein rekombinanter ICAM-1 Rezeptor kloniert, der in eukaryotischen Zellen exprimiert werden kann. Das geeignetste Verhältnis von Virus zu Lipid wurde mit  $3.4 \times 10^{-6}$  gefunden. Höhere Viruskonzentrationen führten zur Zerstörung der Membran, genauso wie als Kontrolle zugegebenes Detergens, wodurch der RT Mix verdünnt wurde und keine cDNA mehr transkribierte. Dies deutet auch wieder auf die Bildung einer Pore für den Transfer von minor group RNA hin. Mit dem Nanocontainer System wurde ein RNA Transfer verstärkender Effekt von Calcium und ein gegenteiliger von dem antiviral wirkenden Molekül Amiloride gefunden.

Sobald der neu klonierte ICAM-1 Rezeptor exprimiert ist, könnte das Nanocontainer System ein einfach abzuänderndes Modell für den RNA Transfer von allen HRVs sein.

## 2 Introduction

### 2.1 Picornaviridae

#### 2.1.1 Classification

Currently two modes of virus classification are in use. The first is the Baltimore classification. It was developed in 1971 by David Baltimore [1] on the basis of viral genomes and the mode of replication. All viruses are classified into seven groups, named in Roman numerals. Their shared genome implies also a common mode of infection and replication, allowing a constricted transmission of investigational data between species within one class. For replication in a host cell, it is mandatory to transcribe the viral genome, no matter in what form it enters the cell, into mRNA, a positive stranded RNA which can be used for translation. Figure 2-1 depicts the seven viral groups according to their genome class and their intermediate steps on the way to produce mRNA.

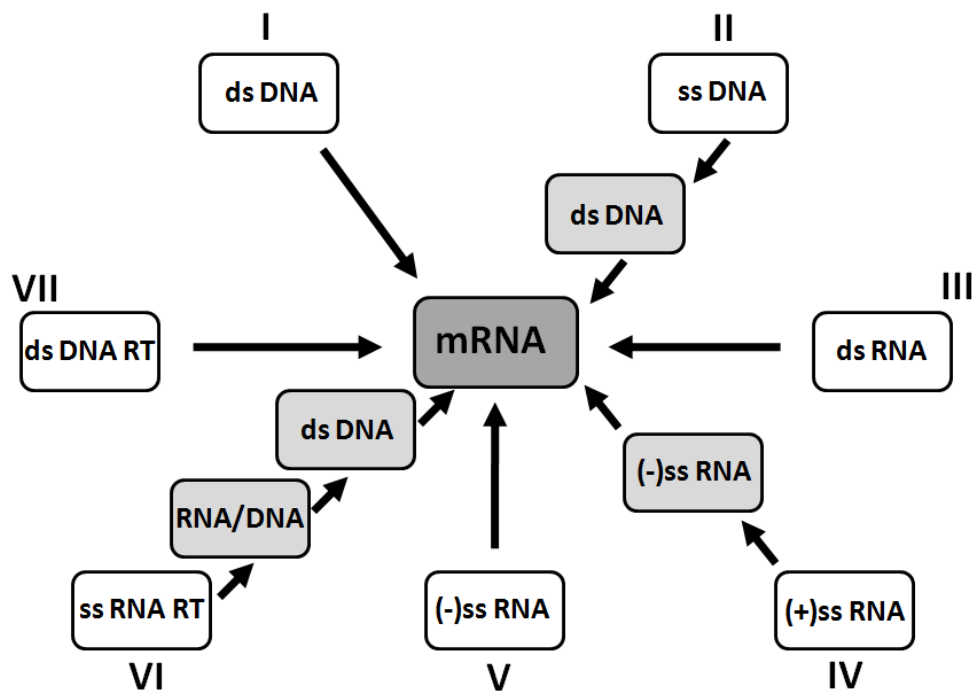


**Figure 2-1.** Baltimore classification scheme of viruses. White background signifies the viral genome, double stranded (ds) or single stranded (ss) and the directionality (+ or -) is given, reverse transcription (RT) as replication strategy noted. Light gray background indicates the necessary intermediate steps of genome replication until mRNA (dark grey) is produced which serves as universal template recognized by the host cellular replication and translation machinery.

Picornaviruses belong to the group IV, comprising all positive sensed single stranded RNA viruses. They need one intermediate step, negative single stranded RNA from which more positive stranded RNA is transcribed.

### **Introduction**

---

Further classification and taxonomy of viruses is taken care of by the International Committee on Taxonomy of Viruses (ICTV) (see Figure 2-2). According to the decisions made by the ICTV, the family picornaviridae belongs to the higher order of picornavirales, also including the families dicistroviridae, iflaviridae, marnaviridae which are all animal infecting viruses, and secoviridae, which include the subfamily comovirinae and comprises all plant picornaviruses. All families share certain characteristics; since similarities in genome structure are a principal indicator for classification, sequencing provides additional proof and often changes of classification. At present, the family Picornaviridae comprises 12 genera, one of them is the genus enterovirus, others are aphthovirus (the species Foot-and-mouth disease virus belongs to that genus) or hepatovirus (holding the species Hepatitis A virus). The genus enterovirus comprises 10 virus species, including Human Enterovirus C, which was formerly known as Poliovirus, and all serotypes of Human Rhinovirus, organized as the species Human Rhinovirus A, Human Rhinovirus B and Human Rhinovirus C. Other enterovirus species are Bovine enterovirus, Human enterovirus A, Human enterovirus B, Human enterovirus D, Porcine enterovirus B, Simian enterovirus A. See Figure 2-2 for an overview of ICTV Picornaviridae classification.



<i>Picornaviridae</i>	order
<i>Enterovirus</i>	family
<ul style="list-style-type: none"> <li>• Human Rhinovirus A</li> <li>• Human Rhinovirus B</li> <li>• Human Rhinovirus C</li> <li>• Bovine enterovirus</li> <li>• Human enterovirus A</li> <li>• Human enterovirus B</li> <li>• Human enterovirus C</li> <li>• Human enterovirus D</li> <li>• Porcine enterovirus B</li> <li>• Simian enterovirus A</li> </ul>	species
<i>Aphthovirus</i>	
<ul style="list-style-type: none"> <li>• Foot-and-mouth disease virus</li> <li>• Bovine rhinitis B virus</li> <li>• Equine rhinitis A virus</li> </ul>	
<i>Avihepatovirus</i>	
<ul style="list-style-type: none"> <li>• Duck hepatitis A virus</li> </ul>	
<i>Cardiovirus</i>	
<ul style="list-style-type: none"> <li>• Encephalomyocarditis virus</li> <li>• Theilovirus</li> </ul>	
<i>Erbovirus</i>	
<ul style="list-style-type: none"> <li>• Equine rhinitis B virus</li> </ul>	
<i>Hepatovirus</i>	
<ul style="list-style-type: none"> <li>• Hepatitis A virus</li> </ul>	
<i>Kobuvirus</i>	
<ul style="list-style-type: none"> <li>• Aichi virus</li> <li>• Bovine kobuvirus</li> </ul>	
<i>Parechovirus</i>	
<ul style="list-style-type: none"> <li>• Human parechovirus</li> <li>• Ljungan virus</li> </ul>	
<i>Sapelovirus</i>	
<ul style="list-style-type: none"> <li>• Porcine sapelovirus</li> <li>• Avian sapelovirus</li> <li>• Simian sapelovirus</li> </ul>	
<i>Senecavirus</i>	
<ul style="list-style-type: none"> <li>• Seneca Valley virus</li> </ul>	
<i>Teschovirus</i>	
<ul style="list-style-type: none"> <li>• Porcine teschovirus</li> </ul>	
<i>Tremovirus</i>	
<ul style="list-style-type: none"> <li>• Avian encephalomyelitis virus</li> </ul>	
<i>Dicistroviridae</i>	
<i>Iflaviridae</i>	
<i>Marnaviridae</i>	
<i>Secoviridae</i>	

**Figure 2-2. Viral classification according to the ICTV (of July 2010) with particular focus on the order picornaviridae.**

### 2.1.2 Morphology

Picornaviridae are small viruses with 27-30 nm diameter of their non-enveloped icosahedral capsid. An icosahedron has 20 identical equilateral triangular faces (*eikosi* is Greek for twenty). In picornaviruses, the outer capsid is made up by three different proteins, the viral proteins 1-3 (VP 1-3). Although their amino acid sequences are different, they share the general structure: each viral protein consists of eight antiparallel  $\beta$ -sheets which together form a  $\beta$ -barrel. One copy each of VP 1-3 form a triangular protomer, which consequently consists of 3  $\beta$ -barrels. A triangulation number ( $T$ ) = 3 capsid consists of 180 structurally identical  $\beta$ -barrels, and although picornaviral capsids look similarly, they are formed by 3 different proteins and hence exhibit  $P = 3$  (pseudo  $T = 3$ ). In total, the picornaviral capsid is composed of 60 protomers. Five of these protomers are located around a 5 fold axis (see Figure 2-3 for icosahedron assembly).

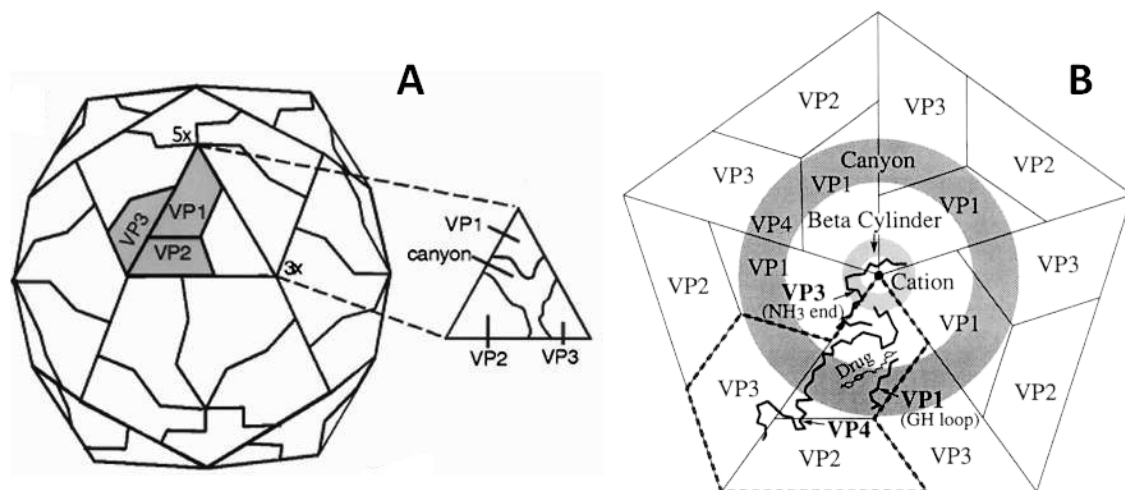


**Figure 2-3. Assembly of the icosahedral picornavirus capsid. (A) Each protomer consists of one copy each of VP1-3. Five of these protomers form a pentamer around a fivefold axis (5x). Taken from Hogle and Racaniello [2] (B) Top view of one of the 12 pentamers of the icosahedron, which contains a cation, probably  $\text{Ca}^{2+}$ , in the middle. A canyon (dark grey) encircles the axis. Structures supposedly playing a role in viral uncoating are indicated for one protomer: VP1 GH loop, VP3 N-terminus and part of VP4. Also a drug binding to the canyon and inhibiting viral infection is shown. From Giranda et al.[3].**

A binding site for divalent ions, most probably calcium, has been observed in this central position, supposedly playing a role in virion stabilization [4]. Each protomer features a canyon which encircles the fivefold axes. It is 15 Å deep and 12 Å wide at its narrowest point. The canyon is the binding site of several receptors. The outer surface of the capsid is made up by the C-termini of only VP1, 2 and 3, the fourth and smallest structural protein VP4 is inside the capsid. The N-termini of VP3 form a  $\beta$ -cylinder at the fivefold axis. This structure is surrounded by the N-termini of VP4 and VP1, the interaction is mediated by a myristic acid which is covalently linked to the terminus of VP4 [5]. This myristoylation is not only necessary for correct assembly, it also plays a role in infectivity.

Inside the capsid, the RNA is tightly packaged to fit into the small space. Picornaviral RNA is about 7500 nucleotides (nt) in length. In contrast to eukaryotic mRNA, the 5' end of the picornaviral RNA is covalently linked to a peptide, the viral protein genome-linked (VPg). This protein functions as a primer for RNA replication. The 3' end is formed of a polyA-tail - like mammalian mRNA - although it is an actual part of the viral genome and not added posttranscriptionally like in mammalian mRNA. Both sides of the RNA contain an untranslated region (UTR), the longer one with around 600-1200 nt on the 5' end and a shorter 50-100 nt at the 3' end.

### **2.1.3 Replication pathway**

The viral life cycle of Picornaviridae has been studied very well in poliovirus, therefore it often serves as model for this virus family. Figure 2-4 presents a schematized summary of the poliovirus life cycle as an example for picornaviruses.

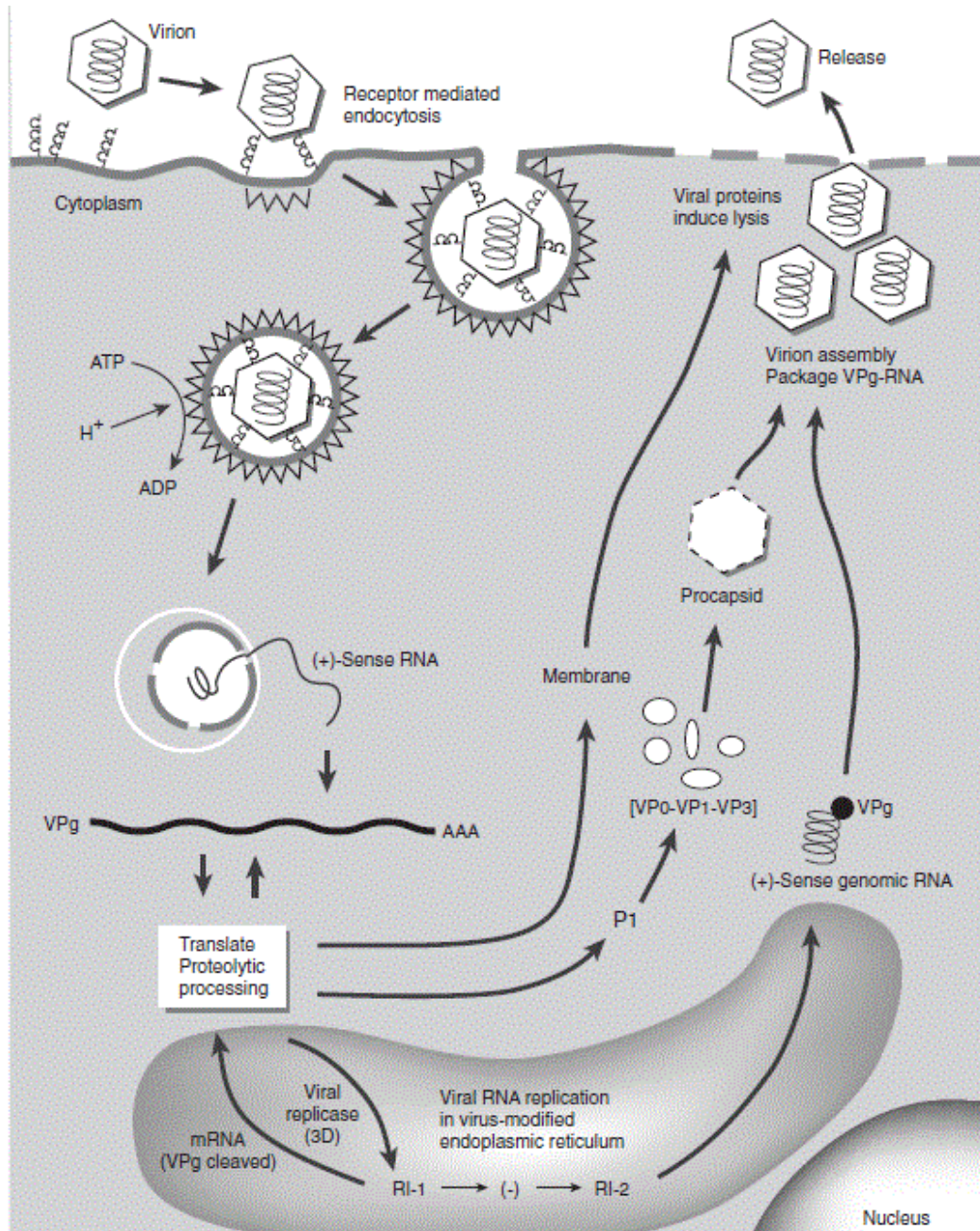


**Figure 2-4. Picornaviral life cycle depicted by the example of poliovirus.** The native virion attaches to its receptor on the plasma membrane of the host cell, which internalizes the particle into an early endosome. Upon maturation to the late endosome, the pH inside the vesicle is decreased, which causes the transfer of the viral RNA into the cytoplasm of the cell, either through a pore or via disruption of the endosomal membrane. The positive sense viral RNA can be translated and the resulting polyprotein proteolytically cleaved into its mature viral proteins. One of the proteins is viral replicase which uses the viral RNA as a template for RNA replication with a negative stranded RNA as an intermediate. Viral RNA with attached VPg on the 5' end can be packaged in the procapsid consisting of the structural proteins VP1, VP3 and VP0, the latter one is cleaved to VP2 and VP4 for full maturation of the virion. Viral proteins also shut off the translation of cellular proteins and lyse the host cell membrane, releasing the new viral particles. From Basic Virology [6, p. 238].

Picornaviruses abuse different cell surface molecules as receptors and co-receptors for attachment to the host cell surface. The picornaviral RNA is either directly transferred across the cell membrane, or the virion is first internalized into endosomes and the RNA

transferred across the endosomal membrane into the cytoplasm of the host cell [5] p. 810. The (+) RNA is translated, using a special region within the 5' UTR, the internal ribosome entry site (IRES), for ribosome recruiting. The translation termination signal is close to the 3' end, allowing for the translation of a single large polyprotein. This polyprotein is the precursor of all viral proteins. It is at first cleaved intramolecularly by two viral proteases to produce 3 large precursor proteins: P1-3. P1 is further cleaved into VP1, VP3 and VP0, the latter further into VP2 and VP4 during virion maturation. All non-structural viral proteins are derived from P2 and P3, including the viral replicase (P3D, an RNA-dependent RNA polymerase), VPg and host cell modulating proteins and enzymes. Already at an early stage of infection the virus shuts off the translation of host mRNA by proteolytic digestion of the translation initiation factor eIF-4G, which functions in ribosomal recognition of 5' capped mRNA. Picornaviruses do not need the 5' cap for translation initiation, but rather use the IRES instead; all resources of the host cell are exploited for the translation of viral proteins.

P3D replicates the RNA genome. It has quite a high error rate compared to DNA polymerases (one mutation per  $10^4$ - $10^5$  nt as compared to  $10^7$ - $10^9$  nt for Pol II), not only because of the low specificity of the replicase, but also because of the absence of a proof-reading function. The high error rate causes a high variability in progeny virions, making fast adaption to the surroundings possible. It is also a way of escape from the immune system of the host or specially designed drugs.

Replication needs uridylylated VPg as a primer. Partly cleaved precursor proteins from P2 and P3 bind to the template RNA strand, either at the polyA-tail or to the origin of replication internal (oriI) [7], one of them being the replicase which catalyzes the attachment of VPg or its uncleaved precursor. In the presence of UTP, the Tyr-3 hydroxyl of VPg is used as a nucleophile to form VPg-pU, the 3'-OH which, in turn, serves as the nucleophile to form VPg-pUpU [7]. The uridylylated VPg is moved to the 3' end of the template RNA strand and acts as a primer for the viral replicase to start RNA transcription of either a positive or negative strand. Negative sense strands serve as template for further positive sense strands, which in turn are used for translation of more viral proteins when the VPg is cleaved off, or are packaged with an attached VPg. The procapsid, consisting of equimolar quantities of VP1, 3 and VP0, encapsulates the (+)ssRNA-VPg and matures to the full virion via cleavage of VP0 to VP2 and VP4. Mature virions accumulate in the cytoplasm of the host cell until the cell membrane is lysed, releasing the progeny virions.

## 2.2 Human Rhinovirus

### 2.2.1 Pathogenesis

The word *rhino* is Greek for nose. The name was chosen because human rhinoviruses infect the polarized epithelial cells of the upper and to some extent also the lower airways of humans. Ciliated cells, which hardly express any ICAM-1 in the absence of inflammation, are rarely infected. Estimated 50% of all mild infections of the upper respiratory tract are caused by rhinoviruses, they also provoke more severe diseases like exacerbating asthma or chronic obstructive pulmonary disease. Due to the variety of serotypes it is difficult to develop immunity, resulting in a high prevalence and many lost working / school days. Although common cold infections are generally mild, the sheer number of infections lead to around \$40 billion spent alone in the USA on medication and loss of working time per year [8]. The large number of serotypes and variability within them also makes it difficult to develop medication. Rhinoviruses are spread via aerosols and smear infections and can be stable at ambient temperatures on commonly touched surfaces like door handles for days. About 1-4 days after infection, the typical symptoms become evident: discharging or blocked nasal passages, accompanied by a general malaise, cough, sore throat, edema of the connective tissue etc at the peak of the infection. The nasal secretion contains a high virus titer. The direct tissue destruction through replication of virus and lysis of its host cell is actually quite marginal; the symptoms experienced are rather caused by the immune reaction of the infected cells, increased by released histamine. The first defense reaction of infected cells includes production of interferons which stimulate other cells to produce antiviral proteins (they break down viral RNA and inhibit elongation during protein translation) and class I MHC molecules and activate the immune system to kill infected cells. Specific immune response includes the production of antibodies, IgA is secreted from the nasal mucosa and provides immunity to the infecting HRV serotype for 1-2 years. As mentioned, this immunity does not prevent further common cold infections caused by one of the many other serotypes. Treatment is normally restricted to relieving the symptoms and not directly antiviral. Other viruses causing diseases with similar symptoms include parainfluenzaviruses, coronaviruses and enteroviruses.

### 2.2.2 Taxonomy

Currently, there are 106 HRV serotypes known. They are categorized into Human Rhinovirus A, B and C, according to the results of genetic typing of a nucleotide sequence between VP4 and VP2. There are 74 HRV-A, 25 HRV-B and 7 HRV-C serotypes acknowledged right now, although there are more to expect. HRV 87 showed closer relationship to the species human enterovirus D than to any other HRV serotype and was

therefore reclassified as human enterovirus 68 [9]. The long time distinction of rhinoviruses and enteroviruses based on their acid stability/lability has been superseded by this new classification and the taxonomical grouping of picornaviruses was revised. The distinct genera enterovirus and rhinovirus were grouped together as a single genus with the name enterovirus.

Another often used classification founds on the employed receptor. Sixty-two HRV-A and all HRV-B use ICAM-1, which is therefore called the major group receptor; the remaining 12 HRV-A bind to the minor group receptor which is a member of the low-density lipoprotein (LDL) receptor family: LDLR, very low-density lipoprotein receptor (VLDLR) or lipoprotein receptor related protein (LRP). Also heparan sulphate can be used by some major group viruses for attachment. HRV-C has only been recognized as a species recently and its receptor(s) have not yet been described.

Depending on their stage of uncoating, subviral particles have been given particular names. The native HRV particle sediments at 150 Svedberg (S) upon centrifugal sedimentation in a sucrose density gradient and is therefore also called 150S particle. During infection, the particle undergoes structural changes, in a first step the amphiphilic N-terminus of VP1 is externalized and the capsid protein VP4 is lost. These molecules are believed to insert into host cell membranes, ensuring binding of the particle closely to the membrane and maybe forming a pore for RNA transfer. On the outside of the virion, VP4's hydrophobic myristic acid contributes to the lipophilicity of the particle and the destabilization of its interior. This first intermediate particle sediments at 135 S and is therefore called 135S particle or also A (altered) particle. Further conversion leads to RNA release. This empty viral shell sediments at 80 S; it is called 80S particle or B particle. Since 80S particles are hydrophilic, the externalized N-termini of VP1 must be somehow hidden, but not all structural changes can be reversed. An opening at the fivefold axes, a 10 Å wide channel, can be found in 80S particles and causes an about 4% larger capsid compared to the 150S particle.

### **2.2.3 Virion structure and properties**

In general, rhinoviruses are typical picornaviruses: they have the non-enveloped icosahedral capsid, the genome is a single stranded, positive sensed RNA of about 7100 – 7300 nt length. It is covalently connected to VPg at the 5' end and featuring a polyA tail at the 3' end. Translation produces a single 2100-2200 amino acids (AA) large polyprotein from one open reading frame (ORF), which is subsequently cleaved into structural and non-structural proteins (see Figure 2-5 for a scheme of HRV genome and proteome). The 5' UTR is 610-625 nt long, the 3' UTR 40-47 nt.

## RNA transfer of HRV through model membranes

### Introduction

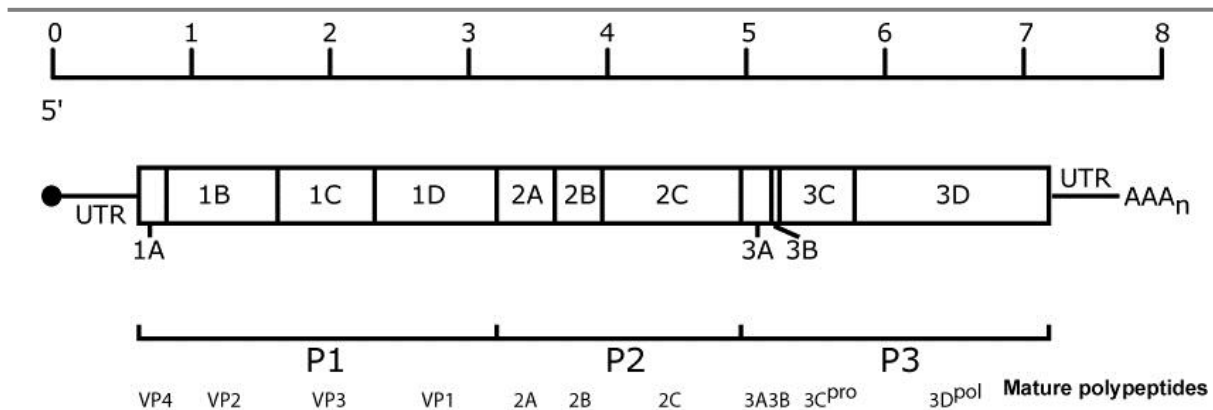


**Figure 2-5. Scheme of the Human Rhinovirus genome.** Upper row indicates the length of the RNA strand in 1000 nt steps from 5' on the left to 3' on the right. Middle row represents the RNA with genes indicated. Note the VPg on the 5' end and the polyA-tail on the 3' end, both followed or presided, respectively, by the UTR. Lower row depicts the large polyprotein and its mature cleavage products. Figure from [www.uq.edu.au/vdu](http://www.uq.edu.au/vdu).

There is a great variability between the serotypes. Best studied representatives of HRV are HRV2, a minor group HRV-A, and HRV14, a major group HRV-B. So far, little is known about HRV-C. The HRV icosahedral capsid features star-shaped domes formed by VP1 at the fivefold axes. These domes are stabilized from the inside by VP3 and are encircled by around 2 nm deep canyons formed by VP1, VP2 and VP3. Beneath the canyon floor, within VP1, is a hydrophobic cavity, the pocket, which is filled in some serotypes with a fatty acid derived from the host cell, but has been found to be empty in others. The fatty acid is believed to stabilize the capsid and has to be expelled prior to uncoating. The canyon has been identified as the binding site for the major receptor ICAM-1, the high specificity ensures that only humans can be infected with HRV. The binding geometry for the minor receptor is totally different and the binding sites are located at the dome.

The so-called “breathing” is a process of structural changes of the viral capsid [10]. VP4 is known to be buried inside the capsid around the fivefold axis, only VP1-3 are exposed on the external surface. But VP4 is transiently exposed on the viral surface, which can be inhibited by antiviral drugs: binding of WIN 52084 to the pocket of the canyon stabilizes the HRV14 virion in the closed conformation with VP4 on the inside; infectivity of these virions is strongly reduced [10], purportedly because the WIN compound serves like a pocket factor for the stabilization of the virion in the closed conformation.

A characteristic trait of rhinoviruses, which separates them from other enteroviruses and has been used for their identification, is their acid lability. Whereas enteroviruses retain their infectivity in a pH below 3, which is necessary when passing through the stomach to reach the intestinal system, rhinoviruses become inactivated at pH values <5.6. When using epithelial cells of the respiratory tract for replication, the pH stability is not necessary. The mode of uncoating of viruses mirrors stability or lability at low pH.



Acid lability allows for uncoating at the low pH in endosomes, acid stable viruses need another trigger for uncoating like receptor attachment.

Another physico-chemical property is the buoyant density in cesium chloride, which reflects the permeability of the capsid. For comparison, the completely tight poliovirus capsid reaches 1.34 g/ml, the foot-and-mouth disease virus, whose capsid features pores, reaches 1.45 g/ml [5, p. 797]. Rhinoviruses reach an intermediate value with 1.40 g/ml, although also lower values have been reported [11]. Internal polyamines limit the amount of cesium ions entering the viral capsid, but more ions can enter at long centrifugation times in high cesium salt concentrations, contributing to an alteration of the buoyant density.

#### **2.2.4 Viral infection**

Viral replication of HRV takes place in the cytoplasm of the host cell. Therefore, it is mandatory for the virus to release its genomic RNA from the viral capsid and transfer it across the host cell membrane. Not all virions are able to initiate infection. They can fail to complete one of the steps of their life cycle, including attachment, RNA release, genome replication and virion assembly. Due to the high error rate of the replicase, also one of the numerous incorporated point mutations during replication can be the reason for inactivation. The ratio between particles and infectious virus is calculated by counting particles (by electron microscopy or spectrophotometrically) and determining the plaque forming units (PFU) of a sample. It ranges between 30 and 1000 for picornaviruses [5, p. 797].

Human Rhinoviruses exploit several different cell surface molecules for attachment to the host cell, the most important ones being ICAM-1 and LDLR. The binding site of ICAM-1 is at the base of the canyon, whereas the VLDL receptor footprint in HRV2 is on the star-shaped dome of the icosahedral fivefold axis formed by the BC and HI loops of VP1 [12]. The uncoating process is probably different for major and minor group viruses. While ICAM-1 interaction seems to be enough to initiate conformational changes in the capsid proteins to allow RNA transfer through the membrane, the LDLR activity is limited to the mediation of a clathrin dependent internalization of the virus-receptor complex. The receptor causes engulfment of the virion in the cell membrane until a vesicle is formed, which proceeds to an early endosome. The endosome matures to a late endosome by fusion with other vesicles, associated with a decrease of the pH to a slightly acidic value of 5.4 – 5.6, depending on the cell type. A conformational change of the receptor and the virus due to the low pH releases the RNA from the viral capsid and transfers it across the endosomal membrane into the cellular cytoplasm. Elucidating the influence of an acidic surrounding on capsid structure, studies in FMDV have shown that the low pH causes protonation of histidines along the pentamer interface. Protonated histidine residues

repulse each other and therefore the neighboring protomers, causing disassembly of the capsid. Affirming the role of histidines in the acid lability of the capsid, mutation of histidines causes higher stability of the virion at low pH [13-14]. Similar effects are presumed in rhinoviruses which also undergo structural changes upon exposure to a low pH. Structural changes of the capsid are necessary to allow for its expansion and the opening of 10 Å wide pores for RNA release. It has to be kept in mind that the later on presented uncoating processes for major and minor group HRVs are presumed models and the exact events of RNA translocation are controversial and have not been visualized yet. It is still especially difficult to explain how the RNA can be threaded through a 10 Å pore, since it forms complicated secondary structures inside the capsid with mostly double stranded regions of at least 20 Å diameter. Either the RNA has to be disentangled into a single stranded structure, although it is not known where the energy for unfolding would come from, or the pore has to extend, at least temporarily, maybe during the process of breathing.

Once the RNA has reached the cytoplasm of the cell, it is immediately translated by the host cell translational machinery. Viral replication follows the events described for all picornaviruses (see section 2.1.3). Once a viral infection is manifested, it induces further ICAM-1 receptor expression of surrounding cells, reinforcing viral spreading.

#### 2.2.5 Major Group Receptor: Human ICAM-1

The Intercellular adhesion molecule 1 (ICAM-1) (also called CD54) is an integral membrane protein and part of the immunoglobuline (Ig) protein superfamily. Its physiological ligand is the lymphocyte function-associated antigen 1 (LFA-1), which is expressed on the surface of lymphocytes. Hence, ICAM-1 is normally intended to play an important role in the host cell's immune system and is therefore expressed on a wide range of cell types, including epithelial cells in the nasopharynx of humans, the hunting ground of Human Rhinoviruses. It is also a receptor for some coxsackieviruses. ICAM-1 consists of 532 AA which are segmented into a 27 AA signal peptide followed by the extracellular topological domain, a helical transmembrane domain and an intercellular cytoplasmic domain (see Figure 2-6 for ICAM-1 structure). The extracellular domain consists of 5 repeats of Ig-like C2-type domains. The actual binding site of ICAM-1 on HRVs is the first amino-terminal located Ig-like domain [15-16]; its BC, CD, DE and FG loops mediate the direct contact of the receptor with the virus. Notably, the virus is kept at quite a distance from the membrane via the 5 Ig-like domains. The ICAM-1 protein is modified by several glycosylations, phosphorylations and disulfide bonds.

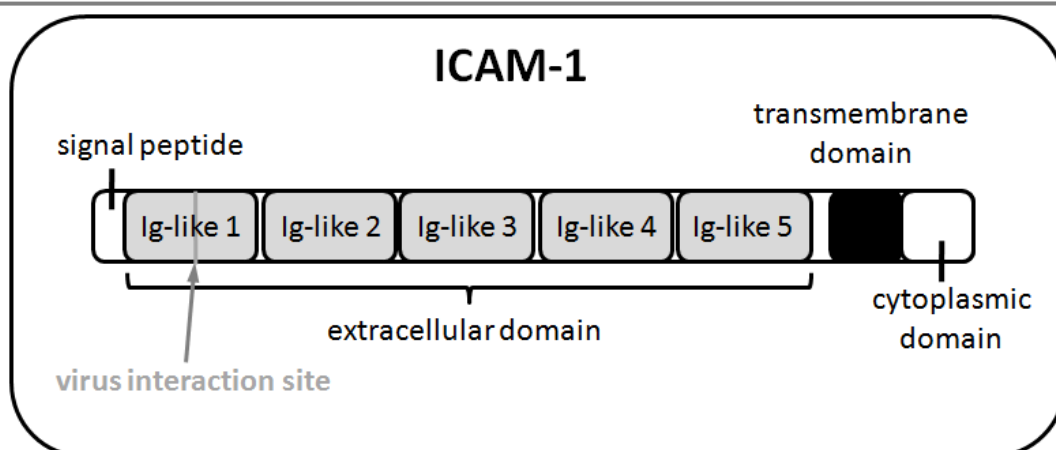


**Figure 2-6. Schematized structure of ICAM-1, indicating the main areas and domains, from N-terminus to C-terminus: a signal peptide, the extracellular domain consisting of 5 immunoglobulin-like domains, a transmembrane domain and the cytoplasmic domain. The virus binding site is situated within the first immunoglobulin-like domain.**

The receptor attaches to the viral canyon which encircles the fivefold axis [17]. The interacting sequences on the canyon base are contributed by VP1 and VP3 and are highly conserved, although they differ in HRV-A and HRV-B. If a pocket factor is present, it is pushed out by the receptor to make the buried binding sites accessible and room for structural rearrangements. Possibly the virus undergoes the structural changes by itself during breathing and the receptor attaches in the right moment and stabilizes the virion in the open conformation. Upon binding to the receptor, the major group virus HRV14 experiences several structural changes. The tight connection between the protomers loosens up, allowing an expansion of the viral capsid of about 4%, especially pronounced at the domes of the fivefold axes. VP1 forms a channel of about 10 Å diameter at the fivefold axes [18], the believed exit point for the RNA. Another important structural change of the viral capsid is the loss of VP4 in the process of uncoating. Presumably, it inserts into the membrane due to its hydrophobic character and could form a channel which would serve as connection between the viral capsid and the cytoplasm. Major group viruses probably use the N-terminus of VP1 and the rigid ICAM-1 receptor in addition to VP4 to completely disrupt the endosomal membrane concomitantly to RNA release [19].

Still, for most serotypes the receptor only mediates the attachment of the virus and is just an additional trigger to an acidic pH for RNA release. Tightly bound virus leads to internalization of the receptor-virus complex. Although the low pH in late endosomes is necessary in addition to the ICAM-1 interaction for RNA release, the contribution of both differs in various serotypes, since some are more acid stable than others. The uncoating process is also strongly temperature dependant. Only very acid sensitive serotypes can infect without ICAM-1 via heparan sulphate, whereas infection via ICAM-1 still works at least at a low level in the presence of the H<sup>+</sup>-ATPase inhibitor bafilomycin.

### 2.2.6 Minor Group Receptor: LDLR family

LDLR family molecules, including LDLR, VLDLR and LRP, are typical endocytic recycling receptors: they are found on the plasma membrane surface but also to a great extent in recycling endosomes. Since they possess at least one clathrin-coated pit localization signal, they are constitutively internalized via clathrin-dependent endocytosis and recycled after ligand detachment. Ligands, either the low-density lipoprotein or HRV, dissociate at the mildly acidic pH in early endosomes with the help of a  $\beta$ -propeller domain. While the ligand is transported to late endosomes and finally lysosomes, the receptor is recycled to the plasma membrane. Members of the LDLR superfamily consist of varying repeats of the same domains. The ligand-binding domain contains several, in the case of LDLR seven, LDL receptor type A repeats. Each repeat consists of 40 residues with three disulphide bonds forming a negatively charged surface which coordinates a  $\text{Ca}^{2+}$  ion. The second conserved region contains LDL receptor type B repeats consisting of EGF-like repeats and YWTD domains (they form the  $\beta$ -propeller). An O-linked glycosylation domain is present in LDLR and VLDLR, but not LRP. The receptor is membrane-bound via a transmembrane domain, followed by the cytoplasmic tail containing one or two consensus sequences Asn-Pro-Xaa-Tyr (NPxY) for receptor internalization signaling via phospho-tyrosine binding (PTB) domains. The  $\beta$ -propeller is the reason for the acid-dependent structural changes of the receptor which results in ligand dissociation. Figure 2-7 depicts the LDLR in open and closed conformation, depending on the pH.

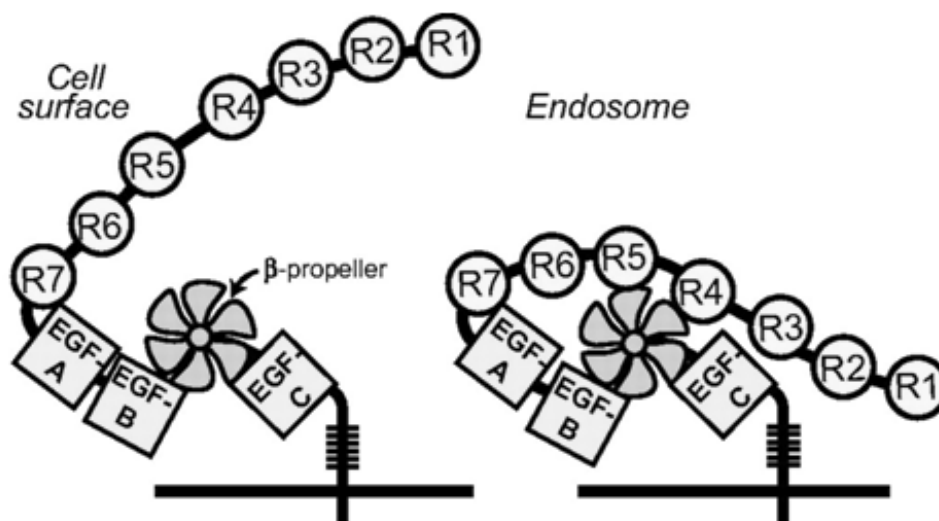


**Figure 2-7.** The low density lipoprotein receptor at a mildly basic pH on the cell surface (left) and at an acidic pH in the endosome (right). Note the structural change at low pH, a turning of the  $\beta$ -propeller causes the extended ligand-binding domains to fold back to a closed structure and thereby release the bound ligand. Figure from [20]

The LDLR family is used as receptor by 12 members of the HRV-A species. There are several important differences between attachment of HRV to LDLR and to ICAM-1. Upon

binding to the LDL receptor the virus does not automatically undergo structural changes like it is the case with the major group receptor ICAM-1. Also the attachment geometry of the virus is different: LDLR does not bind to the canyon encircling the fivefold axis, but to the dome on the fivefold axis itself [21]. Therefore it is not able to stabilize the virion in the open conformation and it is strictly dependent on the low pH ( $\leq 5.6$ ) in late endosomes for RNA release and transfer. This was shown with an inhibitor of the V-ATPase which blocks the pH decrease in endosomes [22-23]. The result was strong inhibition of infection.

Upon exposure to low pH, also minor group viruses exhibit an expanded capsid and pore formation at the fivefold axes. The empty capsids have lost all VP4, in contrast to major group capsids. Also, they have an extended  $\beta$ -cylinder at all 12 fivefold axes. Minor group virions probably stay inside the endosome and only transfer their RNA through the channel into the cytoplasm. In contrast to the ICAM-1 mediated infection pathway, the subviral particles can be found in late endosomes and lysosomes, whereas the RNA escapes the lysosomal degradation, indicating that the RNA has been released within the endosome and was transferred via an ion-conducting pore to the cytoplasm, leaving the empty capsid behind.

The minor group receptor is either LDLR or LRP. For VLDLR a very high binding affinity has been demonstrated, but due to its tissue distribution (it is mainly found in skeletal muscle, heart and organs except liver) it is unlikely to be used as HRV receptor *in vivo*. Nevertheless its high affinity has been utilized for recombinantly produced receptor models. The highest binding affinity was achieved by cloning a concatemere of five domains 3 of the VLDLR. By linking them to a maltose binding protein (MBP) and a His<sub>6</sub>-tag [24-25], the soluble MBP-V33333-His<sub>6</sub> receptor can be attached to the Nickel complexing lipid DOGS-NTA incorporated in liposomes. This provides an artificial model system for the complex and difficult to study *in vivo* cellular situation.

## 2.3 Nanocontainers

To study viral infection, in particular the poorly understood process of RNA release from the virion and transfer across the endosomal membrane, the complex system of cells is a major problem. So far, no structure of uncoating intermediates on cellular membranes could be resolved. High magnifying microscopy like cryo-electron microscopy of cellular compartments is difficult, therefore high resolution pictures of the bound virus during the uncoating process have not yet been taken. Also elucidation of viral infection and the inhibitory effect of different molecules on it is a tricky process in cell culture. Cells are complex systems and modifying just one specific parameter without causing unintended additional changes is merely impossible. Liposomes have been established as a simple and easy to modify model of a cell or cellular compartment. They can be employed for tackling different questions, only using the minimal requirements to make the process work. That

way these requirements can not only be identified, but also manipulated with drugs or high concentrations of a compound which would kill cells and stop any further study. The lipid composition of biological membranes is crucial for their functional properties, therefore to make results obtained with this model as relevant for the *in vivo* situation as possible, it is mandatory to mimick the host cell membrane as closely as possible. The uncoating of HRV occurs at the endosomal membrane, hence that one has to be employed for RNA transfer studies like they were done in the course of the present thesis.

#### 2.3.1 Endosomal Membranes

Endosomes are transport vesicles inside eukaryotic cells. Their function is to collect cargo from the plasma membrane, e.g. free or loaded receptor, and navigate it through the cell, as well as the other way around, to release membrane-bound or soluble molecules on the plasma membrane of the cell. Depending on the cargo's destiny, it has to be sorted into different cell compartments. The plasma membrane derived vesicles fuse with early endosomes which have an only mildly acidic pH. Upon maturation into late endosomes the pH decreases via the action of V-ATPases. Molecules intended for recycling are concentrated in tubules which bud off the early endosomes and transport their cargo back to the plasma membrane as recycling endosomes. Late endosomes fuse with lysosomes, forming the lysosomal endosomes, which feature high density, an acidic pH and degrading enzymes.

The membrane of early endosomes is similar to the plasma membrane, but on maturation to late endosomes there are some dramatic shifts of lipid composition. According to two-dimensional chromatography and autoradiography of  $^{32}\text{P}_i$ -labeled phospholipids of purified late endosomes, the membrane consists besides 1/3 of cholesterol of around 32 % PC, 13% PE, 3% PI, 1% PS, 6% SM and 11% LBPA [26-27]. Figure 2-8 depicts the mean of the concentrations given in the references. Phosphatidylcholine (PC) self-organizes spontaneously as a typical planar bilayer in which each lipid molecule has a nearly cylindrical molecular geometry, with the lipophilic tails facing each other and the polar headgroups facing the aqueous phase. They also account for the membrane fluidity at room temperature [27]. In contrast to PC, Phosphatidylethanolamine (PE) has a conical molecular geometry because of the relatively small size of its polar headgroup, hence exerting influence on the membrane shape. Also it has been found that the various lipids are asymmetrically distributed between the two bilayer leaflets, adding another factor that contributes to curvature stress in biomembranes. Phosphatidylserine (PS) is mainly a part of the inner plasma membrane leaflet and is found in traces in the cytosolic leaflet of endosomes and lysosomes. Several signalling and fusogenic effector proteins with specific phosphatidylserine-binding domains can direct vesicle fate via PS. Phosphatidylinositol (PI) is also important in the physiological system as a signaling lipid which is necessary for

defining the organelle identity and recruiting of proteins. Sphingomyelin (SM) consists of ceramide as a hydrophobic backbone plus oligosaccharides. Due to their saturated fatty acid tail they are able to form tightly packed solid phases which have to be fluidized by other lipids like sterols. Cholesterol (Ch) is the main non-phosphorylated lipid in mammals. It belongs to a family of polycyclic compounds known as sterols which are not only important for membranes but for lipid metabolism in general as they are also part of vitamins, hormones and bile acids, amongst others [28].

### 2.3.2 Liposomal membrane

For the *in vitro* production of liposomes the lipids were chosen in a way to closely resemble the lipid composition of physiological late endosomes and at the same time incorporate functional lipids for subsequent experiments, like proposed by Gerhard Bilek [29]. The small portion of functional lipids of the mammalian cellular late endosomes like PI and PS were omitted, since their signaling activity for messenger proteins is of no interest in a pure liposome sample used for viral infection experiments. Instead, up to 10 mol% of dioleoylglycerol-succinyl-nitriloacetic acid (nickel salt) (Ni-DOGS-NTA) were incorporated as attachment site for His<sub>6</sub>-tagged proteins and, if required, 1 mol% of nitrobenzoxadiazol phosphocholine (NBD-PC), a fluorescence labeled lipid, were applied for liposome tracing. The used 30 mol% cholesterol were comparably to the *in vivo* situation, the second-frequent lipid PC was represented by a share of 20 mol% palmitoylcholine (POPC). The rest was made up by 20 mol% PE and 20 mol% SM. A comparison of membrane compositions of late endosomes according to the literature [26-27] and of the liposomes produced here is presented in Figure 2-8.

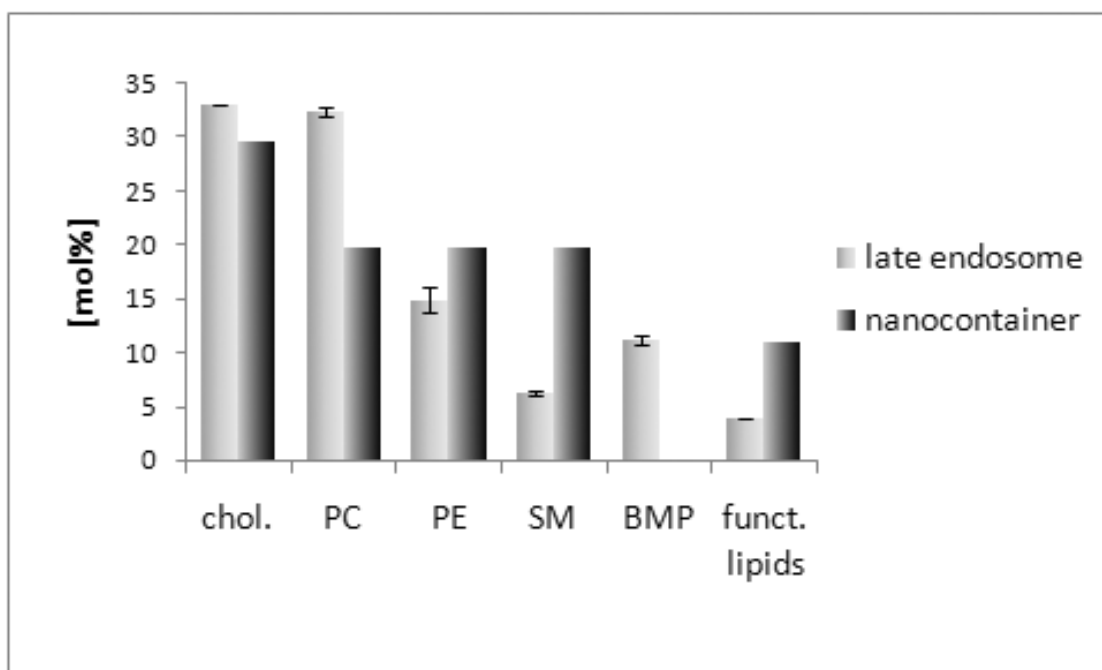


Figure 2-8. Comparison of the lipid compositions of physiological late endosomes according to van Meer and Kobayashi [26-27] and here presented nanocontainers.

#### 2.3.3 Proof of RNA transfer

It is difficult to prove RNA transfer into liposomes. Normally, RNA is detected by reverse transcription (RT) and subsequent polymerase chain reaction (PCR) or quantitative PCR (qPCR). For these methods, the liposomes carrying RNA in their lumen have to be separated from viral particles and from not correctly transferred RNA on the outside. This is tricky and the result can be flawed by loss of correctly transferred RNA or by accidentally detecting outside RNA. Direct detection of the RNA inside the liposomes is by far preferable. A method had been developed by Bilek [29], where liposomes of the above presented composition were prepared and filled with all classical components for reverse transcription except the template, i.e. enzyme-specific buffer, dNTPs, reverse primer, DTT, reverse transcriptase and an RNase inhibitor; these liposomes are as from now on called “nanocontainers”. They were decorated on the outside with the recombinant soluble minor group receptor MBP-V33333-His<sub>6</sub> [25, 30]. HRV2 was allowed to attach to the receptor and was then triggered to release its RNA and transfer it into the nanocontainers where it was transcribed into cDNA by the RT kit. The liposomes were permeabilized with a detergent and the cDNA amplified via PCR to give a visible signal on an agarose gel.

When putting the theory into practice the model system appeared to be unreliable, often giving no signal, whereupon it was not known if the system failed in transferring the RNA or in subsequently detecting it.

#### 2.4 Aim of the project

The present diploma thesis focuses on solving the above described problem of unreliability of the newly developed model system for viral RNA transfer through lipid membranes. HRV2 RNA should be detected reliably upon transfer into liposomes decorated with a recombinant VLDLR and filled with a reverse transcription kit, called nanocontainers. Furthermore, the model system should be refined, characterized and extended to major group HRVs by cloning a soluble ICAM-1 receptor.



### 3 Materials and methods

#### Buffers

abbreviation	name	ingredients
<b>TrisNaCl</b>	50 mM Tris, 80 mM NaCl, pH 8.3	3 g Tris (AppliChem) 2.5 g NaCl conc. HCl ad pH 8.3 dH <sub>2</sub> O ad 500 ml
<b>NaAc</b>	1 M NaAc pH 5.0	136 g sodium acetate glacial acetic acid ad pH 5.0 dH <sub>2</sub> O ad 1000 ml
<b>TBS</b>	10 x TBS 250 mM Tris pH 7.5, 1.5 M NaCl	250 ml 121 g Tris (AppliChem) conc. HCl ad pH 7.5 dH <sub>2</sub> O ad 1000 ml 300 ml 146 g NaCl dH <sub>2</sub> O ad 500 ml 450 ml dH <sub>2</sub> O
<b>CaCl<sub>2</sub></b>	1 M CaCl <sub>2</sub>	147 g CaCl <sub>2</sub> dH <sub>2</sub> O ad 1000 ml
<b>TBSC</b>	25 mM Tris, 150 mM NaCl, 10 mM CaCl <sub>2</sub>	100 ml 10x TBS 10 ml 1 M CaCl <sub>2</sub> dH <sub>2</sub> O ad 1000 ml
<b>TAE</b>	50 x TAE	242 g Tris (AppliChem) 57.1 ml glacial acetic acid 37.2 g Na <sub>2</sub> EDTA.2H <sub>2</sub> O dH <sub>2</sub> O ad 1000 ml
<b>Running buffer</b>	10 x SDS-PAGE running buffer	144 g glycine (AppliChem) 30 g Tris (AppliChem) 10 g SDS (BioRad) dH <sub>2</sub> O ad 1000 ml
<b>NaOH</b>	1 M NaOH	40 g NaOH dH <sub>2</sub> O ad 1000 ml
<b>borate buffer</b>	50 mM boric acid, pH 8.3	3.1 g boric acid (Sigma-Aldrich) 3 M NaOH to pH 8.3 dH <sub>2</sub> O to 1000 ml

Chemicals were purchased from Merck, Darmstadt, Germany if not indicated otherwise. Other suppliers: Bio-Rad Laboratories, Hercules, CA, USA; Sigma-Aldrich, St. Louis, MO, USA; AppliChem, Darmstadt, Germany.

**Lipids**

name	abbreviation	Avanti Polar Lipids catalog#
<b>1-palmitoyl-2-oleoyl-<i>sn</i>-glycero-3-phosphocholine</b>	POPC	850457P
<b>L-<math>\alpha</math>-phosphatidylethanolamine</b>	PE	841118P
<b>sphingomyelin</b>	SM	860062P
<b>1,2-dioleoyl-<i>sn</i>-glycero-3-[(N-(5-amino-1-carboxypentyl)iminodiacetic acid)succinyl] (nickel salt)</b>	Ni-DGS-NTA	790404P
<b>cholesterol from ovine wool</b>	Ch	700000P
<b>1-Oleoyl-2-[12-[(7-nitro-2-1,3-benzoxadiazol-4-yl)amino]lauroyl]-<i>sn</i>-Glycero-3-Phosphocholine</b>	NBD-PC	810133P

All lipids were purchased from Avanti Polar Lipids, Inc., Alabaster, Alabama, USA (<http://www.avantilipids.com>) via Instruchemie, Delfzijl, Netherlands.

**3.1 Liposome Preparation****Preparation of multi-lamellar vesicles (MLV):**

Lipophilized lipids (Avanti Polar Lipids via Instruchemie, Delfzijl, Netherlands) were dissolved in chloroform p.A. to 10 mM stocks of POPC, PE, SM and cholesterol. Ni-DGS-NTA and NBD-PC stocks were 10 mg/ml which corresponds to 9.3 and 11.3 mM, respectively. Stocks were stored in glass vials with teflon lined caps, covered with N<sub>2</sub>, at -20°C. A lipid membrane was prepared, consisting of POPC : PE : SM : Ch : Ni-DGS-NTA and NBD-PC, the latter only if the liposomes were intended for fluorescence detection upon flotation. A total of 5  $\mu$ mol dissolved lipids in the ratio 1 : 1 : 1 : 1.5 : 0.5 (: 0.05) were mixed in a 25 ml pointed bottom glass flask, that corresponded to 100  $\mu$ l POPC, 100  $\mu$ l PE, 100  $\mu$ l SM, 150  $\mu$ l cholesterol, 54  $\mu$ l Ni-DGS-NTA and 4.5  $\mu$ l of the NBD-PC stock if necessary. The flask was rotated (55 rpm) under a constant stream of nitrogen gas on a Büchi Rotavapor for at least 3 hours to evaporate all traces of solvent and dry the lipid film on the glass wall. It was then hydrated for 2 hours under further constant rotation (45 rpm) with a reverse transcription kit composed of 30  $\mu$ l 10  $\mu$ M reverse primer (GAAACACGGACACCCAAAGTA, according to Lu et al. [31] (1  $\mu$ M end concentration), 15  $\mu$ l 10 mM dNTP mix (Promega), 60  $\mu$ l 5x RT first strand buffer (Invitrogen), 15  $\mu$ l Recombinant RNasin Ribonuclease Inhibitor (Promega), 15  $\mu$ l SuperScript III Reverse Transcriptase (Invitrogen) and 165  $\mu$ l nuclease free water (Qiagen) to a total volume of 300  $\mu$ l. No dithiothreitol (DTT) was added. Three short intervals of vortexing during the last 30 min of hydration helped detaching the lipid film from the wall. The resulting 17 mM lipid suspension consisted of MLV (multi-lamellar vesicles) and was stored at 4°C until extrusion.

**Extrusion of MLV to LUV:**

To form LUVs (large unilamellar vesicles) of uniform size, a Mini-Extruder (Avanti Polar Lipids) was employed at room temperature.

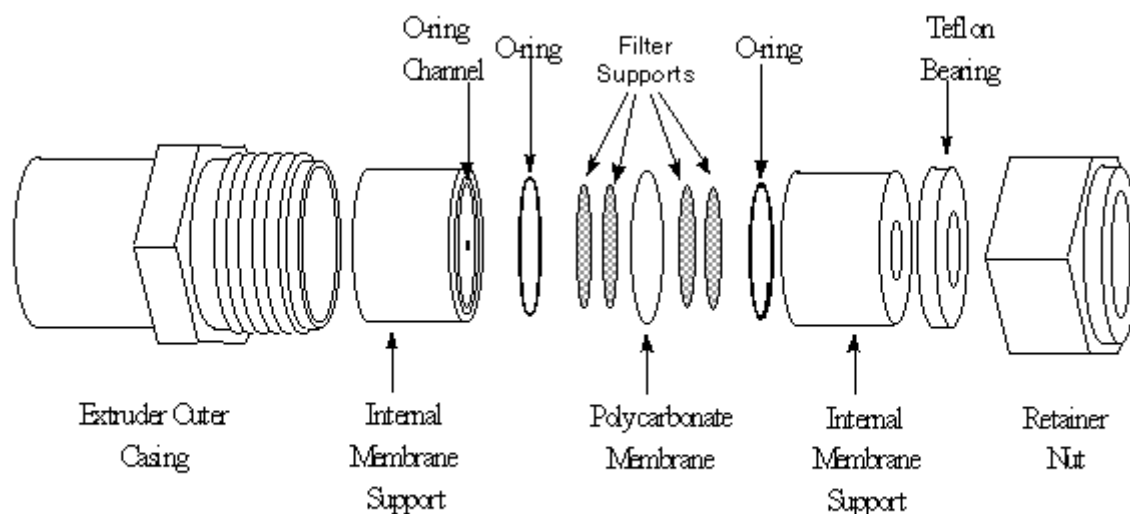


**Figure 3-1. Parts of the Mini Extruder (Avanti Polar Lipids) in the order of their assembly. Multilamellar vesicles are applied to the extruder with a syringe inserted either in the left or right Internal Membrane Support and pushed through the extruder into a second empty syringe on the other side. Taken from Avanti Polar Lipids, Inc., <http://www.avantilipids.com>**

Assembly of the extruder (depicted in Figure 3-1) started with washing all parts with water to remove dust and soaking four pieces of Filter Supports (Avanti Polar Lipids, catalog# 610014, purchased via Instruchemie, Delfzijl, Netherlands) in dH<sub>2</sub>O. After fitting the black rubber rings (O-rings) into the cylindrical Internal Membrane Supports, two wet Filter Supports were placed in the middle of each ring. One support complex was slid into the metallic Extruder Outer Casing and covered with two polycarbonate membranes (Nucleopore Track-Etch Membrane, 19 mm, 0.4 µm pore size, Whatman, catalog# 800282) with a pore size of 400 nm. The second support complex was inserted, extended with the white teflon Bearing ring and the extruder was closed with the metallic Retainer Nut, not using a wrench. The void of the extruder was wetted and filled with 50 mM Tris 80 mM NaCl 3 mM MgCl<sub>2</sub> buffer. The MLV suspension was applied to the extruder with a flat-needle Hamilton syringe and passed through the polycarbonate membrane pores 41 times into a second syringe at room temperature. If liposomes of smaller size were desired, it would have been possible to continue the extrusion with a polycarbonate membrane of a pore size of 0.2 µm. LUVs were either directly used in experiments or stored at 4°C. After total disassembly of all extruder parts and also syringes, every part was washed first with water and then ethanol.

### Purification by mini-size-exclusion-chromatography (mSEC):

Sephadex G-50 (medium) (Amersham Biosciences) was swollen in 50 mM Tris 80 mM NaCl (short: Tris NaCl) buffer over night at 4°C and used to pack a Spin-X Centrifuge Tube Filter equipped with a 0.45 µm pore size cellulose acetate membrane (Corning, purchased via Szabo-Scandic). 900 µl swollen Sephadex were used in two steps for each column, excess buffer was removed by centrifugation (see Figure 3-2 for a scheme of the mSEC procedure).

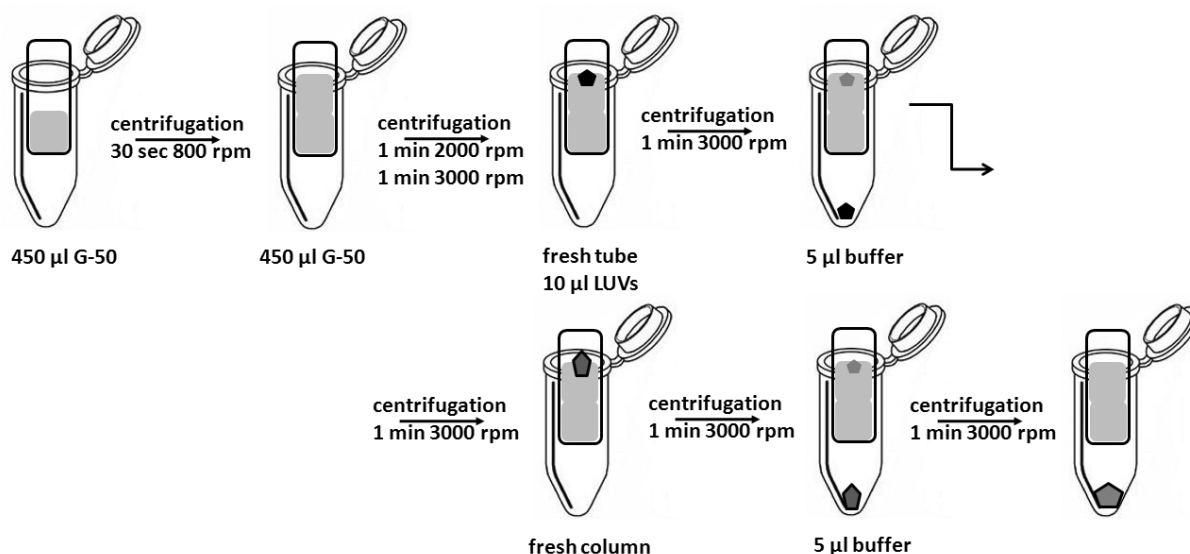


**Figure 3-2. Mini Size Exclusion Chromatography.** First two steps serve the Sephadex G-50 column formation, two columns have to be prepared for each sample. Then the nanocontainer sample is applied on top of the first column and centrifuged through. After a step of washing, the flow-through is applied to the second column and purified in the same way.

First the column was filled with 450 µl Sephadex and centrifuged for 30 seconds at 800 rpm in an Eppendorf 5424 tabletop centrifuge, then it was filled with another 450 µl Sephadex and centrifuged for 1 min at 2000 rpm and 1 min at 3000 rpm. 10 µl of LUV suspension, which had shortly been reloaded with 1.3 mM final concentration NiCl<sub>2</sub>, were applied to the column and sieved by centrifugation at 3000 rpm for one minute. 5 µl buffer were used in the same way for rinsing. The filtrate was subjected to a second round of purification on a fresh column which produced 1:4 diluted but well purified liposomes.

### Nanocontainer system:

The standard procedure of performing RT-PCR with the nanocontainer system is depicted in Figure 3-3.

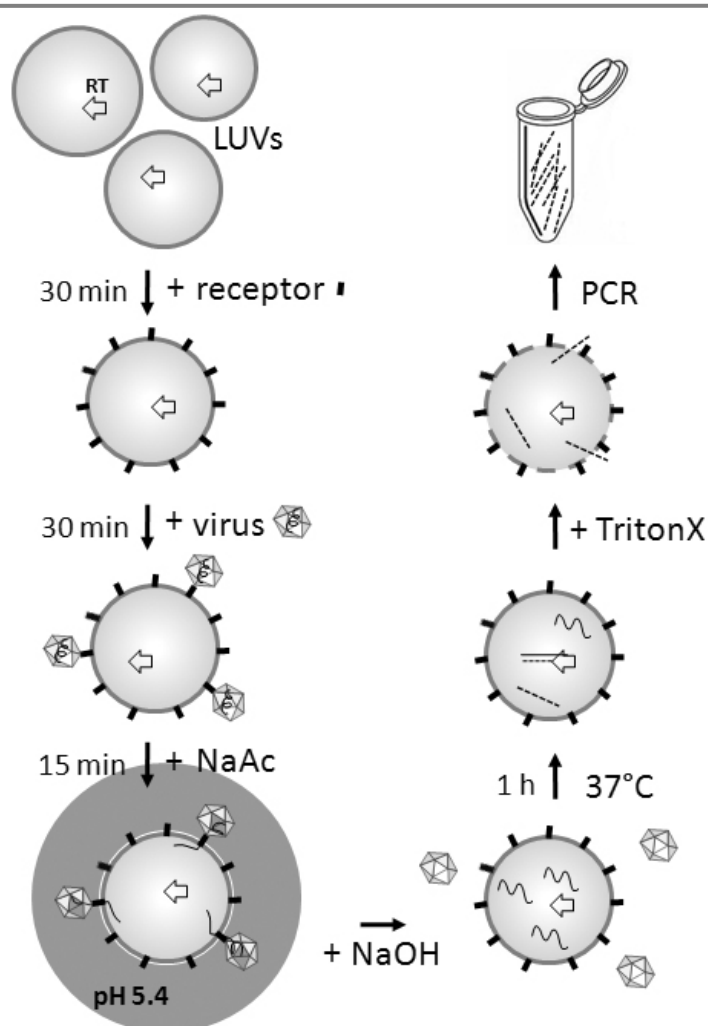


**Figure 3-3.** Standard RT-PCR reaction employing the nanocontainer system. 15  $\mu$ l LUVs purified by mSEC were decorated with receptor and then virus, each for 30 min at room temperature. Typical amounts for one sample were 64 nmol lipid, 36 pmol receptor and around 90 fmol HRV2 in TrisNaCl buffer in a total volume of 19.4  $\mu$ l. Decorated liposomes were exposed to a low pH of 5.4 for 15 min by addition of 1.2  $\mu$ l 1 M NaAc buffer pH 5.0, followed by reneutralization with 0.6  $\mu$ l 1 M NaOH to a pH of 8.3 and 1 hour at 37°C to perform the reverse transcription. After the enzyme was inactivated at 70°C for 15 min, the liposomes were disrupted with 1  $\mu$ l of 20% Triton X-100 and 2.5  $\mu$ l of the sample were used as template in a 50  $\mu$ l PCR reaction. The amplified product was applied to an agarose gel.

Controls and application of the system for different purposes made it necessary to customize the procedure accordingly, by omitting or adding one or several steps of the standard protocol or changing the concentrations. The PCR product was made visible on an agarose gel. Individual steps are described below.

### Decoration:

15  $\mu$ l of mSEC purified LUVs (corresponding to 64 nmol lipid) were mixed at ambient temperature with 1  $\mu$ l (corresponding to 36 pmol) recombinant V33333 receptor or dilutions of that if indicated and incubated for 30 min. The same incubation time was applied after addition of virus, concentrated or diluted in Tris NaCl buffer (amount is indicated for each experiment, it differed from around 1 to 1000 fmol) in a total sample

volume of 19.4  $\mu\text{l}$ . After decoration of the liposomes with receptor and virus, the RNA release of the virus was triggered by pH adjustment to 5.4 for 15 min with 1.2  $\mu\text{l}$  1 M NaAc pH 5.0. Reneutralization to a pH of 8.3 was achieved with 0.6  $\mu\text{l}$  1 M NaOH.

#### Calculation virus : liposome ratio:

The calculations were performed in Microsoft Excel. Starting point was the material liposomes are made of: 5 different lipids, each with a certain size (POPC [32], PE [33], SM [34], Chol [35], DGS-NTA [36]). Weighed according to their share of total lipid, the mean surface for one lipid molecule was 0.54 nm<sup>2</sup>. The surface of a 400 nm diameter sphere consisting of a double layer was calculated to be 980491 nm<sup>2</sup> with the formula  $4 \times \pi \times r^2 \times 2$ . Dividing the spherical surface by the mean lipid surface resulted in the number of lipid molecules incorporated in one liposome. The total amount of lipid used for liposome preparation was known to be 0.017 M, multiplication with  $6,022 \times 10^{23}$  (Avogadro constant) gave the number of lipid molecules per liter preparation. By dividing the number of lipid molecules/liter by the number of lipid molecules/liposome, the amount of liposomes/liter preparation could be estimated. Via division by the Avogadro constant this amount can also be expressed as mol liposome/liter preparation. One RT-PCR sample contained 3.75  $\mu\text{l}$  concentrated liposomes, which corresponded to  $3.5 \times 10^{-14}$  mol.

Virus input was calculated from 7.3 mg/ml virus. HRV2 has a relative molecular mass of 8 MDa, therefore the virus stock contained, according to the formula  $n = m/M$ ,  $9.1 \times 10^{-13}$  mol virus/ $\mu\text{l}$ . Thus 1  $\mu\text{l}$  of a 1:10 dilution of virus, a typical amount for one sample, would correspond to  $9.1 \times 10^{-14}$  mol virus in the RT-PCR sample. Dividing the calculated mol virus by the mol liposomes present in one sample gave the desired mol virus/mol liposome.

The amount of employed virus could also be expressed as TCID<sub>50</sub>. Applying the same TCID<sub>50</sub> : total liposomal surface ratio to the surface of an average cell, the corresponding TCID<sub>50</sub> : cell ratio was deduced and compared to usually employed values of MOI in cell culture.

#### Reverse transcription:

As a control of reverse transcription, 20  $\mu\text{l}$  positive control samples consisting of: 10  $\mu\text{l}$  H<sub>2</sub>O, 2  $\mu\text{l}$  1  $\mu\text{M}$  reverse primer, 1  $\mu\text{l}$  10 mM dNTP mix, 4  $\mu\text{l}$  5x first strand buffer, 1  $\mu\text{l}$  RNasin (Promega), 1  $\mu\text{l}$  diluted HRV as template and 1  $\mu\text{l}$  SuperScript III reverse transcriptase (Invitrogen) were prepared. HRV dilution was varied between 1:10 and 1:1000 (corresponding to 91 fmol to 0.9 amol) and RNA release was triggered comparably to the samples containing nanocontainers with a pH of 5.4 for 15 min. This control also acted as a size standard for the desired PCR product. The reverse transcription reaction

was performed with all samples for 1 h at 37°C, followed by 15 min at 70°C to inactivate the enzyme.

**PCR:**

Each 50 µl PCR reaction contained 40 µl H<sub>2</sub>O, 5 µl 10x pfu buffer, 1 µl 10 mM dNTP mix (Promega), 0.5 µl 10 µM primer forward (CPXGCCZGCGTGGC according to Lu et al. [31], obtained from Exiqon, Vedbaek, Denmark; also see primer list in attachment), 0.5 µl 10 µM primer reverse, 2.5 µl cDNA template and 0.5 µl pfu DNA polymerase (Promega). After an initial step of 2 min at 95°C for enzyme activation, the amplification was performed during 60 cycles of 45 s 95°C for denaturation, 45 s 60°C for primer annealing and 2 min at 72°C for elongation, followed by 10 min at 72°C for final elongation in an Eppendorf Masterycler gradient.

**Agarose gel:**

1% agarose gels were prepared with 0.4 g standard electrophoresis agarose (genXpress) and 40 ml 0.5x TAE buffer. If intended for RNA instead of DNA the buffer was prepared with DEPC treated water. GeneRuler 1 kb DNA ladder (Fermentas) was used as a size standard, the samples were loaded with 6x DNA loading buffer (Fermentas) or RNA loading buffer and the gel was usually run at 80 V for 20 min. It was then incubated for 15 min in an ethidium bromide bath before taking a photograph under UV illumination in a GelDoc-It TS Imaging System (UVP).

**ImageJ:**

Signal intensity of agarose gel bands was quantified with ImageJ (<http://rsbweb.nih.gov/ij/>), a program which integrates intensity and area of a gel band into numbers, according to an online user manual (<http://panic.berkeley.edu/~ghe/GelDoc/UsingImageJ/>). In short: A grayscale photograph of the gel is necessary for this purpose. First the area around the bands was selected with the Rectangular selection tool and appointed by Ctrl + 1. The rectangle was dragged to an appropriate area above, which only contained background and appointed by Ctrl + 2. By pressing Ctrl + 3, the program gives a grayscale profile of both the lanes and the background. Peaks had to be separated by hand via drawing vertical lines between them with the Straight line selection tool (pressing Shift at the same time makes sure the line is really vertical). The area of each peak plus associated background peak was annotated with the Wand tool, the program automatically gave the results after Analyze/Gels/LabelPeaks had been opened. The results, which included the area of each peak and its percentage of the total area, were copied into an Excel file. There the

background area was subtracted from the band area to give the final signal intensity, which was then plotted in a bar chart.

#### **Transmission Electron Microscopy:**

Microscopy was performed by Angela Pickl-Herk. Carbon-coated copper grids were taken from the vacuum storage box and glow discharged for 30 s at 20 mA. They were loaded with 4 µl sample, incubated for 1 min and drained with filter paper. The samples were stained by incubation with 4 µl 2% Na-phosphotungstate (PTA) pH 7.3 twice for 1 min. The loaded grids were stored in vacuum until pictures were taken at 80 kV with the FEI Morgagni transmission electron microscope (FEI, Hillsboro, Oregon, USA) using an 11 Mpixel CCD camera.

#### **qPCR virus dilution series:**

HRV2 was serially diluted, RNA release was triggered by exposure to 56°C for 10 min and the sample was subjected to reverse transcription in a 19.4 µl total volume RT mix. In addition, 1 µl of concentrated virus was added to an RT mix, triggered to release its RNA, reverse transcribed and diluted to give the same dilution series. Five µl of the solution containing the cDNA template were mixed at ambient temperature with 12.5 µl 2x Taq polymerase Red Mix (Ampliqon), 0.1 µl 100 µM primer forward, 0.1 µl 100 µM primer reverse, 0.25 µl 1 µM Fluorescein additive (Eurogentec), 1 µl 25x SYBR Gold and 6.05 µl H<sub>2</sub>O to a total volume of 25 µl. Negative controls with dH<sub>2</sub>O instead of cDNA template were included in every run. Samples were run on a Bio-Rad iCycler with iQ5 optical unit or an Eppendorf realplex Mastercycler with following parameters: 2 min 95°C to initiate the enzyme, 45 cycles of 15 sec 95°C for denaturation, 15 sec 60°C for primer annealing and 1 min at 72°C for elongation and fluorescence measurement, followed by the production of a melting curve between 50° and 95°C. Threshold cycles and corresponding virus dilutions were applied for the calculation of a standard curve using Microsoft Excel.

#### **RNA *in vitro* transcription:**

pBluescriptHRV2, a T7 promoter containing vector which carries the cDNA of HRV2, was used as template in a PCR with forward primer HRV2\_3end 6849 and reverse primer HRV2\_5end 561-583 (see primer list in section 8.2). The same PCR mix was used as described before, except for only 0.3 µl pfu DNA polymerase. The protocol started with 2 min 95°C, 35 cycles of 45 s 95°C, 45 s 50°C and 9 min 72°C, followed by 10 min 72°C. To control the product, 5 µl were applied to an agarose gel. The DNA was ethanol precipitated by filling up the finished PCR reaction to 100 µl with dH<sub>2</sub>O, 1 ml 96% ethanol and 50 µl 3 M NaAc pH 5.2, incubating for 30 min at -80°C, pelleting the DNA at 13000 rpm in an Eppendorf tabletop centrifuge, 4°C, for 20 min, washing the pellet with 750 µl 70%



ethanol and resuspending it in 15 µl dH<sub>2</sub>O. For *in vitro* transcription, using the MEGAscript Kit (Ambion), 0.3 µl of that template were used. It was adhered to the given protocol, allowing transcription for 4 hours. The produced RNA was extracted by Phenol-Chloroform-Extraction (see in section 3.2) and resuspended in 50 µl H<sub>2</sub>O (Ambion). The RNA concentration was measured with a NanoDrop (peqlab) and the quality of the product was checked on a DEPC agarose gel.

### Capillary Electrophoresis:

This was realized in cooperation with Xavier Subirats on a capillary electrophoresis machine (Hewlett-Packard 3D CE). For determination of the EOF, DMSO was used in a 1:200 dilution as neutral marker that would run in front of the virus and benzoic acid as a second internal standard that would run behind the virus. 1 µl virus sample was mixed with 0.7 µl 1:200 diluted DMSO, 0.9 µl benzoic acid and 12.4 µl 100 mM borate buffer pH 8.3 (sample buffer) to a total sample volume of 15 µl. A blank had the same composition except for replacing the virus with buffer. Vials with 1 M NaOH, H<sub>2</sub>O and an empty one were prepared and placed into the CE vial chamber. NaOH was set as Inlet and waste as Outlet and the capillary was flushed for 5 min. Then the Inlet was changed to H<sub>2</sub>O and it was flushed for another 5 min. The background electrolyte (BGE) was prepared by adding 10 mM Thesit to the sample buffer, 3 vials were filled with exactly the same volume (350 µl) of BGE. The capillary was flushed with BGE at the end of the washing procedure. After setting the Inlet to the sample vial, the run was started and the time and absorbance at 200 and 260 nm were measured. Since the migration time usually changes from run to run to some extent, the electrophoretic mobility of the peaks was determined from the total length of the capillary ( $L_{tot}$ ), length of capillary from sample uptake until detector ( $L_{eff}$ ), time of peak appearance of DMSO ( $t_{DMSO}$ ) and time of peak appearance of analyte ( $t_A$ ). Effective mobility of the analyte ( $\mu_{eff}$ ) is the value of  $\mu_{obs}$  minus  $\mu_{EOF}$ , which can be calculated by the following equations:

$$(1) \mu_{obs} = 1/t_A * L_{eff} * L_{tot} / V$$

$$(2) \mu_{EOF} = 1/t_{DMSO} * L_{eff} * L_{tot} / V$$

$$(3) \mu_{eff} = \mu_{obs} - \mu_{EOF}$$

### Flotation in a sucrose step gradient:

For the sucrose step gradient, fresh sucrose solutions of 67% and 25% w/v (6.7 and 2.5 g sucrose, respectively, were brought to 10 ml with Tris NaCl buffer) were prepared, dissolving was accelerated by heating to 80°C in a water bath. Liposomes with incorporated NBD were prepared with receptor and virus at different molar ratios like described for liposomes for RT-PCR (above) and diluted with Tris NaCl buffer to a total volume of 50 µl. Each sample was mixed with 150 µl 67% sucrose solution to give 200 µl

50% sucrose solution, which was transferred to the bottom of an 11x34mm centrifuge tube (Beckman). It was overlaid with 900 µl 25% sucrose solution slowly drop by drop on the wall of the tube and with 900 µl Tris NaCl buffer as 0% sucrose solution. The tubes were evenly balanced and placed in a TLS55 swing out rotor. Centrifugation was performed on an Optima TLX Ultracentrifuge (Beckman) for 4 hours at 4°C, 45000 rpm. Aliquots of 167 µl were taken from the top and transferred to a 96 well plate. Fluorescence of NBD-PC in each aliquot was determined by a Wallac Victor<sup>2</sup> plate reader (PerkinElmer) and corresponded to the amount of liposomes. The fraction with the highest liposome concentration was chosen for TEM imaging. A TCID<sub>50</sub> assay was performed with a 2 µl aliquot of each fraction of a sample with receptor and a control sample without receptor. Aliquots containing most of the liposomes were combined and exposed to a pH of 5.4 for 15 min by the addition of 1 M NaAc pH 5.0 to trigger the RNA release (660 µl floated liposomes + 39.6 µl 1 M NaAc). After reneutralization to a pH of 8.3 with 1 M NaOH (19.6 µl), reverse transcription was performed at 37°C for one hour, then the enzyme was inactivated by heating to 70°C for 15 min. Produced cDNA was precipitated after disintegration of the liposomes with 1% TritonX by addition of 1/10 volume 3 M NaAc, 2 µl 20 mg/ml glycogen and 2.5 times the volume 96% ethanol and incubation at -80°C for 30 min. Precipitate was pelleted by centrifugation at 14000 rpm for 15 min at 4°C in an Eppendorf tabletop centrifuge, washed with 700 µl 70% ethanol and another 5 min centrifugation and then left to dry for some minutes at room temperature. The pellet was dissolved in 20 µl H<sub>2</sub>O and subjected to PCR. 1/4 of the PCR reaction was applied to a 1% agarose gel and the DNA was stained with ethidium bromide. A positive control consisting of the RT mix alone was included in RT, precipitation and PCR.

#### **Median tissue culture infective dose (TCID<sub>50</sub>) assay:**

TCID<sub>50</sub> assays were performed by Irene Goesler. Hela cells in 100 µl infection medium (MEM + 2% FCS, 1% pen/strep, 1% glutamine, 30 mM MgCl<sub>2</sub>) were seeded in 96 well plates and grown overnight at 37°C. Samples containing virus were serially diluted in infection medium to give 10 fold dilutions. A sample from each dilution was spread on the cells of 12 wells and incubated at 34°C for 5 days. The wells were stained with 80 µl 0,1% crystal violet in H<sub>2</sub>O per well for 10 min and cell free wells were counted.

### **3.2 Cloning of soluble ICAM-1 receptor**

#### **Stock of pCDM8ICAM1:**

The plasmid carrying the ICAM-1 encoding gene was obtained from Addgene (plasmid# 8632) in the bacterial host strain MC1061/P3. Bacteria were spread on an agar plate containing 12.5 µg/ml ampicillin and 16 µg/ml tetracycline and incubated overnight at 37°C. A single colony was used for inoculation of 100 ml LB+Amp+Tet, which were again incubated at 37°C overnight. 500 µl of culture were mixed with 500 µl 87% glycerol and frozen in liquid nitrogen for storage at -80°C. The rest of the culture was used for a Midi prep to gain a stock of purified pCDM8-ICAM1 plasmids at a NanoDrop determined concentration of 4.6 µg/µl. This plasmid DNA was the starting material for both cloning strategies.

**Mini prep employing the Invisorb Spin Plasmid Mini Kit (Invitex):**

A single colony was picked with a sterile pipette tip and transferred to a test tube containing 2 ml LB+antibiotic. Incubation overnight at 37°C and constant shaking allowed bacterial replication. Suspension was transferred to a 2 ml tube and centrifuged for 1 min at 14000 rpm on an Eppendorf tabletop centrifuge. Supernatant was discarded and pellet resuspended in 200 µl Resuspension Solution of the Invisorb Spin Plasmid Mini Kit (Invitex). 200 µl Alkaline Lysis Solution were applied and lysis was performed for up to 5 min. After the addition of 200 µl Neutralization Solution it was mixed by shaking the tube and then centrifuged at 14000 rpm for 5 min. The supernatant was decanted into the prepared Spin Filter which had been placed into a 2 ml Receiver Tube and 200 µl Binding Solution were added. The tube was inverted to mix the solutions and centrifuged for 1 min at 8000 rpm in an Eppendorf tabletop centrifuge. After discarding the filtrate 750 µl Wash Buffer PL were centrifuged through in the same way. The emptied tube was subjected to 3 min of centrifugation at 14000 rpm for drying and the filter was moved to a 1.5 ml Receiver Tube and 60 µl Elution Buffer P were applied and allowed to soak for 10 min. To elute the plasmid DNA, centrifugation was performed for 1 min at 8000 rpm.

**Midi prep employing the NucleoBond Midi Kit (Macherey-Nagel):**

100 ml LB+antibiotic were inoculated with bacterial suspension derived from a single colony and incubated on a shaker at 37°C overnight. Bacteria were pelleted by centrifugation at 4°C, 4200 rpm for 15 min in a Megafuge 1.0R (Heraeus Instruments) centrifuge. The NucleoBond Midi Kit (Macherey-Nagel) was used to extract the plasmid. The pellet was resuspended in 4 ml buffer S1+Rnase A. After addition of 4 ml buffer S2 the tube was inverted 8 times and incubated at ambient temperature for up to 5 min. 4 ml pre-chilled buffer S3 were added, the tube again inverted 8 times and then cooled on ice for 5 min. While centrifuging at 12000 rpm at 4°C for 25 min in a Sorvall RC5C centrifuge (Sorvall SS34 rotor), the provided AX100 columns were equilibrated with 2.5 ml buffer N2. The supernatant was applied to the column. Once the sample had passed the filter the

column was washed with 10 ml buffer N3. Elution was done with 5 ml buffer N5, directly into a tube containing 3.5 ml isopropanol. DNA was pelleted by centrifugation at 14000 rpm at 4°C for 30 min in an Eppendorf 5415C tabletop centrifuge, followed by a washing step with 3 ml 70% ethanol and again centrifugation at 14000 rpm, now at ambient temperature for 15 min. The supernatant was aspirated off, the pellet left to dry at room temperature for 10 min and then resuspended in 100 µl pure H<sub>2</sub>O (Qiagen). The DNA concentration was determined by NanoDrop (peqlab) measurement.

#### **Phenol-Chloroform-Isoamyl alcohol extraction:**

The sample containing DNA or RNA was adjusted to 500 µl with H<sub>2</sub>O (Qiagen) and mixed by vortexing with 500 µl phenol-chloroform-isoamyl alcohol. Phases were separated by 2 min of centrifugation at 14000 rpm (Eppendorf 5424 tabletop centrifuge). The upper, aqueous layer was transferred to a new tube and complemented by 50 µl 3 M sodium acetate pH 5.2 and 1 ml 100% ethanol. After vortexing, precipitation was allowed at -80°C for 30 min, followed by centrifugation at 4°C, 14000 rpm for 10 min. The supernatant was sucked off and replaced by 750 µl 70% ethanol. After another round of centrifugation for 5 min at 14000 rpm, the supernatant was sucked off again and the pellet was left to air dry for about 10 min, then it was resuspended in 20 – 50 µl H<sub>2</sub>O (Qiagen).

#### **Restriction digest:**

Either 0.5 - 2 µg or all purified DNA from phenol-chloroform-extraction was mixed with 3 µl 10x buffer (NEB) as required by the enzyme, 0.3 µl 100x BSA if required by the enzyme, 0.5 µl enzyme 20 u/µl (NEB) and dH<sub>2</sub>O to a total of 30 µl. After incubation at 37°C for 2 h the enzyme could be deactivated by heating to 65°C for 20 min or if necessary, religation could be inhibited by addition of 1 µl alkaline phosphatase (Calf Intestinal Alkaline Phosphatase (CIP) (NEB)) and incubation at 37°C for 45 min. Restricted DNA was analyzed on an agarose gel.

#### **Isolation of DNA from agarose gel:**

A Promega kit (Wizard SV Gel and PCR Clean-up System) was used for this purpose. The 0.5% gel was viewed under UV light and the correct band was excised as economically as possible to have all DNA in a small portion of gel. This gel slice was weighed, soaked in 10 µl per 10 mg Membrane Binding solution and heated to 50°C for 10 min with occasional shaking. After total solubilization, the mixture was transferred to a SV Minicolumn placed in a Collection Tube and incubated for 1 min at ambient temperature. Centrifugation was performed for 1 min at full speed on a tabletop centrifuge (Eppendorf). After discarding the flow through, the membrane was washed with 700 µl Membrane Wash Solution and centrifugation like before. After addition of another 500 µl Membrane

---

Wash Solution, the column was centrifuged for 5 min at full speed. The emptied tube was dried with one additional minute of centrifugation. Elution was performed with 50 µl Nuclease-free water after the filter had been moved to a fresh 1.5 ml microcentrifuge tube. Following 1 min incubation at room temperature the tube was centrifuged for 1 min at 14000 rpm.

**Ligation:**

Backbone DNA and insert are mixed preferably in a ratio of 1:3 molecules, starting with about 100 ng of vector. They were mixed with 1 µl 10x ligation buffer, 0.5 µl T4 DNA ligase [400 u/µl] and dH<sub>2</sub>O to a total volume of 10 µl and incubated at room temperature for 1-3 h. A negative control for autoligation of the backbone was included where the insert DNA was replaced by H<sub>2</sub>O.

**Heat-shock transformation:**

Competent MC1061/P3 bacteria (Invitrogen) were thawed on ice. 100 µl were mixed with 5 µl of ligation mix (approximately 100 ng DNA) or 10 pg control plasmid, and incubated on ice for 30 min. The bacteria were heat-shocked in a 42°C water bath for 30 s and then put back on ice for 2 min. After addition of 800 µl SOC medium (Invitrogen) or LB, the suspension was incubated at 37°C for 1 h. 100 µl and the pellet of the transformation mixture were spread on agar plates + 12.5 µg/ml ampicillin and 16 µg/ml tetracycline and incubated at 37°C overnight or longer, if growth was very slow.

**Sequencing and alignment:**

Primer which bind to the pCDM8 backbone (PF 2130-2148, PR 2692-2717) were diluted to 5 µM in H<sub>2</sub>O and sent together with a few µl of sample DNA (approx. 1 µg) to the I.M.P. sequencing service (IMP, VBC, 1030 Vienna). Results were obtained by e-mail and sequences were aligned to normal and the reverse complement of the pCDM8 sequence and the ICAM-1 sequence with the program "BioEdit" (<http://www.mbio.ncsu.edu/BioEdit/bioedit.html>).

**Site directed mutagenesis:**

This method introduces a point mutation in a plasmid by PCR. To be able to remove the not mutated template, it has to be produced in bacteria with an active Dam methylase. In this case, MC1061/P3 E.coli were used. The forward primer ICAM\_SacI\_mut\_1591 (see primer index in section 8.2) was designed to hybridize to the sequence of ICAM-1 exactly on the position of the SacI restriction site except for one nucleotide: the guanine on position 1602 was exchanged for an adenine which resulted in the same amino acid glutamic acid but destroyed the recognition site of SacI. The reverse primer

ICAM\_Sac\_mut\_1590b was designed to bind directly adjoining to the forward primer, not leaving out a single nucleotide (see Figure 3-4 for a scheme of the point mutational primer design).

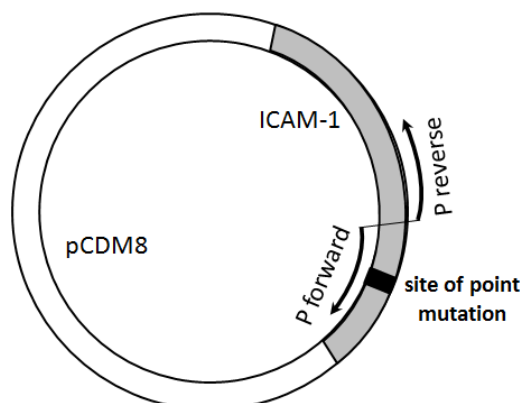


**Figure 3-4. Scheme of a PCR set-up for the introduction of a point mutation in a plasmid. One primer encloses the site of the intended point mutation, containing a single mismatch nucleotide. The end of the second primer directly adjoins to the end of the first primer, leaving no gap in the circle after ligation of the linear PCR product.**

Replication with primers designed this way results in linear plasmids with one changed nucleotide compared to the template introduced by the primer. To allow the recirculation of the plasmid, the primers have to be phosphorylated. For that purpose 5  $\mu$ l of 100  $\mu$ M primer were mixed with 5  $\mu$ l kinase reaction buffer (NEB), 2  $\mu$ l 25 mM  $\text{MgSO}_4$ , 1  $\mu$ l 100 mM ATP, 1  $\mu$ l T4 polynucleotide kinase (NEB) and water to a final volume of 50  $\mu$ l. The preparation was incubated at 37°C for 1 hour and the enzyme was deactivated during 20 min at 65°C. 1.8  $\mu$ l of the phosphorylated forward primer and 2.6  $\mu$ l of the phosphorylated reverse primer were mixed with 100 ng template DNA (plasmid pCDM8-ICAM1), 5  $\mu$ l 5x pfu polymerase buffer (Promega), 1  $\mu$ l 10 mM dNTP mix (Promega), 1  $\mu$ l pfu polymerase (Promega) and  $\text{H}_2\text{O}$  to a total volume of 50  $\mu$ l. The PCR program consisted of 2 minutes at 95°C, 25 cycles of 1 min 95°C, 45 s 55°C, 22 min 72°C, followed by a final elongation step for 10 min at 72°C. After checking 5  $\mu$ l of the preparation on an agarose gel, the original template was digested by addition of 2  $\mu$ l of DpnI and incubation at 37°C for 1 hour. Finally, the linear PCR products were ligated to again form circular plasmids by mixing 2  $\mu$ l of PCR product with 0.5  $\mu$ l 10x T4 DNA ligase buffer (NEB), 0.5  $\mu$ l T4 DNA ligase (NEB) and 2.3  $\mu$ l  $\text{H}_2\text{O}$  and incubating it overnight at ambient temperature.

### **Production of competent MC1061/P3 bacteria:**

P3 is a low copy number, 60 kb plasmid that carries the drug resistance genes for kanamycin (Kan), tetracycline (Tet), and ampicillin (Amp), whereas only the Kan gene is fully active and can be used for selection of the P3 helper plasmid. The Tet and Amp genes carry amber mutations which have to be suppressed to render the resistance markers

active. Some expression vectors, e.g. pCDM8, do not contain any resistance genes themselves, but the suppressor F (supF) gene. Bacterial strains transformed with both, P3 and pCDM8, are therefore resistant to Kan, Tet and Amp. Since the rate of spontaneous reversion associated with the amber mutants is quite high, there should always be used the double selection Tet and Amp. It should be noted that the growth rate of the genetically modified MC1061/P3 can be quite low.

To find a single colony which has not lost the P3 helper plasmid, a few  $\mu\text{l}$  of a fresh MC1061/P3 suspension were spread on an agar plate + 40  $\mu\text{g/ml}$  Kanamycin and incubated overnight at 37°C. 25 single colonies were picked, numbered and patched on a plate + 10  $\mu\text{g/ml}$  Tet, a plate with 50  $\mu\text{g/ml}$  Amp and a fresh Kan plate. After incubation at 37°C overnight, a single colony from the Kan plate was picked which did not grow on either Amp or Tet and used for inoculation of 5 ml LB + 40  $\mu\text{g/ml}$  Kanamycin. After overnight growth in a 37°C shaker, 1 ml of the suspension was used for inoculation of 200 ml LB + 40  $\mu\text{g/ml}$  Kanamycin. It was further incubated until an  $\text{OD}_{600}$  of about 0.25-0.3 was reached. The culture was chilled on ice for 15 min and distributed to 50 ml tubes. Also 0.1 M  $\text{CaCl}_2$  solution and 0.1 M  $\text{CaCl}_2$  plus 15% glycerol were precooled on ice. The cells were centrifuged for 10 min at 3300 g at 4 °C. The supernatant was removed and the pellets resuspended in 4x 20ml cold 0.1 M  $\text{CaCl}_2$ . Incubation for 30 min on ice was followed by another round of centrifugation like above. The cell pellets were resuspended in 12 ml 0.1 M  $\text{CaCl}_2$  solution plus 15% glycerol and distributed in 300  $\mu\text{l}$  aliquots, which were frozen in liquid nitrogen and stored at -80°C.

### 3.3 V33333 receptor production

#### Growth of transformed DH5 $\alpha$ 1 bacteria:

8 liter LB medium were prepared by dissolving 25 g/l LB powder in dH<sub>2</sub>O and having it autoclaved. After autoclavation 100  $\mu\text{g/ml}$  ampicillin (Amp) were added. An overnight culture was prepared by inoculation from a pMALc2b-MBP-V33333-His<sub>6</sub> transformed DH5 $\alpha$ 1 glycerol stock of 200 ml LB-Amp. 800 ml culture were prepared and shaken over night at 37°C. 100 ml were used for inoculating 1 L of fresh LB-Amp, for further growth the bacteria were kept at 32°C on a 130 shakes/min shaker.

#### Induction of protein expression:

After reaching an  $\text{OD}_{600}$  of 0.7 as determined by an Eppendorf BioPhotometer, protein expression was induced by adding IPTG (peqlab) to a final concentration of 0.3 mM. Expression was performed at 32°C over night, since slower protein expression yields higher quality proteins.

**Protein isolation:**

Bacteria were pelleted by centrifugation at 4200 rpm, 4°C for 20 min in a Megafuge 1.0R (Heraeus Instruments) centrifuge. All pellets were combined and resuspended in 150 ml TBSC buffer (25 ml Tris buffer pH 7.5, 30 ml 5 M NaCl, 10 ml 1 M CaCl<sub>2</sub>, 935 ml dH<sub>2</sub>O plus 10 mM CaCl<sub>2</sub>, autoclaved). Bacteria were broken by 3x 30 s ultrasonication in a Bandelin Sonopuls HD200 on ice and centrifuged at 17000 rpm for 30 min in a Sorvall RC5C centrifuge employing a Sorvall SS43 rotor. The soluble protein-containing supernatant was transferred to a new tube and supplemented with 25 µl / 50 ml protease-inhibitor Leupeptin. It was stored at 4°C over night. Ni-NTA slurry was used to pack a column, which was then washed with 5 column volumes TBSC (1 column volume = 10 ml) before applying the supernatant. Unspecific bound protein was washed away with 10 column volumes of TBSC + 10 mM Imidazole. The V33333 receptor carries a His<sub>6</sub>-tag which binds specifically to Ni-NTA. It was eluted with 6 column volumes TBSC + 250 mM Imidazole, the first 5 ml flow through were collected separately because it could be expected that they still contained contaminating protein. See Figure 3-5 for the binding chemistry between Ni<sup>2+</sup> and the histidines of the His<sub>6</sub>-tag and how Imidazole competes with the amino acid for binding sites during elution of the protein.

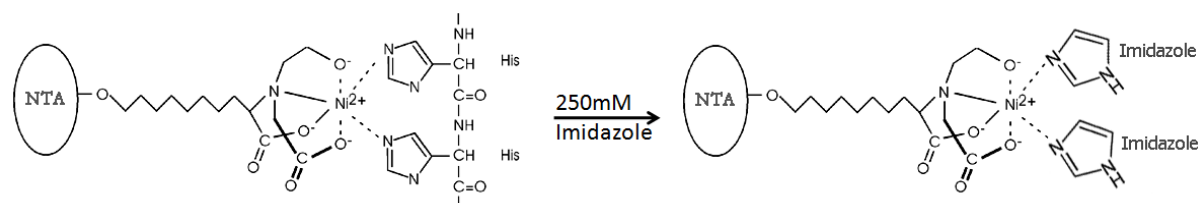


**Figure 3-5.** Histidine residues of a His<sub>6</sub>-tag coordinated to the Ni<sup>2+</sup> of Ni-NTA (left), and their replacement by 250 mM Imidazole (right). Scheme was modified from <http://pages.usherbrooke.ca/bcm-514-bl/5e1.html>.

**SDS PAGE:**

10 µl of each elution fraction were checked on a 15% SDS PAGE gel for content of receptor protein (around 68500 Da) and impurities. A 15% SDS PAGE gel consisted of a resolving gel (1.25 ml 4x buffer: 0.5 M TrisHCl pH 6.8 0.4% SDS, 1.25 ml dH<sub>2</sub>O, 2.5 ml acrylamide, polymerized with 25 µl 10% APS and 2.5 µl TEMED) and a 4.5% stacking gel (1.5 ml stacking gel mixture [consisting of 1.25 ml 4x buffer, 3 ml H<sub>2</sub>O and 750 µl acrylamide], polymerized with 25 µl APS, 2.5 µl TEMED). Samples were mixed 1:1 with a 2x reducing sample buffer and heated to 95°C for 5 min. Constant 25 mA per gel were applied for running. The finished gel could be protein stained with coomassie blue by incubation in a staining bath for 5 min and then destaining in hot water.



**Concentration of protein by spin column:**

The membrane of Centriprep columns (Amicon Inc.) with a molecular weight cut off (MWCO) of 30 kDa was wetted with TBSC and a short round of centrifugation. The sample was spun at 2000 rpm, 4°C, until the desired concentration of the sample was reached.

**Dialysis including redox system:**

The dialysis tube had a MWCO of 6-8 kDa which allowed the diffusion of Imidazole. It was pre-wet in dH<sub>2</sub>O, one side was closed with a clamp, the sample was filled in and it was given some air and space before closing with a second clamp, so it would float and be able to expand with the influx of water. It was placed into a beaker containing 5 l TBSC buffer + 1 mM Cystamin + 10 mM Cysteamin. The receptor needed the redox system (Cystamin – Cysteamin) for at least 2 days at 4°C for correct folding. Dialysis was allowed for at least 3 hours or overnight at 4°C under constant slow stirring before replacement of the buffer. It was repeated with fresh buffer 5 times which would give a total dilution of Imidazole of 1:1250.

## 4 Results

### 4.1 Minor group receptor expression

For the specific attachment of HRV2 to the nanocontainer membrane a recombinant receptor was expressed. The recombinant MBP-V33333-His<sub>6</sub> is a soluble, high affinity HRV minor group receptor construct derived from the VLDLR. The virus binding domain 3 had been concatemerized to give 5 repeats and therefore especially high binding affinity and it had been attached to a MBP on the N-terminus for better solubility and a His<sub>6</sub>-tag for attachment to Ni<sup>2+</sup> on the C-terminus [25]. MBP-V33333-His<sub>6</sub> receptor was expressed in bacterial culture from a previously produced pMALc2b-VLDLR33333 plasmid [25] already transformed into Top10 E.coli. To recover the receptor protein from the supernatant of the broken cells, it was purified on a Ni-NTA column. NTA offers 4 metal ion binding sites with only little ion leaching, ensuring such tight binding of the protein that harsh buffers are not enough for elution. Therefore the column was washed with TBSC + 10 mM imidazole to remove all non-specific contaminants and eluted with TBSC + 250 mM imidazole. Imidazole, a metal complexing agent, is a competitor of the His<sub>6</sub>-tag and pushes the histidines out of the Ni<sup>2+</sup> binding site (see Figure 3-5). Eluted material was collected in 6 fractions which were then checked on a 15% SDS-PAGE (see Figure 4-1) for concentration and the presence of impurities.

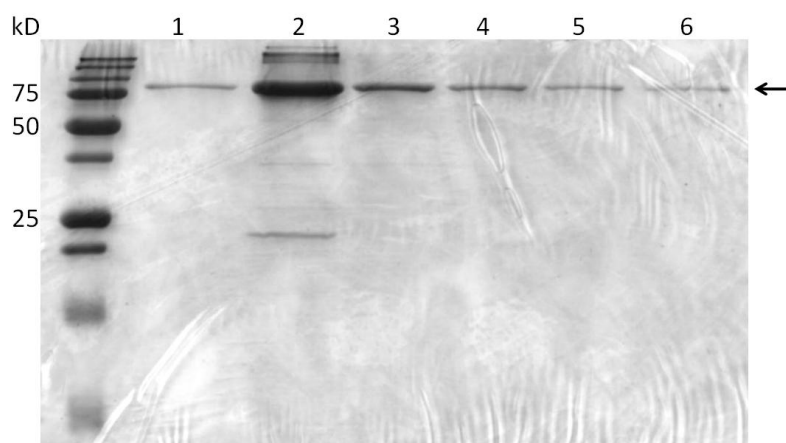


**Figure 4-1. SDS PAGE gel showing elution fractions of MBP-V33333-His<sub>6</sub> eluted from a Ni-NTA column with 250 mM imidazole. Highest 72 kDa receptor (arrow) concentration can be found in fraction 2, which also contains higher molecular weight material, presumably oligomers.**

The 72 kDa receptor protein was mainly found in the second fraction, but also the other fractions showed detectable bands of protein. Fraction 2 also contained visible amounts of higher and lower molecular weight impurities which are probably cellular proteins with a native poly-histidine-tag or oligomers of the V33333 protein. The amount of unspecific proteins was considered neglectable compared to the concentration of V33333, so all fractions were combined and dialyzed several times against five liters of TBSC + 1 mM

Cystamin + 10 mM Cysteamine, a redox system, to reduce the amount of imidazole in the buffer to about 5.8  $\mu$ M, otherwise the imidazole would have inhibited the binding reaction of the receptor protein to the Ni-DGS-NTA of the liposomes. The protein concentration was increased to 2.4 mg/ml.

Binding capacity of the new receptor preparation to HRV2 was checked via CE. Figure 4-2 shows the electropherograms of HRV2 and the freshly prepared MBP-V33333-His<sub>6</sub> at different molar ratios. The complex of receptor and virus formed a shifted peak which drew matter from the peaks corresponding to its individual components. A 1:1 ratio consumed all receptor and gave a small peak for the complex. Application of a 1:12 ratio, which supposedly saturates all receptor binding sites of HRV2, reduced the peak of free virus strongly and at the same time produced several peaks for virus-receptor complexes, apparently created by complexes with differing numbers of bound receptor. The same pattern had already been shown by Konecsni [25]. Also a small share of unbound receptor appeared, this might be due to dysfunctional virus-binding sites of some receptor molecules. Employing an excess of receptor in a 1:18 virus:receptor ratio gave one large peak for the complex, probably with saturated binding sites, all virus was consumed and some receptor stayed unbound.

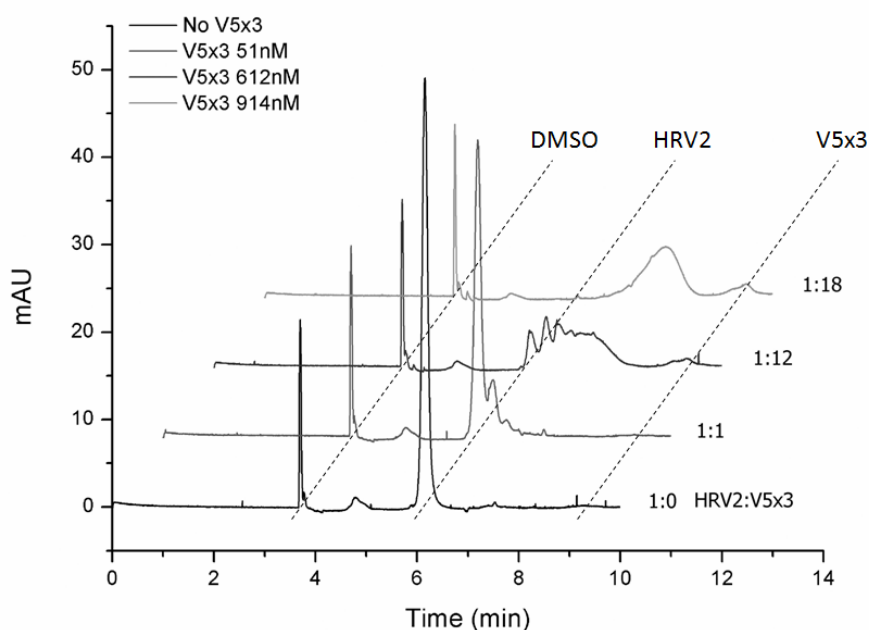


**Figure 4-2.** Electropherograms of virus and freshly expressed receptor V33333 at different molar ratios, detected with UV at 205 nm in CE. BGE: 100 mM borate buffer, 10 mM Thesit, pH 8.3; sample buffer: benzoic acid in 100mM borate buffer, pH 8.3; separation conditions: 25kV, 20°C. Saturation of all 12 binding sites on the viral capsid requires a slight excess of receptor to compensate for dysfunctional molecules, at a molar ratio of 1:18 HRV2:V33333 all virus is saturated with receptor.

## 4.2 Major group receptor cloning

Up to now, the nanocontainer system had only been used with the minor group virus HRV2 and the corresponding recombinant receptor derived from the LDLR family. Since there is a great functional variety between the more than 100 serotypes, especially between major and minor group viruses (differences are described in section 2.2.4), it is not possible to study just one serotype and apply the results gained from that insight on all other serotypes. HRV2 is used as a model for viral infection via the LDLR family of the minor receptor group, the totally different viral infection pathway of the major receptor group via ICAM-1 might be explored with HRV14 as a model. But for these studies the nanocontainer system has to be adapted to major group viruses, which means that the recombinant MBP-V33333-His<sub>6</sub> receptor has to be replaced by a recombinant ICAM-1 receptor. ICAM-1 consists of 5 Ig-like domains, a transmembrane domain and a cytoplasmic domain. For employment of the major group receptor ICAM-1 in the nanocontainer system and in other experiments, it is necessary to make the receptor, originally a hydrophobic transmembrane protein, soluble by cutting off the cytoplasmic and transmembrane domains and adding a His<sub>6</sub>-tag for attachment of the receptor to nickel-DGS-NTA. The gene encoding the major group receptor ICAM-1 was purchased from Addgene. It came inserted in the plasmid pCDM8, a 4356 bp vector (see Figure 4-3).

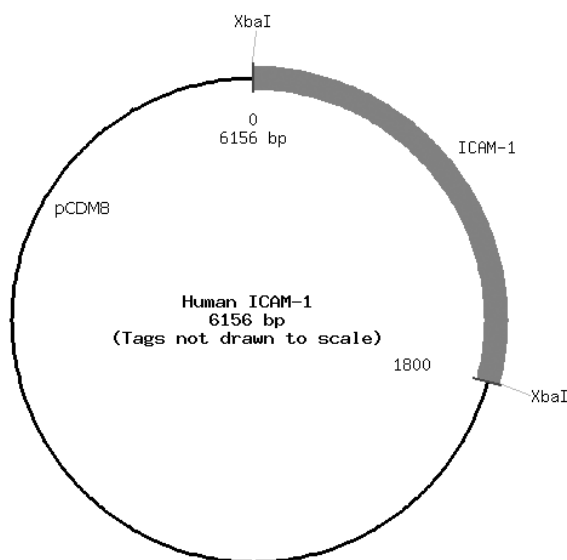


**Figure 4-3.** Plasmid map of pCDM8-ICAM1 as provided by the plasmid source Addgene. The ICAM-1 encoding gene is flanked by two XbaI restriction sites and has a total length of 1800 bp. Map provided by Addgene Inc., Cambridge, MA, USA.

The binding site is situated in the Ig-like domain 1, the full 5 domains keep the virus at quite a distance from the plasma membrane of the host cell and would do so with the liposomal surface in the nanocontainer system. Hence it was decided to produce the receptor in two distinct versions, once full length consisting of all 5 Ig-like domains, and

another version containing just the Ig-like domains 1 and 2. The shortened receptor was intended to keep the virus at a shorter distance from the liposomal membrane and therefore facilitate the RNA transfer into the nanocontainers, in case the full length receptor would function only weakly. *In vivo*, ICAM-1 undergoes several posttranslational modifications. The glycosylations are important for the hydrophilicity of the receptor. The recombinant receptors have to be produced in eukaryotic cells to render the posttranslational glycosylation possible, prokaryotic cells have no mechanism for that. Instead of glycosidic residues it is also possible to add a maltose binding protein (MBP), which aids the solubility of the receptor as well. However, it has to be taken care that the MBP does not inhibit the receptor-virus interaction. Adding it to the recombinant ICAM-1 Ig-1 domain would most certainly interfere with viral interaction, therefore it can only be attached during expression in bacterial suspension and has to be cleaved off via a factor Xa cleavage site before applying it to the nanocontainer system or subjecting it to other virus-interacting experiments.

Therefore, two possibilities for receptor protein expression were considered: fast prokaryotic expression of the protein adjoined to MBP in bacterial suspension and subsequent cleavage of MBP or eukaryotic expression of the receptor protein in mammalian cell culture. It was thus intended to clone 4 different ICAM-1 receptors: ICAM-D5-His<sub>6</sub> for expression in eukaryotic cells (see Figure 4-4 A), ICAM-D2-His<sub>6</sub> also for expression in eukaryotic cells (Figure 4-4 B), MBP-ICAM-D5-His<sub>6</sub> for expression in bacteria (Figure 4-4 C) and MBP-ICAM-D2-His<sub>6</sub> also for expression in bacteria (Figure 4-4 D). Each expression route made a different cloning strategy into different vectors necessary.

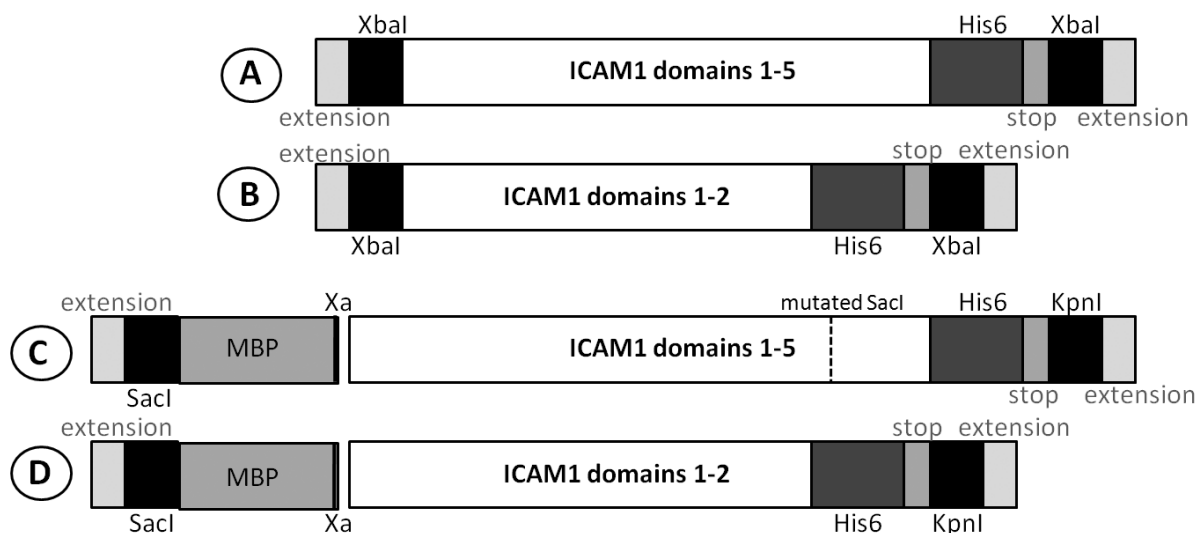


**Figure 4-4. Schemes of the truncated ICAM-1 genes ready for integration into a plasmid for expression in eukaryotic cells (A+B) and in prokaryotic cells (C+D). A+B are flanked on both sides by restriction sites for XbaI and short genome extensions for proper enzyme function. The 3' ends are linked to a His<sub>6</sub>-tag and a stop codon. C+D are flanked by a SacI site on the 5' end and a KpnI site on the 3' end. The SacI site is situated within MBP, hence it is followed by the C terminus of MBP which can be cleaved off of the ICAM1 protein via an Xa cleavage site.**

## Results

The *SacI* site within ICAM1 domain 5 is mutationally silenced. The 3' ends are also linked to a His<sub>6</sub>-tag and a stop codon.

### bacterial expression strategy:

For protein expression in bacteria, the intention was to use the expression vector pMALc2b, the same vector that had been successfully used for V33333 expression and already contained the DNA encoding MBP (note Figure 4-5 for an overview of the cloning steps).

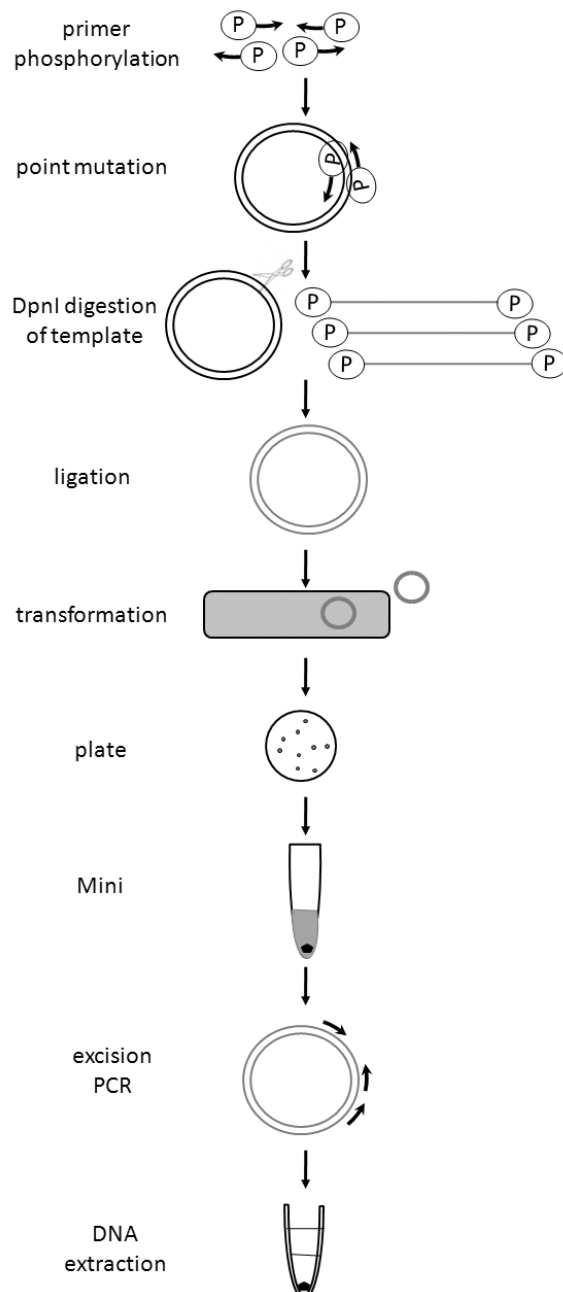


**Figure 4-5. Scheme of the cloning strategy for truncated ICAM-1 expression in bacterial cells.** Primers were phosphorylated prior to mutational PCR, the template plasmids were digested after *SacI* restriction site mutation with DpnI. Linear mutagenized amplicons were religated and the plasmids transformed into MC1061/P3. Single colonies were picked and used for Mini prep plasmid DNA isolation. Domains 1-2 and 1-5 of the *SacI* mutated ICAM-1 were excised and amplified via PCR with primers which added a *SacI* restriction site and part of MBP on the 5' end and a His<sub>6</sub>-tag and a *KpnI* restriction site at the 3' end and the DNA was purified in a chloroform-phenol-extraction.

To cut out the gene for V33333 of the vector pMALc2b, the enzyme *SacI* would have been the best suitable, except for another *SacI* restriction site present within the ICAM-1 gene. Therefore the first step was to introduce a translational silent point mutation into this *SacI*

enzyme recognition site GAG CTC. GAG encodes the amino acid glutamic acid, which is also encoded by GAA, hence the second guanine, on position 1602, was exchanged for an adenine which resulted in the same amino acid, glutamic acid, but destroyed the recognition site of SacI. Primers were designed specifically for that purpose: the forward primer spanned 15 nt upstream and 15 nt downstream of the mutation target to allow tight binding despite the mismatch (ICAM\_Sac1\_mut\_1591), the reverse primer was placed in a way that its first nucleotide directly connected to the first nucleotide of the forward primer, leaving no gap between them (ICAM\_Sac1\_mut\_1590b) (Figure 3-4). Primers were phosphorylated to later allow the ligation of the produced linear plasmid and used in a mutagenizing PCR. Template plasmids were digested with DpnI to ensure that only mutagenized ICAM-1 would be used in the further cloning steps. Linear plasmids were recircularized with DNA ligase and transformed into MC1061/P3 E.coli. Several colonies were picked from the Amp + Tet plate and used for Mini preps. Isolated DNA was checked via SacI restriction digest to ensure that the SacI site within the gene for ICAM-1 was inactive. Figure 4-6 shows the result of the restriction digest of the mutated clones and the non-mutated starting plasmid for comparison. Only one of the clones (lane 5) had been cut twice and hence gave bands at 4500 and 1650 bp like the non-mutated plasmid, all other clones had only been restricted once, proving that the mutation of SacI within ICAM-1 had been successful.

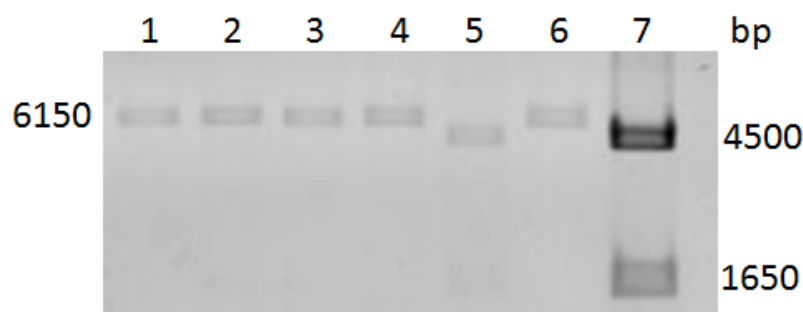


**Figure 4-6.** Agarose gel of 6 clones containing a SacI mutated pCDM8ICAM1 plasmid and a non-mutated control plasmid, digested with SacI. The total plasmid size was 6150 bp, all clones except one met the expected size since they had only 1 SacI restriction site left. The non-mutated control (lane 7) and clone 5 were cut twice by SacI and gave the 2 expected bands for 1650 and 4500 bp. Clone 3 was used for further experiments.

Specifically designed primers were used in PCR to excise domains 1-2 and 1-5 of clone 3 ICAM1mutSacI. The forward primer also added a SacI restriction site and the C-terminal part of MBP until cleaving factor Xa (see Figure 4-4, C and D). This part will be lost when V33333 is cut from the vector pMALc2b with SacI and KpnI. Adding it directly to the new insert will restore the full MBP and the cleavage factor upon ligation of the insert into the truncated vector. Reverse primers added a His<sub>6</sub>-tag and a stop codon to the end of the

### Results

---

truncated ICAM-1 and introduced a restriction enzyme recognition site for KpnI. The amplicon was purified via Phenol-Chloroform-Isoamylalcohol extraction.

At that point the bacterial expression strategy was abandoned in favor of the eukaryotic expression strategy, which was considered to have a higher probability of success. In case the eukaryotically expressed receptor proves to be dysfunctional or not soluble enough, it is still possible to return to the bacterial expression strategy and continue the cloning of that receptor construct by digesting the SacI-mutated ICAMmutSacI (isolated and amplified via PCR with the primer forward ICAM\_SacI\_Xa\_401 and the primers reverse ICAM\_D5\_KpnI\_1759b or ICAM\_D2\_KpnI\_898b, to gain a full length and a shortened version of ICAM-1, respectively) and the pMALc2b-MBP-V33333-His<sub>6</sub> backbone with the enzymes SacI and KpnI. The vector pMALc2b-V33333 and the inserts ICAM1mutSacI-D2 and ICAM1mutSacI-D5 are ready for further usage. After separating the backbone fragment from the old insert via an agarose gel, it can be ligated with the inserts and amplified in Top10 E.coli. After confirming a correct clone via sequencing, the plasmid can be used for protein expression in bacteria.

#### **eukaryotic expression strategy:**

It was planned to excise the desired domains of the ICAM-1 gene from its vector by PCR, add a His<sub>6</sub>-tag, a stop codon and new restriction sites in the same process and religate it back into pCDM8 for larger scale replication in E.coli. The purified plasmid could then be used for protein expression in eukaryotic cells. The sequence of the cloning steps performed is depicted in Figure 4-7.



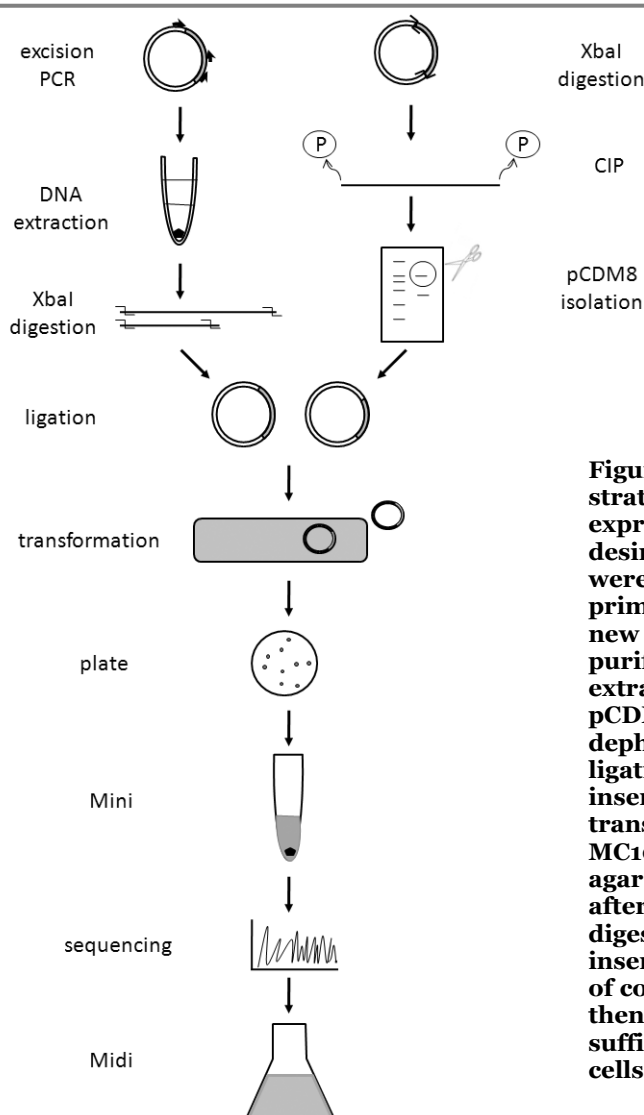


**Figure 4-7.** Scheme of the cloning strategy for truncated ICAM-1 expression in eukaryotic cells. The desired domains 1-2 and 1-5 of ICAM-1 were excised and amplified with primers which added a His<sub>6</sub>-tag and new XbaI restriction sites, the DNA was purified via chloroform-phenol-extraction. In parallel, the vector pCDM8 was isolated with XbaI and dephosphorylated to prevent auto-ligation of the empty vector. D2 and D5 inserts were ligated with the vector and transformed into competent MC1061/P3. Single colonies from the agar plate were used for Mini preps, after screening them by restriction digestion and PCR, sequencing of the insertion area allowed the identification of correctly cloned plasmids which were then amplified in a Midi prep to have sufficient material for transfection of cells.

First, primers were designed for the excision of the domains 1-2 and 1-5. Primer sequences can be found in the primer index (see 8.2). Requirements of well designed primers include a minimal length of 15 binding nucleotides, a melting temperature of at least around 60°C, a Guanine or Cytosine as last nucleotide and no unspecific binding, neither to the template nor its reverse complement strand. Binding of the primer was checked via the program “Bioedit Sequence Alignment Editor” (available at <http://www.mbio.ncsu.edu/BioEdit/bioedit.html>). The forward primer consisted of 4 nucleotides in addition to the recognition sequence for the XbaI restriction enzyme and a pCDM8 complementary region at the beginning of the ICAM-1 gene (ICAM\_pCDM8\_2197) (see primer index 8.2). Two different reverse primers were necessary for cutting once after domain 2 and another time after domain 5. These primers consisted of an ICAM-1 complementary region at the end of domain 2 and 5, respectively, plus a His<sub>6</sub>-tag, a stop codon, the XbaI restriction site and some random nucleotides as extension for the enzyme binding (ICAM\_D2\_Xba1\_898b, ICAM\_D5\_Xba1\_1795b).

**Results**

After excising and amplifying the truncated ICAM-1 genes via PCR, the DNA was purified twice via Phenol-Chloroform-Isoamylalcohol extraction and then treated with XbaI enzyme to get sticky ends. Also, 2.3µg of the pCDM8ICAM1 vector were treated with XbaI to produce an empty backbone, which was then treated with Alkaline Phosphatase for prevention of autoligation. To separate the backbone from the full ICAM1 insert, it had to be applied to an agarose gel, so the band for the backbone could be excised and the DNA purified. The empty backbone pCDM8 and the truncated ICAM1 were religated via the XbaI sites. After heat-shock transformation of the plasmid into competent MC1061/P3, cells which contain the helper plasmid P3, numerous colonies appeared on the Amp + Tet plates. Mini preps of several colonies were prepared and the plasmids were checked after XbaI restriction digestion on an agarose gel to see if the plasmid really contained the desired insert. Bands, in particular the one for the insert, were hardly visible due to the low amount of DNA, so the presence and length of inserts was additionally checked via PCR. Primers, which had been designed to bind to pCDM8, flanking the ICAM1 inserts about 50 nt upstream and downstream of the XbaI restriction sites, respectively, (pCDM8\_2130sequ, pCDM8\_2692sequ\_b), were used.

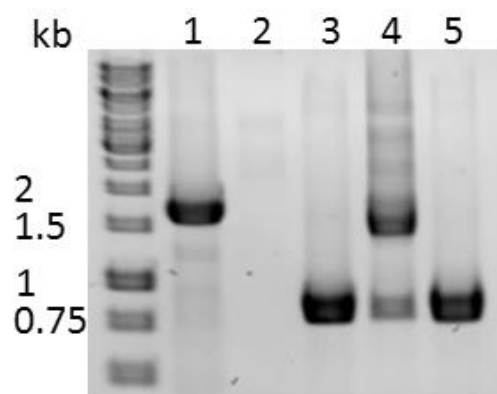


**Figure 4-8. Agarose gel of ICAM1-D5 and ICAM1-D2 inserts from several clones amplified with PCR primers whose amplicon spans the whole inserted region. ICAM1-D5 shows the expected insert size of approx. 1600 nt (lane 1); there was no insert in the clone 1 of ICAM1-D2 (lane 2), the clones 2 and 4 showed the expected insert size of approx. 750 nt (lane 3 and 5), clone 3 contained a double-sized insert (lane 4).**

Figure 4-8 illustrates that some plasmids showed the correct insert length of 1600 bp for ICAM1-D5 (lane 1) and 750 bp for ICAM1-D2 (lanes 3 and 5). Lane 4 contains a band for a much longer product with double the size of ICAM1-D2. Since XbaI was used on both sides, several inserts could ligate as concatemers into the backbone. Plasmids with the correct insert size were sent to sequence analysis with the same primers as for the above mentioned control PCR (pCDM8\_2130sequ, pCDM8\_2692sequ\_b). Pairwise alignment of the sequenced plasmids with pCDM8 and ICAM1 in “Bioedit” made the exact cloning product visible. Another problem caused by the two XbaI sites was found: the insert could also ligate in the reverse direction (Figure 4-8 lane 3). Luckily, one clone each was found

(ICAM1-D5 from lane 1 and ICAM1-D2 from lane 5) which proved to carry the correct insert (check 8.3.2 and 8.3.3 for sequences) and could be further used. Additionally, a point mutation in the ICAM-1 gene was identified (see plasmid sequence of pCDM8-ICAM1-D5-His<sub>6</sub> in section 8.3.3 for position): many published sequences (e.g. NCBI accession number NM\_000201) have an A at the questionable position, sequencing of the cloning product and the first plasmid sample isolated from the purchased pCDM8ICAM1 plasmid resulted in a G at the same position. Probably, already the originally purchased plasmid pCDM8ICAM1 had carried that mutation. The original AA coding triplet GCA is translated into an alanine, the mutated tripled GCG does not change the translational product. Although most published sequences refer to an adenine, also sequences containing the guanine have been published [37] (EMBL X06990). Since it was a silent mutation, no further attention was paid to it.

A total of 315 µg of the plasmid pCDM8-ICAM1-D2-His<sub>6</sub> and 303 µg of the plasmid pCDM8-ICAM1-D5-His<sub>6</sub> were produced via amplification in MC1061/P3 and purified to a 260/280 absorbance ratio of above 1.8 which is a purity high enough for transfection of eukaryotic cells (measured by NanoDrop). Maps are depicted in Figure 4-9 and the sequences can be found in the appendix 8.3. Transfection into eukaryotic cells like CHO can be either transient to check the functionality of the receptor or stable to directly go for high yield production.

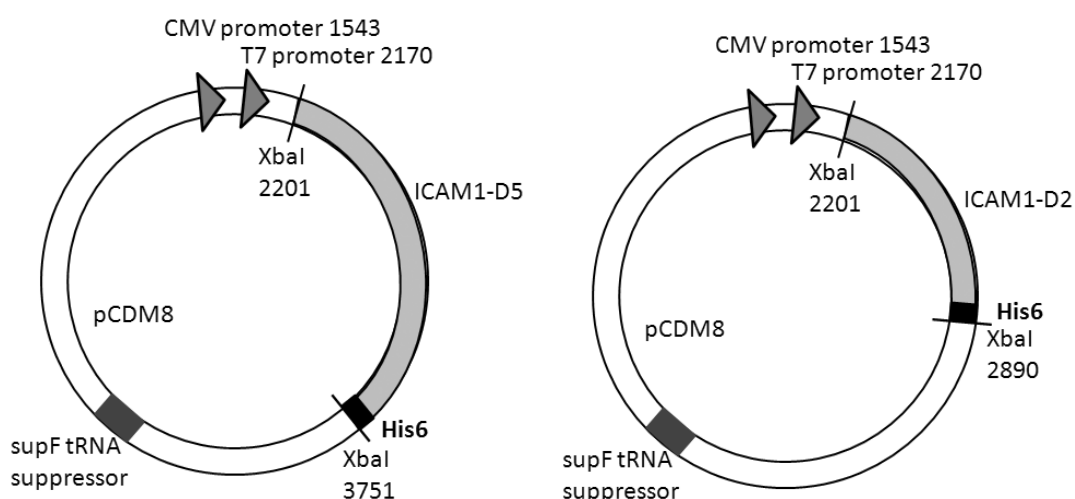


**Figure 4-9.** Plasmid maps of the cloned ICAM1-D5 (left) which is cut off after the domain 5 and ICAM1-D2 (right) which is cut off after the domain 2 of ICAM-1 and have therefore lost their transmembrane and cytoplasmic regions. Both have a His<sub>6</sub>-tag attached to the 3' end and are flanked on both sides with an XbaI restriction site.

Due to time limitations and focus on experiments with minor group viruses further conduction of soluble ICAM1 expression had to be halted.

### 4.3 RNA transfer through liposomal membranes

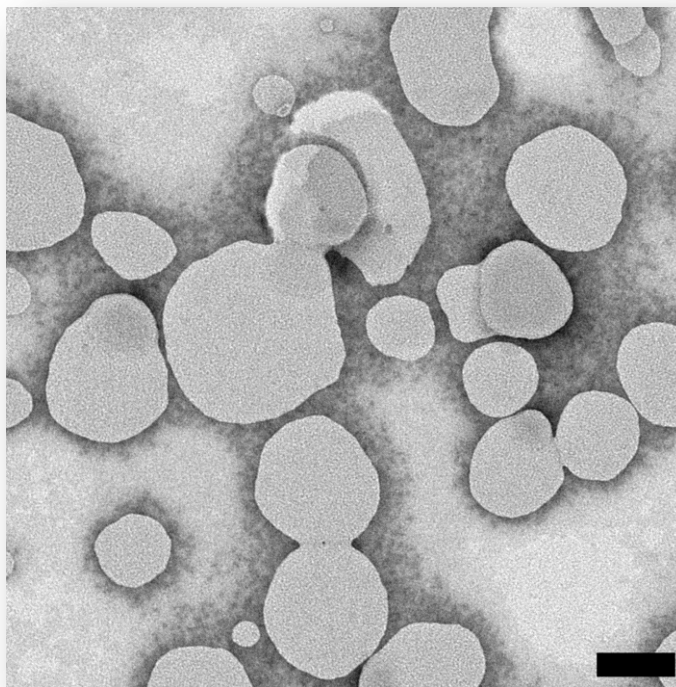
#### **nanocontainer construction:**

For production of nanocontainers, 5  $\mu\text{mol}$  in chloroform solubilized lipids consisting of 20 mol% POPC, 20 mol% PE, 20 mol% SM, 30 mol% cholesterol and 10 mol% Ni-DGS-NTA, in case of flotation experiments also 1 mol% NBD-PC was added for each preparation. The dry lipid film was rehydrated with 300  $\mu\text{l}$  RT mix for 2 hours to give a multilamellar vesicle (MLV) stock of 17 mM total lipid concentration.

The MLV stock was subjected to extrusion through a polycarbonate membrane with 400 nm pore size. Passing it through 41 times, the liposomes were ripped apart and reformed at diameter sizes  $\leq 400$  nm as large unilamellar vesicles (LUV). The use of freshly prepared lipid stocks and elimination of air bubbles inside the syringes ensured good quality of the liposomes.

Prior to their application, LUVs had to be purified to remove non-encapsulated RT mix. This ensured that only RNA which had been transferred across the liposomal membrane was detected, RNA released to the outside buffer could not be transcribed into cDNA and was therefore not detected. For that purpose, liposomes were passed two times through a mini size exclusion chromatography column which retained ions and small molecules and allowed the liposomes to pass through with the buffer. This resulted in dilution of the original LUV stock, especially when Sephadex G-50 medium was used for the mSEC, G-50 fine grade caused a little less dilution. Dilution was standardized at 1:4. The size and shape

**Figure 4-10.** Nanocontainers consisting of 20 mol% POPC, 20 mol% PE, 20 mol% SM, 30 mol% cholesterol and 10 mol% Ni-DGS-NTA, filled with RT mix, extruded to 400 nm and purified with mSEC to exchange the outside buffer to 50 mM Tris 80 mM NaCl pH 8.3. TEM picture was taken at 36k magnification; size bar = 200 nm.



of the purified nanocontainers was checked in EM and is shown in Figure 4-10. All visible

liposomes are about 400 nm or smaller, confirming the efficiency of the extrusion. Also the liposomes appear to be intact and of a healthy round shape.

#### **nanocontainer decoration with receptor:**

To allow specific attachment of minor group HRVs to the liposomal membrane, the nanocontainers have to be decorated with receptor prior to the addition of virus. For each sample, purified liposomes were decorated with the recombinant receptor MBP-V33333-His<sub>6</sub>. It is derived from the VLDLR by taking the virus binding domain 3 and cloning it five times next to each other, flanked by a His<sub>6</sub>-tag for Ni-DGS-NTA attachment and a maltose binding protein (MBP) for better solubility [24, 38]. Ni-DGS-NTA had a share of 10 mol% of the total lipid amount, therefore one sample preparation contained 6.4 nmol Ni-DGS-NTA lipid. 36 pmol receptor were added to the 6.4 nmol Ni-DGS-NTA lipid. Assuming homogenous distribution of the Ni-DGS-NTA lipid across the membrane bilayer, only half of it is presented on the outer liposomal surface, i.e. 3.2 nmol. Consequently, there is almost 90 times more Ni-DGS-NTA present than receptor, ensuring that almost all receptor molecules are bound to the nanocontainer surface. Free receptor is believed to stabilize the virus [39]. When the virus is already bound to liposomes the receptor stabilizes the virion and inhibits the RNA release and transfer across membranes. In solution, the free receptor can saturate all viral binding sites and thereby not only inhibit the uncoating process, but also hinder the attachment of the virion to the liposomal membrane, preventing any possibility of RNA transfer across the membrane. By strongly outnumbering the receptor with Ni-DGS-NTA, this inhibitory effect should be kept to a minimum.

#### **nanocontainer decoration with virus:**

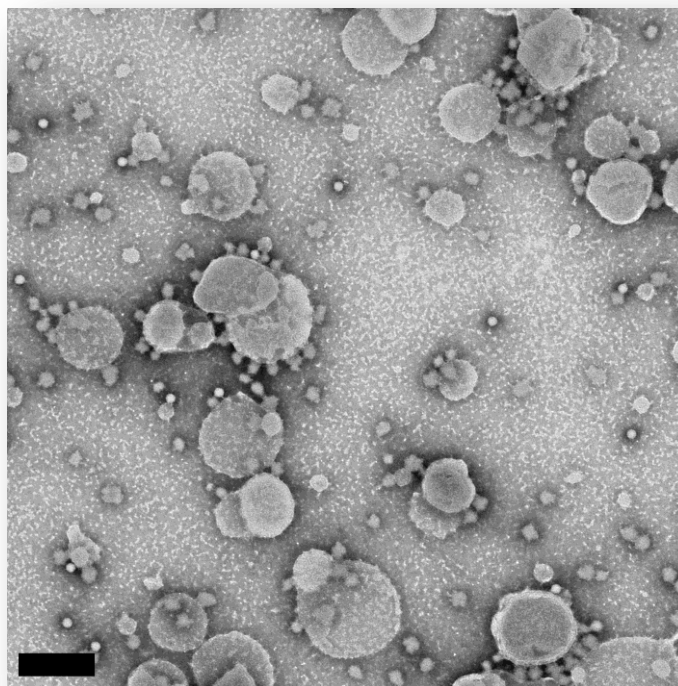
Minor group rhinovirus HRV2 uses LDLR family receptors such as the VLDLR for attachment to the host cell, in the here performed experiments the VLDLR derived recombinant receptor V33333-His<sub>6</sub> was employed. In theory, each virion attaches to up to 12 receptor molecules [25]. Even though it will not use all of these sites it should be bound tightly to the host cell or liposome by one or several receptors. If the virion is using several attachment sites it might fold the membrane around itself, causing invagination. Upon attachment and beginning conversion, the viral particle is thought to insert VP4 and the N-terminus of VP1 into the membrane. Numerous virions doing that next to each other might cause a strong perturbation of the liposomal membrane which could lead to holes and leakage (see discussion 5.3). If too few virions are applied the sensitivity of the assay will not be high enough to detect any RNA at all. Therefore, it is very important to elucidate the best virus concentration which is a trade-off between transferring as much

### Results

RNA into the liposome as possible and not ripping it apart while doing so (see virus dilution series below). Orienting experiments indicated that about  $5.5 \times 10^{10}$  viral particles (corresponds to 91 fmol) had to be used in one sample to get a strong signal by standard RT-PCR.

Since every virus preparation has a different concentration and different percentages of dead and viable virus particles, probably also different amounts of impurities, this concentration has to be determined experimentally with every new virus preparation used. Normally, concentrations between 10 and 500 fmol virus per 64 nmol lipid gave an RT-PCR signal. Virus was diluted in TrisNaCl buffer to the desired concentration, added to the receptor-decorated liposomes and incubated at room temperature for 30 min. The product could be checked in EM. Figure 4-11 shows the high concentration of virus in a standard RT-PCR sample. A lot of virus is denatured, a process which happens most probably during the adsorption of the sample on the grid for EM.

**Figure 4-11.** Standard nanocontainer system sample: purified nanocontainers decorated with receptor and virus (64 nmol lipid, 36 pmol receptor and 91 fmol virus). HRV2 is bound to the liposomal membrane. Native virus appears as well defined white 30 nm large dot. The high amount of broken virus particles (grey dots with undefined border, “popcorn”) is probably caused by the adsorption of the sample to the grid for TEM imaging. Picture was taken at 36k magnification; size bar = 200 nm.



### trigger of RNA release:

During natural infection, rhinovirus virions release their RNA into the cytoplasm of their host cell upon acidification of the endosome they used for entering the cell [40]. That mechanism can also be employed *in vitro* to generate 80S particles. Exposure of native HRV2 to a pH at 5.4 for 15 min resulted in empty virus capsids (80S particles) and externalized RNA [29]. In experiments presented here the pH was lowered by addition of 1M NaAcetat pH 5.0 which resulted in a pH of 5.4 in the sample. Prior experiments had shown that 15 min at pH 5.4, a condition comparable to that prevailing in the interior of

late endosomes, are enough to convert most virions into 80S particles (Pickl-Herk, A., unpublished data). *In vitro* it is also possible to trigger the RNA release at elevated temperature. 10 min at 56°C convert 150S particles of HRV2 to empty 80S particles, given the virus sample is not too concentrated, since a high virus concentration inhibits the full conversion and stops at the intermediate 135S particle [41]. Both methods, pH lowering and high temperature, can be used for triggering the RNA transfer through the liposomal membrane, although it has been found that the pH trigger gives rise to a stronger signal in RT-PCR (data not shown) and is therefore not only more efficient but also the physiologic trigger. After the 15 min at low pH, the samples were reneutralized with 1 M NaOH, except when the sample was intended to be analyzed by EM. Electron microscopy pictures show that the virions stay attached to the liposomes as empty particles after triggering and do not leave the endosomal membrane before reneutralization (see Figure 4-12). The RNA transfer itself does not need the reneutralization, it is completed during the low pH exposure, but reneutralization should ensure that no pH change inhibits the following RT reaction for detection of luminal RNA.

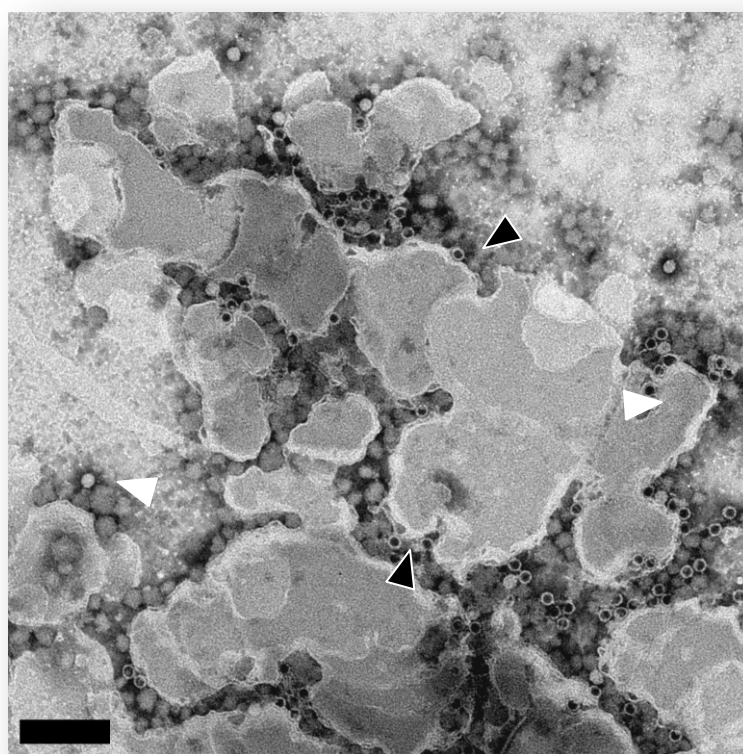


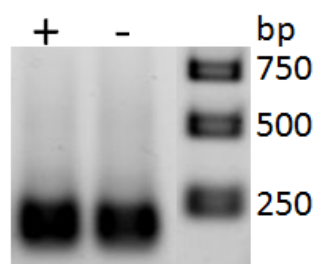
**Figure 4-12.** Nanocontainer system sample (64 nmol lipid, 70 pmol V33333, 91 fmol HRV2) after 15 min at pH 5.4. Most virus particles are converted to 80S particles (light shell with dark core), only very few are still native (full light). TEM picture was taken at 36k magnification; size bar = 200 nm.

### Results

#### reverse transcription without DTT:

Normally, a reverse transcription mixture consists of H<sub>2</sub>O, 5x first strand buffer, reverse primer, dNTP mix, DTT, RNA template, RNasin and reverse transcriptase. For RT liposomes (nanocontainers) this mixture was added to the dried lipid film during liposome production for hydration of the lipid film so liposomes encapsulate the RT mix. Unfortunately, it was noticed that the addition of the mix to the dried lipids POPC, PE, SM, Ch and Ni-DGS-NTA caused a change of color from milky-colorless to orange-brown. To find the responsible component they were added one after the other instead of altogether. The color change happened immediately after the addition of DTT. In a separate experiment DTT also changed the color of NiCl<sub>2</sub> at a slightly alkaline pH. DTT is normally added to break the disulfide bonds of RNases for inactivation and protect the reverse transcriptase from oxidation. Since the final mix also contained RNasin to inactivate ribonucleases, it was decided to try to omit the DTT in the RT mix. No adverse effect was found, the signal for transcribed RNA in RT-PCR was as strong without DTT as with (see Figure 4-13) in an RT mix sample without membranes.

**Figure 4-13. Agarose gel of by PCR amplified RT products transcribed in reaction mixtures with (+) and without (-) DTT. Both yielded strong signals at the expected 200 bp, the RT reaction is not dependent on the presence of DTT.**



#### controls included in RT-PCR:

Once it was found that DTT gave adverse reactions with Ni-DGS-NTA, but could be omitted without reducing the efficiency of the RT reaction, the nanocontainers were produced with the modified RT mix. After receptor and virus decoration, the encapsulated RT mix without DTT was tested for a signal for transferred RNA in RT-PCR (see Figure 4-14, lane 1). This reproducible signal showed that the minimal requirements for RNA transfer were met in the model system set-up. Further characterization of the nanocontainer model system for viral infection required the implementation of several controls. Necessity of different components of the system and steps of the RNA transfer were checked by omitting or changing them. See Figure 4-14 for the RT-PCR signals of the following controls and compare them to the standard sample on lane 1.



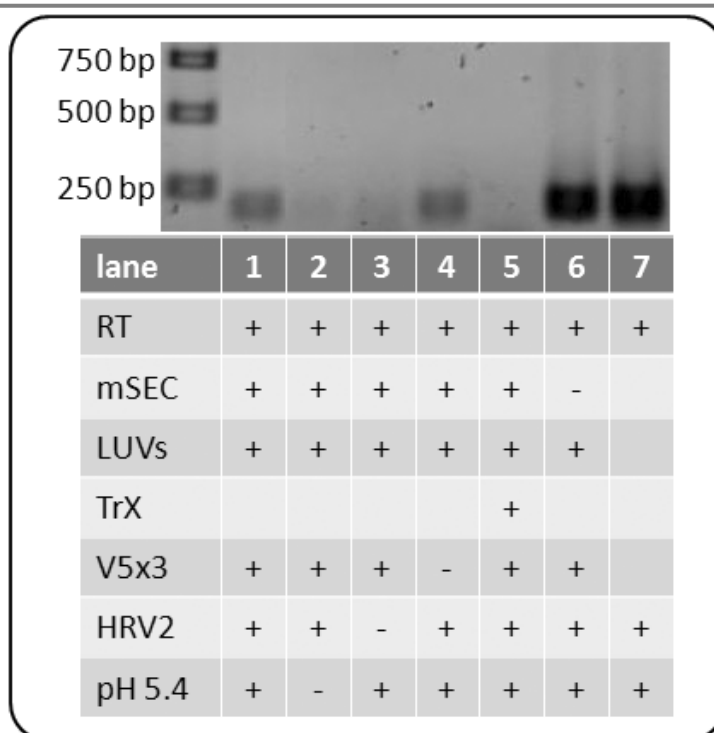


**Figure 4-14.** Agarose gel depicting RT-PCR signals for transferred RNA in nanocontainer system samples. Nanocontainer composition as in Figure 4-10, RT mix was prepared without DTT. Decoration was done with 36 pmol receptor V33333 and 360 fmol HRV2 ( $1.2 \times 10^8$  TCID<sub>50</sub>). RNA release was triggered for 15 min at pH 5.4. Standard sample on lane 1, controls with no RNA release trigger (lane 2), no virus (3), no receptor (4), permeabilized nanocontainers with Triton X-100 (5), nanocontainers not subjected to mSEC purification (6) and an RT mix sample without nanocontainers (7). For a detailed description of the controls note the main text.

To make sure that no contamination of the sample components with traces of nucleic acids would give a false positive signal, one sample was included without any virus. Receptor decorated liposomes were triggered by pH treatment and subjected to RT and PCR reaction. Any signal seen on the agarose gel was considered to be background. Negative control: no virus (Figure 4-14, lane 3) shows that the nanocontainer system does not give a signal without added virus.

RNA transfer takes place *in vivo* inside late endosomes following exposure to a low pH of about 5.6 – 5.4 [42]. This is mimicked in the nanocontainer system by lowering the pH of the liposome surrounding buffer to 5.4 with 1 M NaAc pH 5.0 for 15 min after virus was bound to the receptor. To show the necessity of that trigger for RNA transfer into the liposomes, it was omitted in a control sample. Since the RNA transfer was not induced, there was also no signal seen on the agarose gel. Negative control: no trigger (Figure 4-14, lane 2). A comparable RNA releasing effect is reached by heating the diluted virus to 56°C for 15 min, but a pH trigger is closer to the *in vivo* situation of RNA release and was therefore chosen for the experiments performed here.

Nanocontainers are supposed to only allow transcription of cDNA in their RT mix filled lumen, but not outside. That way, only RNA that had been transferred across the membrane will be detected. Disrupted liposomes will not allow production of cDNA. Components of the RT mix will leak into the surrounding and are therefore missing inside and buffer from the outside will flow into the liposomes and dilute the RT mix. Addition of Triton-X 100 to 1% final concentration disrupts all liposomes and therefore prevents

### Results

---

cDNA production resulting in no PCR product on the agarose gel. Negative control: TritonX (Figure 4-14, lane 5) proves that only intact nanocontainers are capable of cDNA transcription. If they break apart or the RNA is not transferred into their lumen, the RNA will not be transcribed on the outside.

*In vivo*, HRV2 binds to its receptor and is subsequently taken up by the host cell into endosomes. Following the pH decrease, the virion detaches from the receptor and is handed over to the endosomal membrane [43], through which it releases its RNA into the cytosol. Since the liposomes are mimicking the endosome, it is thought that a receptor is necessary to bring the virus close to the membrane before the trigger. The receptor concentrates the virus on the nanocontainers by fishing it from the exterior buffer and holding it close to the membrane. Therefore, when omitting the receptor, no cDNA should be produced because not enough virus particles are bound by chance to the membrane when triggered. However, corresponding experiments still showed strong signals. Negative control: no receptor (Figure 4-14, lane 4) gives a strong signal for transferred RNA. This can be explained by the small sample volume of a standard RT reaction which causes high concentration of liposomes and virus in the sample (visible in Figure 4-12) which increases the probability of virus residing in close proximity of a liposomal membrane at the moment of receiving the trigger for RNA release. Curry et al. [44] showed infection of CHO, murine L and HeLa cells by poliovirus 135S particles without receptor, because 135S particles are hydrophobic and therefore attach to the membrane even without receptor if they are close in the moment of conversion. By externalizing VP4 and the N-terminus of VP1, the 135S particle become hydrophobic and attach to a membrane in close proximity where they can release their RNA into the lumen of the cell.

As demonstrated via flotation experiments, native HRV2 is not able to bind to the plain liposomal membrane by itself. As shown below, receptor is necessary to stably bind the virus to the liposome so that it co-flotates with the liposomes in a sucrose step gradient. When no receptor is present, free native virus and 135S subviral particles, which had not been formed in the presence of the lipid membrane, stay at the high density bottom of the gradient, separated from the liposomes. It is not absolutely mandatory to use the receptor for standard RT-PCR experiments in a small total sample volume of 20 µl, since the virions are close enough to the membranes to bind upon conversion to 135S during low pH exposure. Diluting the sample 10 fold should reduce the probability of close contact by coincidence, but makes the precipitation of cDNA prior to PCR necessary. The small amounts of DNA are easily lost and reproduction of a signal from receptor decorated liposomes in contrast to no signal from plain liposomes was difficult. Therefore, the function of the receptor to concentrate the virus on the liposomal membrane before

triggering the RNA release could not be shown unequivocally, although it is definitely necessary for tight binding of the native virion.

One control sample was included in every run and consisted of all components necessary for reverse transcription, in other words it was a fresh RT mix not encapsulated in liposomes. Triggering RNA release in that sample allowed for 100% cDNA transcription, because no transport across membranes was necessary, all released RNA could be transcribed. In the used set-up, the detection limit was found to be at approximately  $10^5$  virions per RT sample. This sample allowed monitoring of the functionality of the RT and PCR reactions, in case it failed to give a signal there was a problem with the RT or PCR, which explained any simultaneously failed samples. Positive control: RT mix (Figure 4-14, lane 7).

To control the functionality of the encapsulated RT mix without the necessity of RNA transfer the purification step on a size exclusion chromatography column was left out. This resulted in a sample which had the concentrated RT mix not only inside the nanocontainers, but also on the outside. When virus was triggered in that sample, it was not necessary that it was bound to the liposomes and that the RNA was transferred into the liposomal lumen. RNA release somewhere in the sample volume was sufficient to make cDNA transcription possible and therefore resulted in a signal on the agarose gel. Only if the RT mix was not functional, for example due to aged transcriptase, the sample would fail to give a signal. In that way it was possible to exclude the risk of interpreting no signal as the result of no RNA transfer into the liposomes. Positive control: no mSEC (Figure 4-14, lane 6) ensured that the encapsulated RT mix worked properly. The saturated signal was comparably to the positive control on lane 7, since in both controls all RNA released from the virus somewhere in the sample could be transcribed into cDNA. This control showed no decline of enzyme activity due to storage, indicating that the aging of the enzyme was not a very fast process. Therefore nanocontainers could be stored for several days up to weeks without losing their functionality.

#### **virus dilution series:**

Absolute values of cDNA production were subject to a strong variation depending not only on directly influenceable parameters like pipetting accuracy but also on parameters which are difficult to control like the age of the liposomes or the virus preparation used. Especially the aging of the enzyme reverse transcriptase, normally demanding storage at  $-20^{\circ}\text{C}$  but inside the liposomes it can only be kept at  $4^{\circ}\text{C}$ , had a big influence. Freshly prepared liposomes always gave the strongest signal which decreased with every day the liposomes grew older until it became not only weak but also unreliable. Nevertheless, the general picture was reproducible, i.e. some samples with a middle virus concentration

### Results

gave a stronger signal compared to higher and lower virus concentrations of the same dilution series experiment. A dilution series of virus with constant amounts of lipid and receptor was repeated many times and revealed a consistent trend. Two gels are shown which were produced on consecutive days (Figure 4-15).

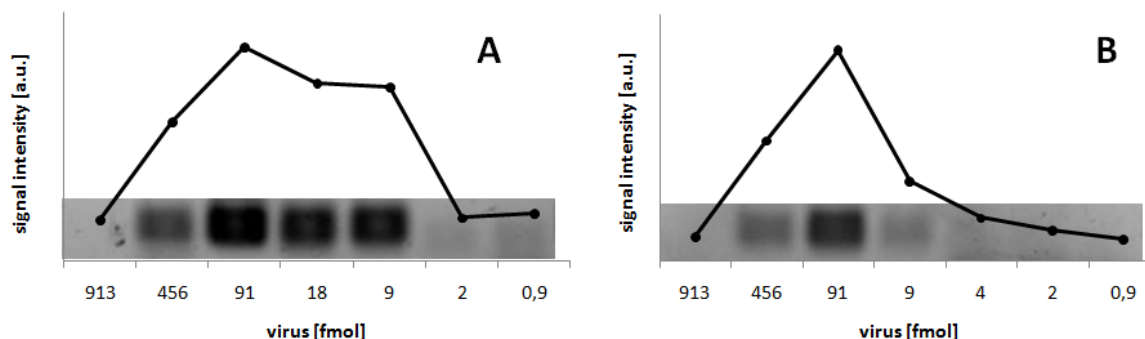


**Figure 4-15.** Two dilution series of virus in RT-PCR samples of the nanocontainer system. Signal intensity on the agarose gels was quantified with ImageJ. Note the different virus dilutions in A and B, the first including a sample with 18 fmol virus which results in a shoulder of the decreasing slope which cannot be found in the dilution series B.

Although their signal intensity is quite different, they share the general pattern: no signal in the first lane with concentrated virus, then increasing signal until a peak is reached in the third lane with 91 fmol virus and then decreases again until background intensity. The agarose gel band intensity can also be quantified with ImageJ to give figures which are easier to compare and interpret. The curves given in Figure 4-15 allow the easy identification of the lane with the strongest signal for RNA transfer. Notably, this is not the lane with the highest virus concentration which would be expected to transfer the most RNA copies. Too many viral particles seem to decrease the cDNA transcription efficiency. A known RT reaction inhibiting effect is the dilution of the RT mix, as it happens in nanocontainers treated with the detergent Triton X. The insertion of many viral proteins in close proximity to each other could cause perturbation of the lipid bilayer, resulting in holes which allow the dilution of the encapsulated RT mix with buffer from the exterior. Although a lot of RNA is transferred across the membrane, the diluted RT mix is not able to transcribe it into cDNA and as a result it is not detected. Below a certain threshold of virus concentration this negative effect of the virus on membrane stability is negligible. The signal intensity from intact nanocontainers for detected RNA is directly related to the amount of applied virus, i.e. the signal intensity decreases depending on the dilution of the virus.

### conversion of native particles to 135S:

Controls for the nanocontainer system showed RNA transfer without receptor mediating the attachment of virus to the liposomal membrane. It is believed that this is an

effect of the small sample volume which causes high concentration of viral particles and membranes, increasing the probability of virus residing in close proximity of a membrane when RNA release is triggered by acidification. Upon pH reduction the viral particle undergoes structural changes which result in the formation of 135S subviral particles with released VP4 and externalized VP1 N-terminus. These hydrophobic peptides are believed to insert into a membrane and allow the RNA transfer across the lipid bilayer. This would make the receptor dispensable for RNA transfer if the viral particles are close to a membrane when triggered. To study 135S particles, they have to be produced *in vitro* without fully converting the viral particle to non-infectious 80S particles.

Native virus particles can be converted to 135S particles by heating the concentrated virus for 10 min to 56°C, either in a heating block or a water bath. Conversion can be confirmed via CE, depicted in Figure 4-16, which shows a large peak for 135S and only a small peak for the remaining native particles. Viral protein is detected at 205 nm, RNA at 260 nm; if peaks show up at both wavelengths at the same time in a virus sample, it can only mean native particles or 135S, because 80S particles have lost their RNA [41].

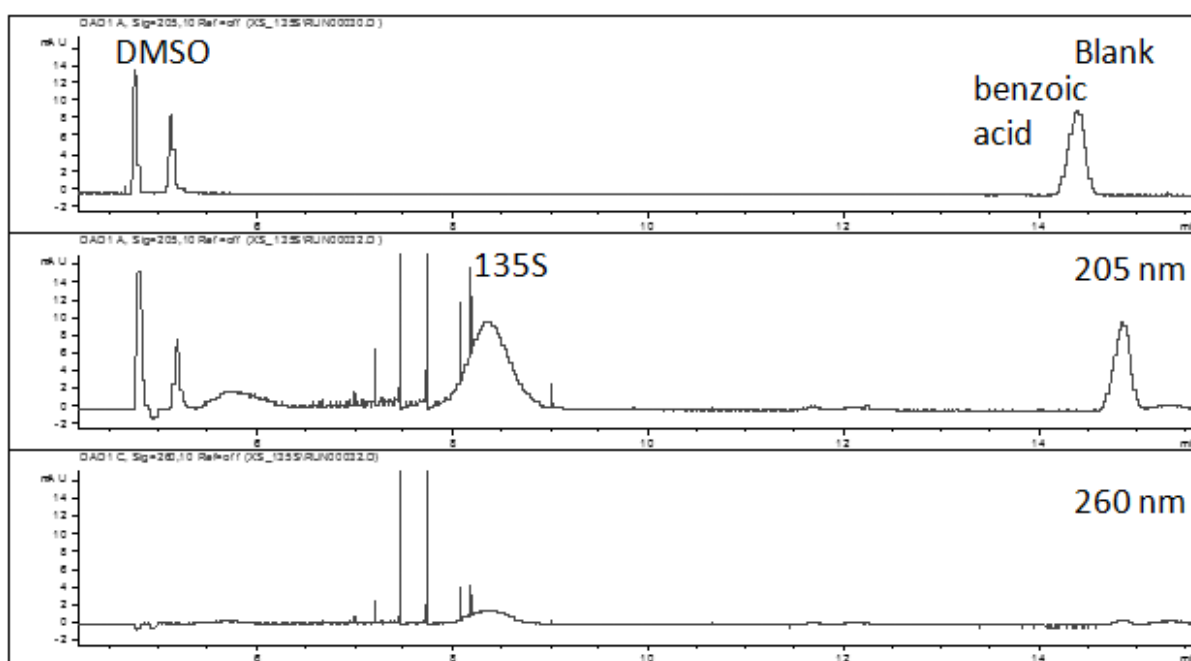


**Figure 4-16.** Electropherograms produced with UV detection of HRV2 run in CE. Blank contained DMSO and benzoic acid as migration markers. Concentrated HRV2 was heated to 56°C for 10 min and its conversion to 135S particles was confirmed in CE, where the viral protein can be detected at 205 nm and the viral RNA at 260 nm. A small peak for native particles remains, but most virus particles are converted to 135S. Spikes probably indicate aggregation of virus particles during conversion. BGE: 100mM borate buffer, 10mM Thesit, pH 8.3; separation conditions: 25kV, 20°C.

Since no detectable peak for 80S particles appeared in CE, it can be concluded that the conversion stopped at 135S particles like expected. These particles could be used for the following flotation experiments to determine the binding capacity of 135S particles to plain liposomes.

**separation of unbound virus from nanocontainers via flotation:**

When preparing samples in the way described above, by just adding nanocontainers, receptor and virus together, one question remains unanswered: how much of the virus is really bound to the liposomes and how much is residing in the buffer without being able to transfer its RNA into the liposomal lumen? Performing the RT in the negative control without receptor resulted in a strong positive signal for cDNA production (see Figure 4-14, lane 4). One might believe that the receptor plays no role at all in the nanocontainer system and could be left out. To show the necessity of receptor for tight attachment of virus to the liposome, flotation in a sucrose step gradient was employed as the method of choice to separate unbound virus from the liposome. The position of the liposomes could be determined by fluorescence measurement with the Victor plate reader and the position of the virus by a TCID<sub>50</sub> assay. Liposomes with 1 mol % fluorescent NBD-PC were decorated with receptor and virus, exactly like for RT-PCR, and mixed with 67% w/v sucrose in TrisNaCl buffer to give a 50% w/v sucrose solution which was overlaid with 25 and 0% w/v sucrose solutions. Centrifugation at 45000 rpm moved liposomes to their corresponding sucrose density whereas virus particles stayed at the high density bottom of the gradient. Fractions were taken from the top to the bottom and their lipid content was determined based on the fluorescent lipid NBD-PC (see Figure 4-17).

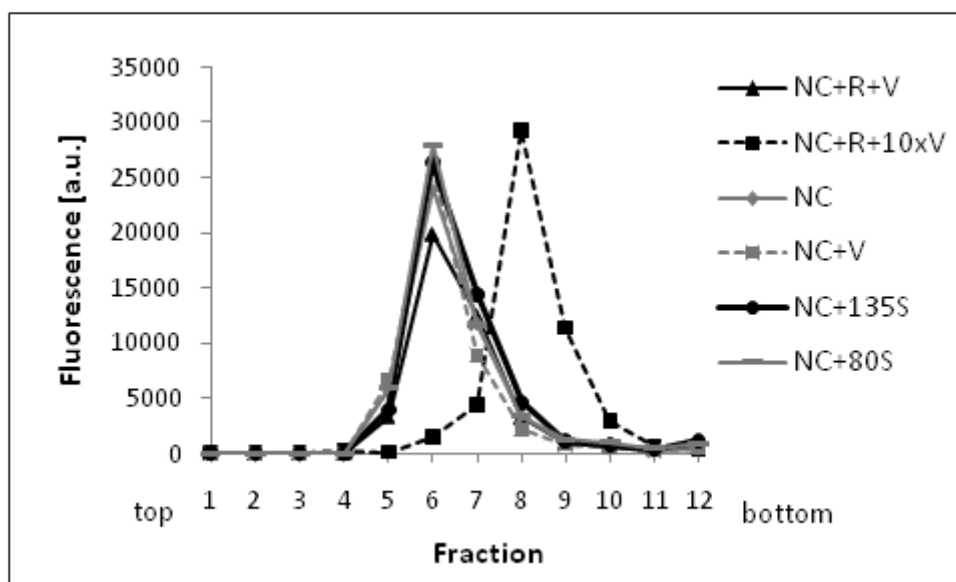


**Figure 4-17. Liposomes in of sucrose gradient fractions after flotation. Plain nanocontainers or nanocontainers decorated with only a few virus particles both flot at the top of the 25% sucrose step (fraction 6), whereas a high virus concentration causes a shift to the bottom of the same step (fraction 8). Fluorescence of NBD-PC was determined in a Victor plate reader (Wallac).**

Plain nanocontainers (NC) were mainly found in fraction 6, just as nanocontainers which had not been decorated with receptor and then mixed with native virus particles, 135S or

80S. Receptor decorated nanocontainers with 91 fmol virus / 64 nmol lipid had a similar flotation pattern, their corresponding peak was just a bit broader. This was caused by a slight distribution of the liposomes depending on the amount of virus bound to each nanocontainer. The peak-shifting effect of virus bound to the membrane became especially obvious with a sample consisting of receptor decorated nanocontainers and 10 times more virus. Due to the contribution of the high number of virus particles bound to the liposomes, the complex was shifted to fraction 8.

Unbound virus had been separated from the liposomes and only receptor-coupled virus co-floated, which was shown by a TCID<sub>50</sub> assay of aliquots of all fractions of a sample with receptor and one without receptor (depicted in Figure 4-18). Without a receptor, most of the virus accumulated at the bottom of the gradient, whereas receptor bound to the liposomes caused a shift of the virus to the same fractions which also contained liposomes.

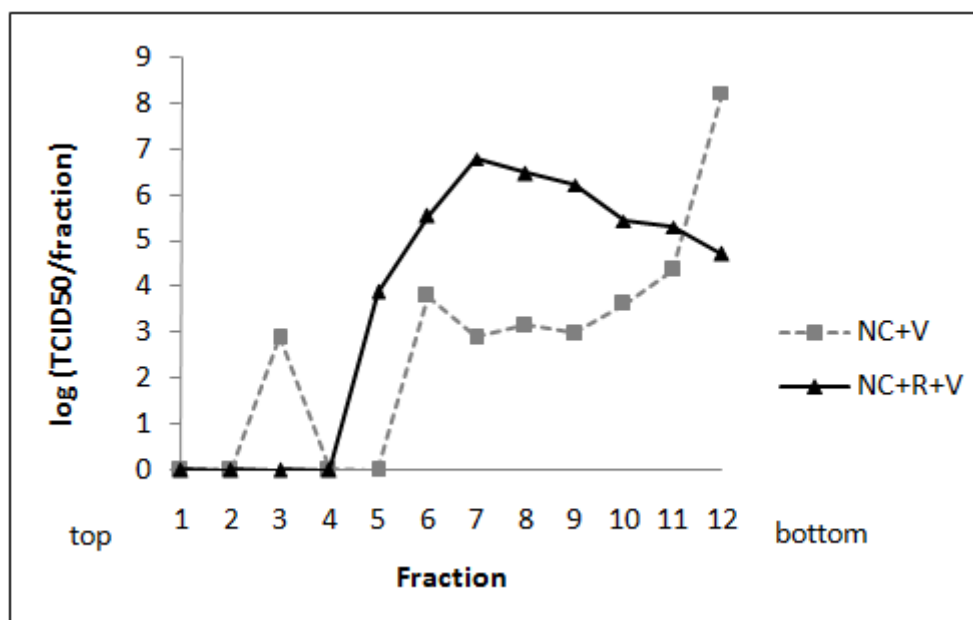


**Figure 4-18.** TCID<sub>50</sub> of fractions of the sucrose step gradient after flotation of a sample consisting of nanocontainers decorated with receptor and virus (NC+R+V) and another sample of just nanocontainers and virus (NC+V). The receptor binds the virus to the nanocontainers which causes more than 90% of infectious virus to float in fraction 7, whereas unbound virus remains at the bottom of the gradient in fraction 12. The bound virus gives rise to a signal for RNA transfer, which cannot be seen in a floated sample without receptor (see Figure 4-21).

From pictures of the liposome-receptor-virus complexes taken by electron microscopy, it was possible to count virus particles per liposome and compare that actual number with calculated ratios. On the pictures (Figure 4-19 A, floated standard nanocontainer system sample) not all virus particles are still bound to the liposomes, nevertheless they must have adhered during flotation, otherwise it would not be possible to find them in the same fraction as the liposomes in the upper 25% sucrose area (picture of a sample without receptor is not shown because only plain liposomes can be seen, comparably to Figure 4-10; the virus alone flotates at the bottom of the gradient in the high density sucrose, shown by the TCID<sub>50</sub> assay).

## Results

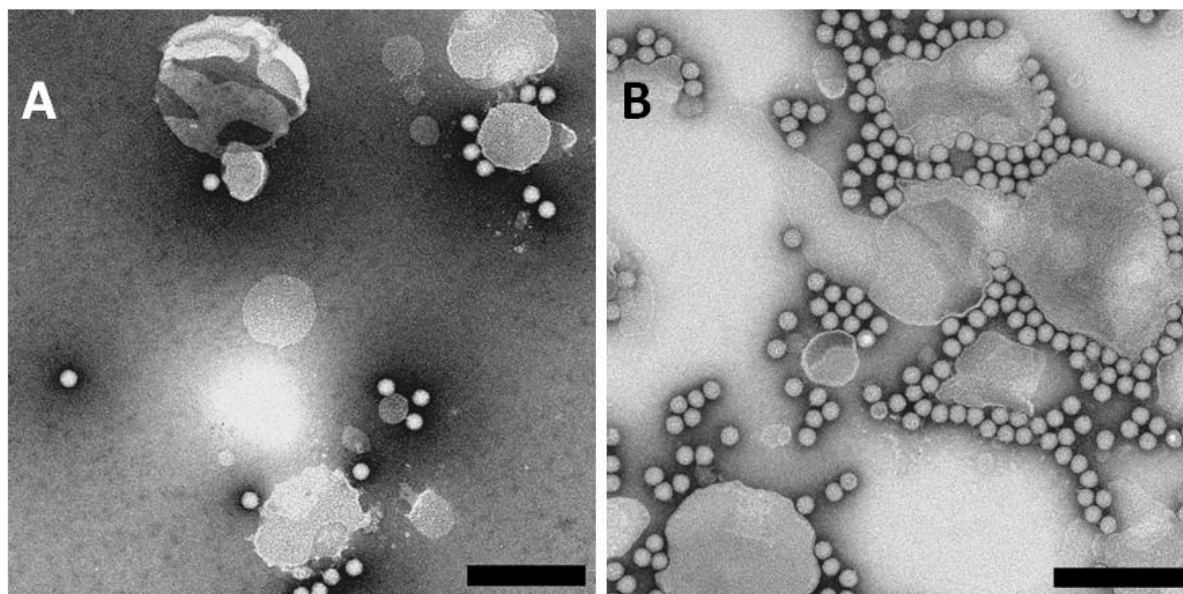


**Figure 4-19.** TEM pictures of a standard nanocontainer system sample with 91 fmol virus / 64 nmol lipid (A) and with 10x HRV2 (B) after flotation, taken at 56k magnification. In average, 3 virus particles are bound to each liposome in the standard sample, 10 times more virus causes aggregation of the liposomes. Size bar = 200 nm.

It was found that the calculation of about 3 virus particles per liposome in the case of 91 fmol virus / 64 nmol lipid had been quite accurate and could be trusted to really reflect the situation in liposome decoration for RT-PCR. A shift of the fraction containing the liposomes can be reached by applying a very high virus concentration. When binding around 30 virus particles per liposome (see Figure 4-19 B), the density increased and forced the liposomes to flotata close to the interface between 25% and 50% sucrose. The highly concentrated virus also crosslinked the liposomes to form big aggregates. This caused the liposomes to contract to a small area, reflected by the high and sharp peak in fluorescence measurement. Aggregation can also be seen on pictures taken with the microscope.

Most 135S particles, converted prior to their addition to the nanocontainers, could not bind to the liposomal membrane and were not found in the same fraction as the nanocontainers after flotation (see Figure 4-20, A). Addition of 80S had a similar outcome, since the fully converted particles have no hydrophobic residues for membrane attachment externalized, no particle co-flotated with the liposomes (see Figure 4-20, B). Conversion to 135S in the presence of the liposomal membranes was not possible because addition of liposomes to the virus would cause dilution of the viral sample. As already described by Weiss [41], conversion of a diluted virus sample results in 80S instead of a halt at the 135S intermediate. Only conversion in the presence of membranes is expected to result in several viral particles adhering to the membrane via the externalized VP4 and VP1 N-terminus. Once these peptides are lost, the particle is not able to anchor itself to the membrane anymore.



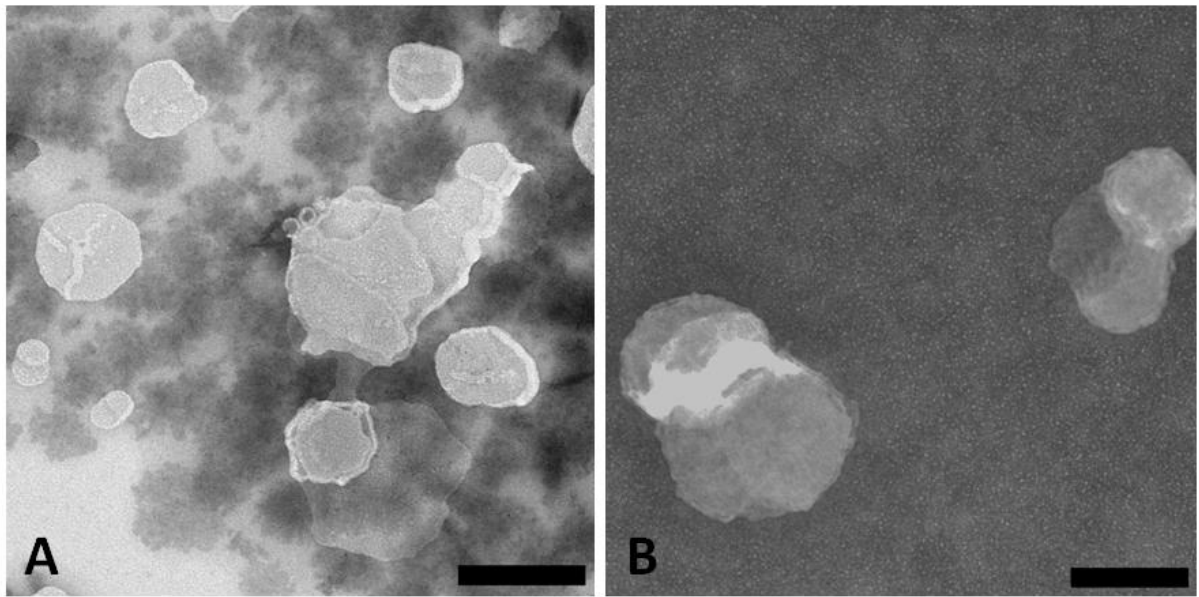


**Figure 4-20.** TEM pictures of nanocontainers with 135S (A) and 80S (B) after flotation. 135S were produced prior to their addition to the liposomes and did not adhere tightly enough to co-flotate with them, only very few were found on the liposomal membrane. Preformed 80S did not bind to the liposomal membrane. Magnification 56k; size bar = 200 nm.

Together with the results from virus-decorated samples (Figure 4-19) this indicates the necessity of a receptor for tight binding of the virus to the liposomal membrane, unbound native virus or subviral particles do not adhere by themselves.

To make sure that the tightly bound virus alone is enough to give a detectable signal for RNA transfer in RT-PCR and the additional free virus from normal RT-PCR is not needed, liposome containing fractions were combined after flotation, bound virus was triggered by pH 5.4 and the RT reaction was performed. Transcribed cDNA was precipitated with ethanol and 3 M NaAc using glycogen as a carrier and amplified by PCR (for result see Figure 4-21). It could be shown that 3 virus particles per liposome are enough to give a positive signal for RNA transfer (lane 1). If no receptor was present to mediate the tight attachment of virus to the liposomal membrane during flotation in the sucrose step gradient, the virus was separated from the liposomes and therefore could not give rise to a signal for RNA transfer (lane 2). The band has the same size and intensity as the background signal determined by RT-PCR of flotated plain liposomes (lane 4). Reduction of the virus concentration by a factor 5 reduced the amount of transferred RNA below the detection limit (lane 3).

## Results

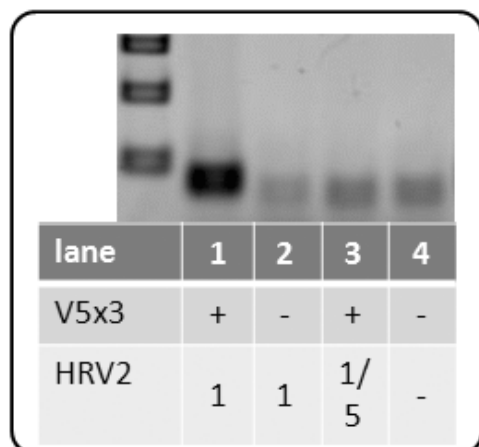
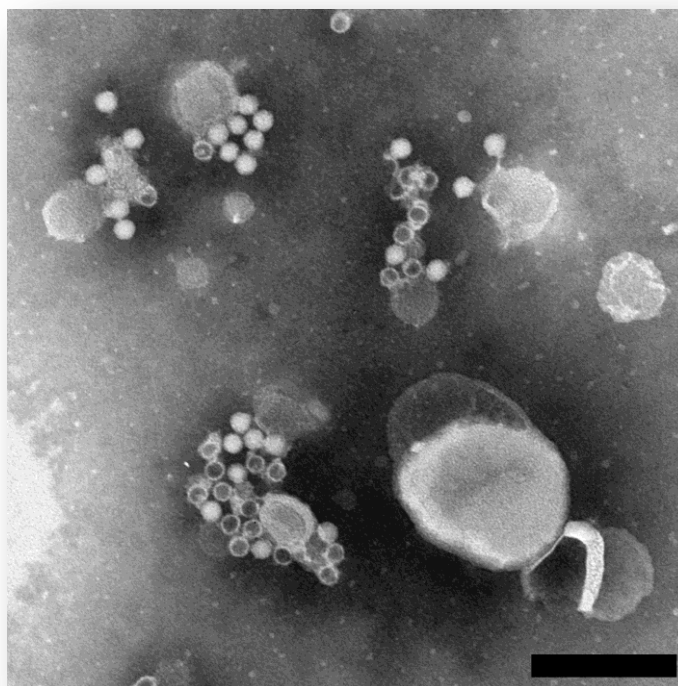


**Figure 4-21.** RT-PCR of flotated nanocontainer system samples. RNA release was triggered after flotation, the cDNA transcribed in RT was precipitated and subjected to PCR. Only the standard sample with NC (64 nmol) + 36 pmol receptor + 91 fmol virus (lane 1) was able to give a signal, when the receptor did not bind the virus to the liposomes (2) or the virus concentration was only 1/5 (3), there was no signal. Background is given by the plain liposomes in lane 4.

The flotation of receptor and virus decorated liposomes at typical nanocontainer system ratios removed all broken virus particles which were not able to bind the receptor. Electron microscopy of such a sample depicted the complexes and the effect of 15 min acidification (see Figure 4-22), which turned part of the native virions into 80S particles.

**Figure 4-22.** TEM picture of a flotated and acidified standard nanocontainer sample (64 nmol lipid, 36 pmol receptor and 91 fmol virus) at a 56k magnification. Many virus particles were converted to 80S particles. Size bar = 200 nm.



In summary, by flotation experiments it was possible to determine if viral and subviral particles were able to adhere to the liposomal membrane by themselves or if they needed a mediating receptor to do so. Decoration of the nanocontainers with MBP-V33333-His<sub>6</sub> resulted in co-flotation of liposomes and native virus. The fraction containing the complex depended on the virus concentration: large amounts of applied virus contributed to a higher overall density of the sample, shifting the complex to a higher density fraction, close to where free virions were found. A high virus concentration, i.e. more than about

0.6 pmol virus / 64 nmol lipids, also crosslinked the receptor-decorated liposomal membranes, forming large aggregates. If fewer virus particles were applied, they attached to the receptor-decorated liposomes but contributed too little density to significantly change the location of the liposomes in the sucrose density gradient in comparison to plain, non-decorated liposomes. Nevertheless, these virions were able to give an RT-PCR signal showing RNA transfer when triggered after flotation. Subviral particles which were converted prior to their addition to the membranes were not able to adhere.

#### **virus per liposome: *in vivo* relevance:**

The nanocontainer system only yields results relevant to *in vivo* infection if the amount of infecting virus per liposome is comparable to the amount of virus infecting a cell *in vivo*. Therefore, the amount of liposomes and virus in one sample preparation was calculated, as to deduce the number of viruses per liposomes. Liposome number was calculated from the known amount of used lipids and their surface, in combination with the inner and outer surface of a sphere of 400 nm diameter. A typical sample containing 91 fmol virus and 35 fmol liposomes would add up to 2.6 virus particles per liposome.

The 91 fmol virus corresponded to  $10^8$  median tissue culture infective doses (TCID<sub>50</sub>), which are distributed all over the total outer liposomal surface. Assuming a typical cell has a diameter of 40 µm, applying the same TCID<sub>50</sub>/surface ratio would give around 50 TCID<sub>50</sub> per cell. This is in a range comparable to the infective doses used for cell infection in tissue culture, which are normally around 10 TCID<sub>50</sub> per cell.

#### **RNA quantification via quantitative PCR:**

RNA transferred into liposomes was transcribed into cDNA via the encapsulated RT kit. The low amount of cDNA could not be seen on an agarose gel, therefore it was amplified in a PCR reaction prior to application on an agarose gel. This was mainly a semi-quantitative method, either there was a band visible or not. Quantification of the band intensity via ImageJ allowed the comparison of RNA transfer efficiencies, but it was not possible to determine the exact number of transferred RNA copies. A method to directly quantify how many viral genomes had entered the liposomes would be desirable. Quantitative PCR is an established method of quantification of starting material.

The reaction mix was composed of Taq DNA Polymerase Master Mix RED, Fluorescein additive, SYBR Gold dye, template DNA and primers which had been designed to recognize all serotypes of HRV [31] (see primer index). Their specificity for all HRVs was rendered possible by targeting a highly preserved region in the viral 5' UTR region with sequences obtained from 100 recognized HRV prototype strains additionally to field

### Results

---

isolates. The qPCR machine chosen to work with here was a BioRad iCycler, after also testing the Eppendorf Realplex Mastercycler and the Roche Lightcycler.

By selecting the primers, the assay can either be optimized for HRV2 or for all HRV serotypes when employing the general primers developed by Lu et al. [31]. The choice of how to produce the standard curve is crucial to gain the desired information about transcribed cDNA amount. At first whole virus particles were employed, they were used for serial dilutions and their released RNA was subjected to RT and qPCR. Calculating from the threshold cycle (T<sub>c</sub>) values of samples back to their RNA content with the help of this virion standard curve could not give exact starting values, since this would only be possible if the number of virus particles was the same as free RNA molecules. This assumption might not be met; the virus preparations contain a large amount of inactive virus particles which do not release their RNA for cDNA synthesis and subsequent qPCR detection. As a result, *in vitro* synthesized HRV2 RNA of a known size, spanning the qPCR amplicon, for an RNA based standard curve would be a better choice. It would allow the determination of the absolute number of RNA strands transcribed into cDNA. For that purpose it was necessary to obtain RNA of exactly one size, spanning the region which was amplified during qPCR, otherwise it was not possible to calculate the RNA copies from total RNA concentration measured by NanoDrop. Unfortunately, the attempts made here proved to be unsuccessful. When applying the *in vitro* transcribed RNA to an agarose gel it was visible that most of the RNA was of the intended size, but some was of smaller or of bigger size (data not shown), tampering with the RNA copy number calculation. The big problem of RNA, fast digestion, made it difficult to synthesize RNA of one distinct size which is the prerequisite for molecule copy number calculation. During the course of these experiments, the overall qPCR sensitivity decreased (shown in Figure 4-23) due to an unidentified factor. Before further advancing the RNA based standard curve, the overall sensitivity has to be increased again.

Although it was aimed at increasing the sensitivity of the assay, in fact it decreased with time. Figure 4-23 depicts several dilution series of HRV2 performed over several months (time-lag indicated).

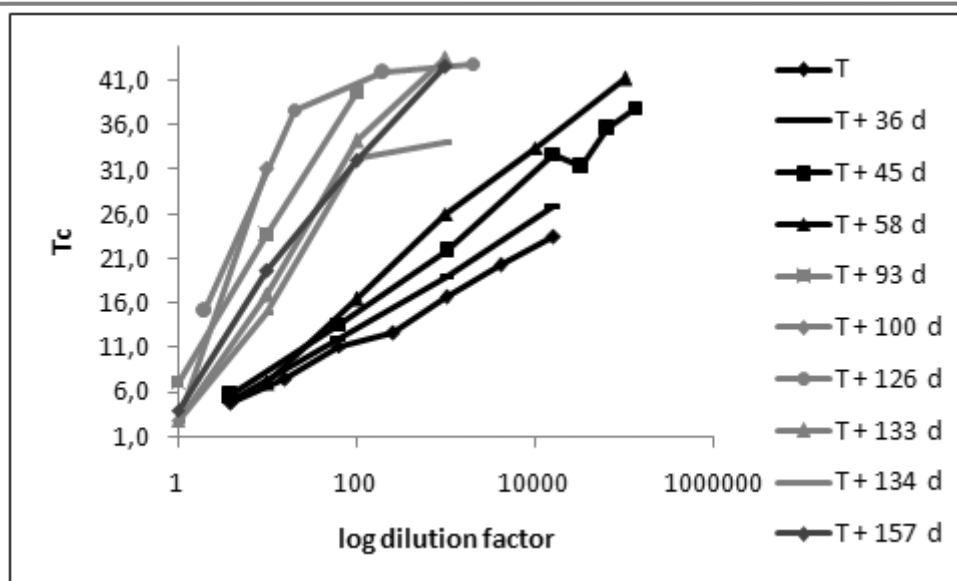


**Figure 4-23. Standard curves for qPCR produced over several months from dilution series of HRV2. Curves created within the first 2 months are indicated in black, later ones in grey. The dark grey graph was measured on an Eppendorf Mastercycler in contrast to all other samples, which were run on a BioRad iCycler.**

Highest sensitivity equals to lowest threshold cycle number ( $T_c$ ) at a given HRV2 concentration. Since the amount of cDNA transcribed in nanocontainers was low, the decreasing sensitivity of the qPCR did not allow the quantification of these samples.

The reason for the loss of sensitivity could not be found. Aging and therefore dysfunction of certain qPCR mix compounds seemed probable since the loss was time dependent, although it could not be solved by using fresh DNA polymerase master mix, SYBR Gold or Fluorescein additive. Only primers could not be replaced, but since the same primers were used successfully in standard PCR it is unlikely that they are the responsible component. Amplification products of the qPCR could be applied to agarose gels to check if the amplification itself worked. Low template amounts did not yield a visible product (data not shown), just as detected by qPCR fluorescence measurement. Hence it was the sensitivity of the amplification that failed and not the in parallel running detection of activated SYBR Gold. It was not possible to solve that problem in time.

#### **inhibition of RNA transfer:**

Several drugs have been used previously in cell culture to inhibit viral infection [45]. Testing their blocking capacity in the nanocontainer system would be a faster and easier way to test a drug's influence on RNA transfer. Experiments to determine their mode of action could be done. Also it is a chance to test the usefulness of the nanocontainer system. Amiloride and its derivatives hexamethylenamiloride (HMA), 5-(N-ethyl-N-isopropyl)amiloride (EIPA) and rimantadine were checked for their RNA transfer inhibiting capacity employing the nanocontainer system. First, each drug was added during liposome decoration between receptor and virus addition and RT-PCR was

## Results

performed. The cDNA transcription was totally inhibited in the sample containing 5 mM Amiloride and to a high extent in the sample containing 0.1 mM HMA, whereas EIPA and rimantadine did not exhibit any inhibitory effect (see Figure 4-24 for results). Separate reverse transcription reactions, which were not encapsulated in liposomes, supplemented with the drugs showed that the drugs did not interfere with the RT reaction. Virus triggered to release its RNA first was added to the RT mix together with the released RNA. The transcription of cDNA showed that the drugs had no inhibitory effect on the RT reaction itself (data not shown). Also virus added in its native form to the sample and triggered by pH lowering in situ led to cDNA transcription. Unfortunately, this cannot be handled as a prove that the drugs did not stop the RNA release from the virus, because it was also detected that the virus prep contains not only closed native virus particles but also enough free RNA to give a strong RT-PCR signal even without triggering the RNA release.

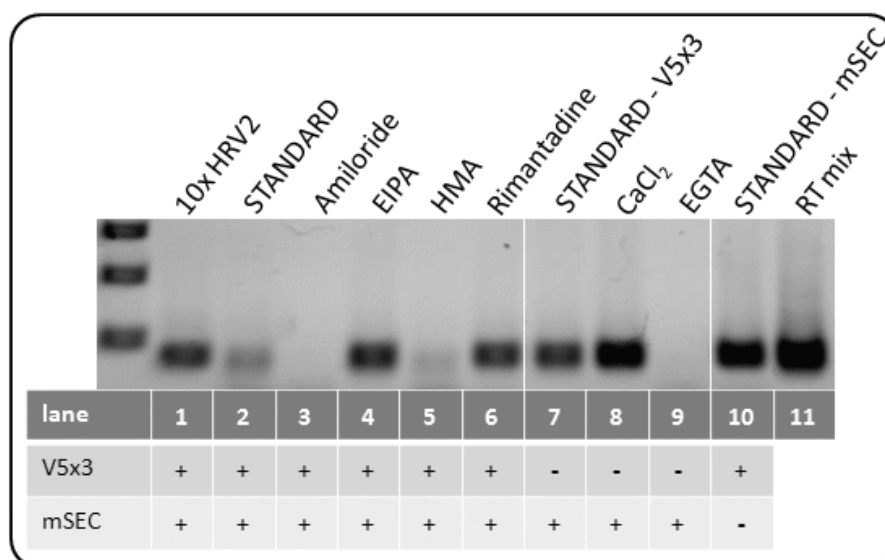


**Figure 4-24.** RT-PCR of nanocontainer system samples treated with antiviral drugs or other chemical compounds which are supposed to have some influence on viral infectivity. The low signal of the standard sample with 91 fmol virus (lane 2) compared to the sample with 10 fold higher amount of virus (1) is due to the use of a low-infectious virus preparation. All other samples were prepared with the standard amount of virus. Standard sample on lane 2 had been treated with different drugs (lanes 3-6). A standard sample without any receptor is shown on lane 7, which had been treated with calcium (8) and a calcium chelator to remove all available calcium from the reaction (9). Positive control of an unpurified standard sample on lane 10 and a RT control on lane 11.

#### effect of calcium and EGTA on RNA transfer:

Calcium is bound to the dome at the fivefold axis of the viral capsid and is supposed to play a role in virion stability and uncoating. It is present to some extent in the receptor decorated liposome samples because the receptor storage buffer contains 10 mM  $\text{CaCl}_2$ , which is needed by the receptor for correct folding. The addition of 1  $\mu\text{l}$  receptor to a 20  $\mu\text{l}$  total volume sample therefore results in the presence of about 0.5 mM  $\text{CaCl}_2$ . To test if the

presence of calcium in the sample would increase the RNA transfer efficiency even without any receptor present,  $\text{CaCl}_2$  was added to 1 mM end concentration in the sample before virus was added. Then, the RT-PCR was performed as usual and the signal intensity was compared to a sample without supplemented calcium (see Figure 4-24, lanes 7 to 9). The signal intensified visibly, clearly stating the RNA transfer supporting role of calcium. Then again it might not be an essential part of RNA transfer and could be omitted without total loss of transfer. This was tested with ethylene glycol tetraacetic acid (EGTA), a calcium-chelating agent which was added to 1 mM end concentration to plain liposomes before virus addition. This sample gave no sign of cDNA production, stating the necessity of ions for the RNA transfer. Calcium may be present in standard samples from receptor buffer and the virus preparation, when the virus imports the ion itself from replication in its host cell. Another ion, which was added as part of the reverse transcription buffer and is also chelated to some extent by EGTA, was magnesium (5x first strand buffer (Invitrogen) contains 15 mM  $\text{MgCl}_2$ ). Since EGTA had an effect on samples containing hardly any calcium, it might be conceivable that magnesium could have the same function as calcium in samples lacking an appropriate amount of the latter ion.

## 5 Discussion

Liposomes as a simple model membrane system for viral infection of host cells have been further evolved into a nanocontainer system where liposomes are filled with an RT mixture and decorated with a recombinant receptor for HRV2 to permit virus attachment and RNA transfer into the nanocontainer upon a trigger. It can not only be used for taking a look at virus attachment from the outside but also for RNA transfer studies, detecting the viral RNA inside the liposomes via RT-PCR. In the current thesis, weaknesses of the system like variability were addressed and, after solving that, the system was characterized and put into use. The nanocontainer system had only been developed for minor group Human Rhinovirus. Limitations are the chosen minor group receptor which is derived from a member of the LDLR family, and the specific primer used for RT. To expand the research applications of the nanocontainer system, a recombinant receptor derived from the major group HRV receptor, ICAM-1, was engineered in the course of this diploma thesis.

### 5.1 Elimination of reactions potentially disturbing the nanocontainer system.

At the beginning, nanocontainers were produced according to the protocol of Gerhard Bilek [29]. Liposomal membranes were made of POPC, PE, SM, Ch, Ni-DGS-NTA and NBD-PC in a molar ratio of 1 : 1 : 1 : 1.5 : 0.5 : 0.05, the hydration buffer, which was encapsulated by the liposomes, consisted of a complete reverse transcription mix, i.e. enzyme specific buffer, dNTP mix, reverse primer, DTT, RNase inhibitor and reverse transcriptase. Already Bilek had experienced difficulties with the reproducibility of the system. It appeared that although the liposomes looked spheric in pictures taken with the electron microscope and the RT mixture worked properly outside of the liposomes, there was hardly any signal detectable in RT-PCR from the inside of nanocontainers. It was not known if the failure was due to a problem inside or outside of the nanocontainers, it might have concerned every step of the virus-receptor interaction, the receptor-liposomal membrane attachment, the RNA transfer, the reverse transcription or the PCR. Many of the reagents were replaced by fresh or different preparations, for example the V33333 receptor was substituted by V123, another recombinant receptor derived of the VLDLR, and a fresh preparation of V33333. The new receptor preparation of V33333 only contained 5.8  $\mu$ M imidazole in the receptor buffer, whereas the previous preparation had an imidazole content of 10 mM. The reduction of this competitor for  $\text{Ni}^{2+}$  might increase the binding capacity of the receptor since fewer Ni-DGS-NTAs are blocked by imidazole. A change in the hydration buffer composition to 10x more primer temporarily resulted in



increased signal intensity, but this was not confirmed in following experiments. Editing of the established RT-PCR program to give the RT reaction more time neither enhanced the signal. A breakthrough was finally made by the alteration of the lipid composition. The fluorescent lipid NBD-PC, although incorporated only in traces compared to the rest of the lipids, gave the membranes a distinct yellow tint. Without this lipid, the preparation should have been transparent to white. When omitting NBD-PC in the liposomal membrane preparation, still a strong color change to rubiginose was noticed upon addition of the hydration buffer. It was found that the  $\text{Ni}^{2+}$  bound to DGS-NTA reacted with DTT at the pH present in the RT mixture. DTT consists of two sulfhydryl groups attached to a four carbon threitol. It has a low redox potential of -0,33 V at a pH of 7 which enables the chemical to keep reduced SH groups unbound and quantitatively reduce present disulfide bridges, oxidizing itself in the process to circularize via an intramolecular disulfide bridge. The Ni-DGS-NTA is a crucial part of the nanocontainer system, as it mediates the attachment of the receptor and therefore virus to the liposomal membrane. Without the active  $\text{Ni}^{2+}$ , the receptor is not able to interact via its His<sub>6</sub>-tag. Since later experiments showed that RNA transfer can also happen without receptor in a concentrated sample, the complexation of  $\text{Ni}^{2+}$  by DTT probably caused complete shielding of the liposomal surface from the interacting virus. DTT is normally added to an RT reaction to protect the enzyme from oxidation following contact with ambient oxygen and to inactivate RNases via reducing their disulfide bridges. Omitting DTT in the RT mixture in order to prevent a reaction with  $\text{Ni}^{2+}$  resulted in functional nanocontainers. RNases were still inhibited with RNasin (Promega), a commercial RNase inhibitor. The oxidation and hence the accelerated aging of the encapsulated enzyme was probably limited inside the membranes or had to be accepted as a trade off.

## 5.2 Generalizing the nanocontainer system for all HRV serotypes.

The viral infection model system of nanocontainers has been improved and characterized. First, composition and procedure of the standard RT-PCR reaction provided by Bilek were optimized. In the beginning, a primer set giving an amplicon on the 3' end of HRV2 and one producing an amplicon on the 5' end of HRV2 were used. Although they generated distinct amplicons for HRV2, they were abandoned in favor of generally applicable primers for all HRV serotypes. This was a step towards broadening the nanocontainer model system for research on all HRV species. The newly introduced primers had been described by Lu et al. [31] and were intended for use in RT-PCR as well as quantitative PCR. Their product was a short amplicon of 204 nt on the border of the 5' UTR of the HRV genomic RNA. The reverse primer was designed in a way that it would

bind to a region highly conserved among all HRV and human enteroviruses (HEVs). In contrast, the forward primer was designed to be complementary to a variable region that contained a signature T indel in HEVs but not HRVs, allowing its exploitation for differential amplification. Locked nucleic acid analogues (LNA) that increase thermodynamic stability were introduced into the short forward primers to raise their melting temperature comparably to that of the longer reverse primer. These primers worked best at an annealing temperature of 60°C although the calculated melting temperature was considerably lower for the reverse primer (see primer index attached).

The second HRV serotype dependent component of the nanocontainer system was the receptor. Only 12 HRV serotypes use the minor receptor, the larger part employs ICAM-1 for internalization. For investigation of the RNA transfer of HRV2, a member of the minor group, a soluble recombinant VLDLR had already been developed by Ronacher et al. [46]. RNA transfer of major group viruses is believed to follow a different pathway. The attachment of virus to ICAM-1 induces structural changes for which the minor group virus needs the additional trigger of acidification [18, 47]. Controlling the moment of uncoating in the nanocontainer system, like it is done via acidification of minor group viruses, could be impossible with major group viruses. For detection of transferred viral RNA by RT in the lumen of the nanocontainers it is mandatory to keep the liposomal membrane intact. This was no problem with minor group viruses, whose viral capsids have been detected in lysosomes after releasing their RNA into the cytosol [48] and endosomal pH was unaffected by successful HRV2 infection [49], pointing at the formation of a pore without disrupting the membrane. Major group viruses seem to disrupt the endosomal membrane and reach the cytosol with the RNA as well as with the capsid [50-51]. Disruption of the nanocontainer membrane would render any RNA detection impossible. Although further studies employing the nanocontainer system would not be possible with the major group virus if this was really the case, it would be interesting to find out if major group viruses disrupt the membrane upon attachment to ICAM-1, if they need the low pH as additional trigger to do so or if they can also form a pore for RNA transfer across the membrane. A recombinant ICAM-1 receptor was cloned in the course of the present work which can be expressed in eukaryotic cells for the addition of glycosidic chains which increase the solubility. The implementation of this receptor extends the nanocontainer system to the use of major group viruses.

### 5.3 Determining the ideal sample composition.

Leakage experiments performed by Weiss et al. [52] on liposomes and different HRV concentrations have shown that a virus concentration above a certain threshold in relation to the used lipid causes leakage of the liposomes, losing its encapsulated fluid to the exterior. If the interior and exterior of the liposomes are different, like it is the case in the

nanocontainer system where an RT mix fills the inside of liposomes which are surrounded by iso-osmotic buffer, the mixture of the two fluids results in a dilution of both. Since diluted RT mix is not able to transcribe RNA into cDNA anymore, the leakage of nanocontainers causes a decrease or total loss of the signal intensity. This causes a trade off, because enough virus has to be applied to the nanocontainers to reach a detectable cDNA template concentration for PCR, but not so much as to cause leakage. A serial dilution of HRV2 with constant amounts of nanocontainers and receptor reflected these two counteracting influences on the signal intensity (see Figure 5-1).

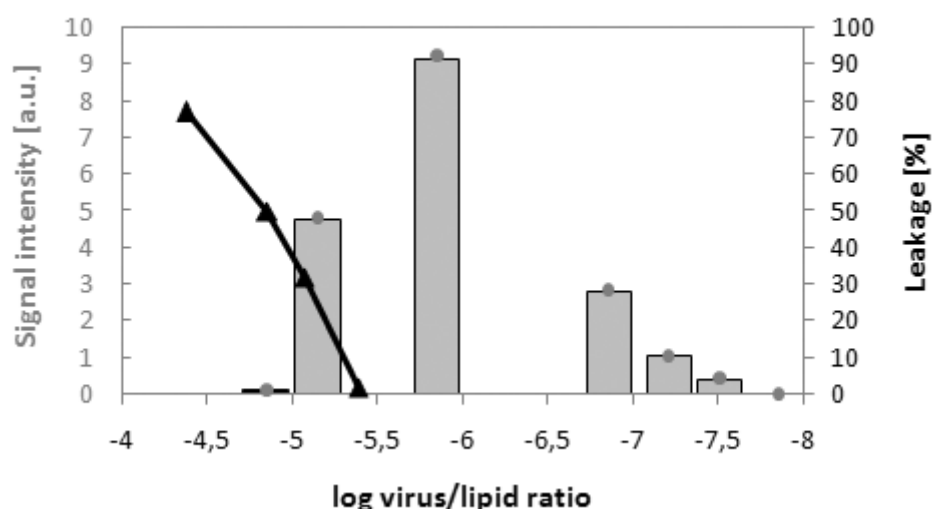


**Figure 5-1.** RT-PCR of a virus dilution series in the nanocontainer system (grey) with leakage in the same virus/lipid ratio range indicated (black). Leakage data according to Weiss et al. [52], RT-PCR signal from agarose gel bands quantified with ImageJ. Highest RT-PCR signal corresponds to the highest virus concentration with 0% leakage (-5.8 log virus/lipid ratio, equivalent to  $10^8$  TCID<sub>50</sub> or 91 fmol virus / 64 nmol lipid).

Upon use of high virus concentration that is supposed to cause 100% of the nanocontainers to leak, the signal obtained from RT-PCR equals zero, because all viral RNA that had been transferred across a liposomal membrane was exposed to a diluted RT mix, which was not able to produce any detectable cDNA. Lowering the HRV2 concentration by half to a range where about 60% of the nanocontainers stay intact, results in a clearly detectable signal in RT-PCR. The signal intensity can be potentiated by decreasing the applied virus to the point where leakage of the nanocontainers can be neglected. The exact virus/lipid ratio at the crossing point to 0% leakage will give the strongest signal because all RNA that reaches the liposomal lumen is transcribed into cDNA. Decreasing the virus concentration further only results in less transferred RNA and therefore reduced signal intensity as is indicated by the declining signal in Figure 5-1. The ideal virus/lipid ratio to yield the strongest signal for RNA transfer was calculated to be around  $3.4 \times 10^{-6}$  from the data provided by Weiss et al., the ratio for the strongest signal in the nanocontainers was  $1.4 \times 10^{-6}$ , i.e. in a similar range, although a little less dilution of

the virus would still be possible without risking leakage. Summarized, the ideal virus – receptor – lipid concentrations are about 90 fmol virus, 36 pmol receptor and 64 nmol lipid (1: 400 : 711111 molar ratio) in one sample preparation.

The RT efficacy-reducing effect of leakage also supports the hypothesis of pore formation for RNA transfer through the lipid bilayer as the first option for transferring the viral RNA to the cellular cytoplasm. The second possibility, total disruption of the membrane by the virus for RNA transfer, would cause 100% leakage of all nanocontainers, resulting in no cDNA transcription at all. Since RT-PCR signals are only produced at a virus concentration below a certain threshold of leakage, the RNA must enter the nanocontainer via a small pore which does not allow any leakage. If many virions bind along the membrane next to each other and each of them starts to fold the membrane around them, the lipid bilayer will be strongly disturbed and finally disrupted, causing leakage.

### 5.4 Ratio total particles to infectious particles.

A virus preparation from cell culture [12], as employed in these experiments, contains varying shares of inactive virus particles. Numbers for virus concentration in mg/ml determined via CE [53] are only little helpful related to their use in infectious assays. The problem is not that parts of the detected virions are non-infectious, but that this part is varying in each new preparation, maybe even in each aliquot. As long as it would remain at a comparable levels the same correction factor could be applied to all preparations and therefore would not be noticed. Unfortunately, sometimes there are very bad preparations with substantially high proportions of inactive virus which give low signals in infection assays when standard virus amount measured in [grams] were used. Several virus preparations used in these experiments are presented below, their concentration in mg/ml determined via CE, their infectivity in TCID<sub>50</sub>/ml and the resultant virus particles / TCID<sub>50</sub> ratios are indicated.

	TCID <sub>50</sub> /ml	mg/ml	virus particles / TCID <sub>50</sub>
<b>1.</b>	1.00 x 10 <sup>12</sup>	7.3	543
<b>2.</b>	3.16 x 10 <sup>11</sup>	18.0	4235
<b>3.</b>	2.31 x 10 <sup>11</sup>	5.8	1867
<b>4.</b>	5.62 x 10 <sup>11</sup>	8.1	1072

This ratio has already been determined for other viruses, for example it is 30-1000 virus particles / PFU in poliovirus [5] and 10-100 virus particles / TCID<sub>50</sub> in adenovirus preparations [54], although it has to be noted that the virus particle number was determined via counting virions in microscopy and not by determining total protein via CE like it was done here. Although our preparations are in a similar range (1 PFU equals 10

TCID<sub>50</sub>), the great variance in our HRV2 preparations (between 540 and 4240) makes it important to express and compare the amount of virus used in an infection assay also in TCID<sub>50</sub> units and consider the quality of the specific preparation. Calculated 2.6 virus particles per liposome as are employed in standard nanocontainer samples could equal to TCID<sub>50</sub> per liposome values between 1.5 and  $4.7 \times 10^{-3}$ .

### **5.5 The influence of drugs and calcium on RNA transfer, determined by the nanocontainer system.**

Many HRV infection influencing actions take place inside the endosomes within the cell. The nanocontainer system makes them easier accessible for study. The drug ethylisopropylamiloride (EIPA; an amiloride-derived analogue) has been shown to inhibit HRV14 infection of human tracheal epithelial cells at a concentration of 10  $\mu$ M [55]. The drug amiloride was used successfully at 5 mM final concentration for the inhibition of HRV2 and HRV14 infection of RD-ICAM cells in cell culture [45]. In the present work, both drugs were tested together with other antivirals, hexamethylenamiloride (HMA) and adamantylethanamine (rimantadine), for their anti-infective capacity in the nanocontainer system. Surprisingly, only amiloride prevented the signal, whereas EIPA was not even effective at a concentration of 1 mM, which is 100x more than the concentration successfully employed in cell culture. This could be explained by the different modes of action of both drugs. EIPA was suggested to inhibit infection by preventing the endosomal acidification [55]. Since acidification of the nanocontainer system is done from the outside and cannot be influenced by EIPA, it is without effect in this artificial system. The discussed effects of amiloride are diverse and include the inhibition of RNA release into the cytosol. The mode of action of this inhibition is not clear. Running liposomes treated with amiloride in CE pointed to a membrane disrupting effect (unpublished data). *In vivo* this would prevent the acidification of the endosome and therefore the RNA release. Disruption of the liposomal membrane in the nanocontainer system would also cause leakage and therefore dilution of the RT mix, rendering the detection of released RNA impossible.

The RT reaction itself has been found to be left undisturbed by all drugs, but RT-PCR of the nanocontainer system has always to be done in combination with leakage experiments in CE to rule out the possibility of detection failure due to dilution of the RT mix. It was impossible to test the direct influence of the drugs on viral uncoating. A non-encapsulated RT mix always gives a signal from free RNA present in every virus preparations. Even if uncoating was inhibited by the drugs, there would still be a signal from free RNA. HMA diminished the signal for RNA transfer but could not totally erase it, rimantadine proved to be ineffective.

It has already been found before that the divalent ion calcium plays an important role in the structure and function of many viruses. Li et al. [56] suggested the implication of calcium in virion assembly, cell attachment and entry and the nucleus entry of simian virus 40 (SV40). Also in icosahedral plant viruses, whose structure resembles rhinoviral capsid structure, implication of calcium in the uncoating process has been shown previously [57-58]. Amino acids that normally bind  $\text{Ca}^{2+}$  in Cowpea chlorotic mottle virus (CCMV) and Tomato bushy stunt virus (TBSV) release the ion via charge repulsion caused by an acidic pH. The resulting conformational changes create a 20 Å wide channel at the quasi three-fold axes by expansion of the whole capsid, a process that is similar to conformational changes observed in HRV for RNA release [18].

Although also a zinc ion is under discussion [59], HRV14 and HRV16 most probably contain a calcium ion on the icosahedral fivefold axis, which plays a role in viral uncoating upon acidification in the endosome [3]. Addition of  $\text{CaCl}_2$  to the nanocontainer system lacking the receptor increased the RNA transfer significantly compared to the same sample without  $\text{CaCl}_2$ . Furthermore it was possible to reduce the RT-PCR signal strongly by the addition of the calcium-chelator EGTA prior to virus challenge of plain nanocontainers. Also RNA transfer through receptor decorated nanocontainers was boosted by  $\text{CaCl}_2$ . The LDLR is known to need calcium to maintain its correct folding, but the above described RNA transfer experiment with nanocontainers not decorated with any receptor points at a function of calcium directly related to the virus. After stabilizing the viral capsid in its native form, the dissociation of the ion due to acidification might favor the transition of the viral capsid to its hydrophobic intermediate state (135S particle) in which it can attach to membranes without receptor and subsequently release its RNA into the cell or liposome, respectively.

## 6 Conclusion

Liposomes with a lipid composition close to endosomal membranes, decorated on their surface with a recombinant receptor derived from the minor group HRV receptor VLDLR, serve as a model system for RNA transfer of HRV2 across a membrane. The direct detection of transferred RNA in the lumen of the liposomes via an encapsulated RT mix (such liposomes are termed “nanocontainers”) was not reproducible at the beginning of the present diploma thesis. The reducing agent DTT, a component of the RT mix, was identified as the main cause. It reacted with the nickel complexed by the lipid DGS-NTA which mediates receptor attachment to the liposomal membrane via a His<sub>6</sub>-tag. The nanocontainer system was found to give the strongest signal with a molar ratio of virus : receptor : lipid of 1 : 400 : 711111, i.e. a virus/lipid ratio of  $1.4 \times 10^{-6}$ . Higher virus concentrations induced leakage of the nanocontainers; consequentially, the diluted RT mix was not able to transcribe any cDNA. Lowering of the virus concentration resulted in proportionally weaker RT-PCR signals. Obviously, single HRV2 particles do not disrupt the membrane during RNA transfer but rather move it through a pore. Although RNA was transferred in a concentrated sample even without any receptor, it could be demonstrated via flotation experiments that the receptor is necessary to tightly bind the virus to the liposomal membrane. Once formed, 135S and 80S particles are not able to tightly attach to the membrane.

The antiviral drug amiloride was found to inhibit signals obtained with RT-PCR from the nanocontainers, in contrast to EIPA and rimantadine and to some extent HMA. Further CE experiments point at a leakage inducing effect of amiloride. High calcium concentrations could be demonstrated to enhance the RNA transfer strongly even without receptor, whereas the calcium chelator EGTA counteracted and prevented any RT-PCR signal, underlining the influence of the ion on the capsid stability and therefore infection efficiency.

For the purpose of making the nanocontainer system applicable to all HRV serotypes, the HRV2 specific primers for RT, PCR and qPCR were replaced by suitable general primers. Truncated ICAM-1 receptors consisting of the extracellular domains 1-2 and 1-5 and a His<sub>6</sub>-tag were cloned for the expression in eukaryotic cells and in bacteria. They are necessary for studying major group HRV.

The nanocontainer system can now be used for various experimental set ups with minor group HRVs, e.g. for studying the antiviral capacity and activity of different chemical compounds, or imaging the process of viral uncoating on endosomal membranes in cryo-EM. Expression of the cloned major group receptor will also allow the same studies with major group HRVs.

## 7 References

1. Baltimore, D., *Expression of animal virus genomes*. Bacteriol Rev, 1971. **35**(3): p. 235-41.
2. Semler, B.L. and E. Wimmer, *Molecular Biology of Picornaviruses*, ed. B.L. Semler and E. Wimmer. 2002, Washington, DC 20036-2904: ASM Press.
3. Giranda, V.L., et al., *Acid-Induced Structural Changes in Human Rhinovirus-14 - Possible Role in Uncoating*. Proceedings of the National Academy of Sciences of the United States of America, 1992. **89**(21): p. 10213-10217.
4. Zhao, R., et al., *Cations in human rhinoviruses*. Virology, 1997. **227**(1): p. 13-23.
5. Fields, B.N., M.D. Knipe, and P.M. Howley, eds. *Virology*. Third Edition, Lipincott-Raven Publishers, Philadelphia, New York. 1996.
6. Wagner, E.K. and M.J. Hewlett, *Basic Virology*. Third ed. 2007: Wiley-Blackwell. 584.
7. Pathak, H.B., et al., *Picornavirus genome replication: roles of precursor proteins and rate-limiting steps in oriI-dependent VPg uridylylation*. J Biol Chem, 2008. **283**(45): p. 30677-88.
8. Fendrick, A.M., et al., *The economic burden of non-influenza-related viral respiratory tract infection in the United States*. Arch Intern Med, 2003. **163**(4): p. 487-94.
9. Blomqvist, S., et al., *Human rhinovirus 87 and enterovirus 68 represent a unique serotype with rhinovirus and enterovirus features*. J. Clin. Microbiol., 2002. **40**(11): p. 4218-4223.
10. Lewis, J.K., et al., *Antiviral agent blocks breathing of the common cold virus*. Proc Natl Acad Sci U S A, 1998. **95**(12): p. 6774-6778.
11. Abraham, G. and R.J. Colonno, *Many rhinovirus serotypes share the same cellular receptor*. Journal of Virology, 1984. **51**(2): p. 340-345.
12. Hewat, E.A., et al., *The cellular receptor to human rhinovirus 2 binds around the 5-fold axis and not in the canyon: a structural view*. EMBO J., 2000. **19**(23): p. 6317-6325.
13. Curry, S., et al., *Viral RNA modulates the acid sensitivity of foot-and-mouth disease virus capsids*. J Virol, 1995. **69**(1): p. 430-8.
14. Ellard, F.M., et al., *Evidence for the role of His-142 of protein 1C in the acid-induced disassembly of foot-and-mouth disease virus capsids*. Journal Of General Virology. Aug, 1999. **8**: p. 1911-1918.
15. Olson, N.H., et al., *Structure of a human rhinovirus complexed with its receptor molecule*. Proc. Natl. Acad. Scie. U.S.A., 1993. **90**(2): p. 507-511.
16. Register, R.B., et al., *Human-murine chimeras of ICAM-1 identify amino acid residues critical for rhinovirus and antibody binding*. Journal of Virology, 1991. **65**(12): p. 6589-6596.
17. Colonno, R.J., et al., *Evidence for the direct involvement of the rhinovirus canyon in receptor binding*. Proc Natl Acad Sci U S A, 1988. **85**(15): p. 5449-5453.
18. Hewat, E.A. and D. Blaas, *Cryoelectron microscopy analysis of the structural changes associated with human rhinovirus type 14 uncoating*. J Virol, 2004. **78**(6): p. 2935-2942.
19. Fuchs, R. and D. Blaas, *Uncoating of human rhinoviruses*. Reviews in Medical Virology, 2010. **(in press)**.
20. Zhang, D.W., et al., *Structural requirements for PCSK9-mediated degradation of the low-density lipoprotein receptor*. Proc Natl Acad Sci U S A, 2008. **105**(35): p. 13045-50.



21. Verdaguer, N., et al., *X-ray structure of a minor group human rhinovirus bound to a fragment of its cellular receptor protein*. Nature Structural Molecular Biology, 2004. **11**(5): p. 429-434.
22. Brabec, M., et al., *Conformational changes, plasma membrane penetration, and infection by human rhinovirus type 2: Role of receptors and low pH*. Journal of Virology, 2003. **77**(9): p. 5370-5377.
23. Bayer, N., et al., *Effect of bafilomycin A1 and nocodazole on endocytic transport in HeLa cells: Implications for viral uncoating and infection*. Journal of Virology, 1998. **72**(12): p. 9645-9655.
24. Moser, R., et al., *Neutralization of a common cold virus by concatemers of the third ligand binding module of the VLDL-receptor strongly depends on the number of modules*. Virology, 2005. **338**(2): p. 259-269.
25. Konecsni, T., et al., *Twelve receptor molecules attach per viral particle of human rhinovirus serotype 2 via multiple modules*. FEBS Letters, 2004. **568**(1-3): p. 99-104.
26. Kobayashi, T., et al., *Separation and characterization of late endosomal membrane domains*. J Biol Chem, 2002. **277**(35): p. 32157-64.
27. van Meer, G., D.R. Voelker, and G.W. Feigenson, *Membrane lipids: where they are and how they behave*. Nat Rev Mol Cell Biol, 2008. **9**(2): p. 112-24.
28. Alberts, B., D. Bray, and J. Lewis, *Molecular Biology of the Cell*. Fourth ed. 2002: Taylor & Francis.
29. Bilek, G., *Functionalized Liposomes as a Model to Reveal Cell-Surface Associated Events of the Human Rhinovirus Infection-Pathway*. 2009, Universität Wien: Vienna.
30. Neumann, E., et al., *A cellular receptor of human rhinovirus type 2, the very-low-density lipoprotein receptor, binds to two neighboring proteins of the viral capsid*. J Virol, 2003. **77**(15): p. 8504-11.
31. Lu, X., et al., *Real-time reverse transcription-PCR assay for comprehensive detection of human rhinoviruses*. J Clin Microbiol, 2008. **46**(2): p. 533-9.
32. Evans, R.W., M.A. Williams, and J. Tinoco, *Surface areas of 1-palmitoyl phosphatidylcholines and their interactions with cholesterol*. Biochem J, 1987. **245**(2): p. 455-62.
33. Felmeister, A., M. Amanat, and N.D. Weiner, *Interactions of gaseous air pollutants with egg lecithin and phosphatidyl ethanolamine monomolecular films*. Atmos Environ, 1970. **4**(3): p. 311-9.
34. Li, X.M., et al., *Sphingomyelin interfacial behavior: the impact of changing acyl chain composition*. Biophys J, 2000. **78**(4): p. 1921-31.
35. Stottrup, B.L. and S.L. Keller, *Phase behavior of lipid monolayers containing DPPC and cholesterol analogs*. Biophys J, 2006. **90**(9): p. 3176-83.
36. Lud, S.Q., et al., *Field effect of screened charges: electrical detection of peptides and proteins by a thin-film resistor*. Chemphyschem, 2006. **7**(2): p. 379-84.
37. Simmons, D., M.W. Makgoba, and B. Seed, *ICAM, an adhesion ligand of LFA-1, is homologous to the neural cell adhesion molecule NCAM*. Nature, 1988. **331**(6157): p. 624-7.
38. Bubeck, D., D.J. Filman, and J.M. Hogle, *Cryo-electron microscopy reconstruction of a poliovirus-receptor-membrane complex*. Nat Struct Mol Biol, 2005. **12**(7): p. 615-8.
39. Marlovits, T.C., C. Abrahamsberg, and D. Blaas, *Very-low-density lipoprotein receptor fragment shed from HeLa cells inhibits human rhinovirus infection*. Journal of Virology, 1998. **72**(12): p. 10246-10250.
40. Madhus, I.H., S. Olsnes, and K. Sandvig, *Different pH requirements for entry of the two picornaviruses, human rhinovirus 2 and murine encephalomyocarditis virus*. Virology, 1984. **139**(2): p. 346-357.
41. Weiss, V.U., *Chip Electrophoresis of Human Rhinovirus and Receptor Decorated Liposomes as Model Membranes for the Analysis of Key Steps in the Viral Infection Pathway*. 2009, Universität Wien: Vienna.

References

42. Gruenberger, M., et al., *Stabilization of human rhinovirus serotype 2 against pH-induced conformational change by antiviral compounds*. J Gen Virol, 1991. **72 (Pt 2)**: p. 431-3.
43. Konecsni, T., et al., *Low pH-triggered beta-propeller switch of the low-density lipoprotein receptor assists rhinovirus infection*. J Virol, 2009. **83**(21): p. 10922-30.
44. Curry, S., M. Chow, and J.M. Hogle, *The poliovirus 135S particle is infectious*. J Virol, 1996. **70**(10): p. 7125-7131.
45. Khan, A.G., et al., *Human rhinovirus 14 enters rhabdomyosarcoma cells expressing icam-1 by a clathrin-, caveolin-, and flotillin-independent pathway*. J Virol, 2010. **84**(8): p. 3984-92.
46. Ronacher, B., et al., *Expression and folding of human very-low-density lipoprotein receptor fragments: neutralization capacity toward human rhinovirus HRV2*. Virology, 2000. **278**(2): p. 541-550.
47. Hooverlitty, H. and J.M. Greve, *Formation of rhinovirus-soluble ICAM-1 complexes and conformational changes in the virion*. Journal of Virology, 1993. **67**(1): p. 390-397.
48. Brabec, M., D. Blaas, and R. Fuchs, *Wortmannin delays transfer of human rhinovirus serotype 2 to late endocytic compartments*. Biochem Biophys Res Commun, 2006. **348**(2): p. 741-749.
49. Brabec, M., et al., *Opening of size-selective pores in endosomes during human rhinovirus serotype 2 in vivo uncoating monitored by single-organelle flow analysis*. J Virol, 2005. **79**(2): p. 1008-1016.
50. Grunert, H.P., et al., *Internalization of human rhinovirus 14 into HeLa and ICAM-1-transfected BHK cells*. Med Microbiol Immunol, 1997. **186**(1): p. 1-9.
51. Lonberg-Holm, K. and B.D. Korant, *Early interaction of rhinoviruses with host cells*. Journal of Virology, 1972. **9**(1): p. 29-40.
52. Weiss, V.U., et al., *Liposomal leakage induced by virus-derived peptides, viral proteins and entire virions: rapid analysis by chip electrophoresis*. submitted, 2010.
53. Okun, V.M., et al., *Analysis of common cold virus (human rhinovirus serotype 2) by capillary zone electrophoresis: The problem of peak identification*. Analytical Chemistry, 1999. **71**(10): p. 2028-2032.
54. Pereira, H.G. and R.C. Valentine, *Infectivity titrations and particle counts of adenovirus type 5*. J Gen Microbiol, 1958. **19**(1): p. 178-81.
55. Suzuki, T., et al., *Bafilomycin A(1) inhibits rhinovirus infection in human airway epithelium: effects on endosome and ICAM-1*. Am J Physiol Lung Cell Mol Physiol, 2001. **280**(6): p. L1115-27.
56. Li, P.P., et al., *Importance of Vp1 calcium-binding residues in assembly, cell entry, and nuclear entry of simian virus 40*. J Virol, 2003. **77**(13): p. 7527-38.
57. Harrison, S.C., et al., *Tomato bushy stunt virus at 2.9 Å resolution*. Nature, 1978. **276**(5686): p. 368-73.
58. Speir, J.A., et al., *Structures of the native and swollen forms of cowpea chlorotic mottle virus determined by X-ray crystallography and cryo-electron microscopy*. Structure, 1995. **3**(1): p. 63-78.
59. Hadfield, A.T., et al., *The refined structure of human rhinovirus 16 at 2.15 angstrom resolution: Implications for the viral life cycle*. Structure, 1997. **5**(3): p. 427-441.

## 8 Appendices

### 8.1 Abbreviations

abbreviation	explanation
<b>A</b>	Ampere
<b>Amp</b>	Ampicillin
<b>BGE</b>	background electrolyte
<b>cDNA</b>	complementary DNA
<b>CE</b>	capillary electrophoresis
<b>Da</b>	Dalton
<b>dNTP</b>	deoxyribonucleotide triphosphate
<b>DTT</b>	dithiothreitol
<b>His<sub>6</sub></b>	Hexa histidine
<b>HRV</b>	Human Rhinovirus
<b>ICAM-1</b>	intercellular adhesion molecule 1
<b>ICTV</b>	international committee on taxonomy of viruses
<b>IRES</b>	internal ribosome entry site
<b>Kan</b>	Kanamycin
<b>LB</b>	luria broth
<b>LDLR</b>	low density lipoprotein receptor
<b>LRP</b>	LDLR related protein
<b>LUV</b>	large unilamellar vesicle
<b>MBP</b>	maltose binding protein
<b>MLV</b>	multilamellar vesicle
<b>MOI</b>	multiplicity of infection
<b>mSEC</b>	mini size exclusion chromatography
<b>NC</b>	nanocontainer
<b>NEB</b>	New England Biolabs
<b>nt</b>	nucleotide
<b>ORF</b>	open reading frame
<b>PAGE</b>	polyacrylamide gel electrophoresis
<b>PCR</b>	polymerase chain reaction
<b>PFU</b>	plaque forming unit
<b>PTA</b>	phosphotungstic acid
<b>RT</b>	reverse transcription
<b>TCID<sub>50</sub></b>	median tissue culture infective dose
<b>TEM</b>	transmission electron microscopy
<b>Tet</b>	Tetracyclin
<b>UTR</b>	untranslated region
<b>VLDLR</b>	very low density lipoprotein receptor
<b>VP</b>	viral protein

## 8.2 Primer index

name	sequence 5'–3'	length [nt]	T <sub>m</sub> [°C]	complimentary to	comments
PF HRV2-7A	GAGTTGACTTACCTATGTCAAC	23	48.9	HRV2 6126-6148	
PR HRV2_3end	CCACTCATGCAAAAGCAAATC	21	52.4	HRV2 7028-7048	
PF HRV2 5end	GACCAATAGCCGGTAATCAG	20	60.1	HRV2 125-144	
PR HRV2_5end	GTCACCATAAGCAAAATATAAAGG	23	47.7	HRV2 561-583	
PF HRV2gen LNA (348)*	CY+AGCC+TGCGTGGC	14	63	HRV2 348-361	general primer for all HRV serotypes
PR HRV2gen(553)	GAAACACGGACACCCAAAGTA	21	51.6	HRV2 532-552	general primer for all HRV serotypes
PF ICAM_pCDM8_2197	AGCTCTAGAGATCCCTCGACCTCGAG	27	61.6	pCDM8 2197-2223	
PR ICAM_D2_Xba1_898b	GATCTAGATTAATGATGGTGATGGT GGTGCCGAGGTCAGTTCAGTGCG	52	67.5	ICAM1 877-898	adds a His <sub>6</sub> -tag, stop codon, XbaI restriction site
PR ICAM_D5_Xba1_1759b	GATCTAGATTAATGATGGTGATGGT GGTGCTCATACCGGGGGAGAG	49	64.8	ICAM1 1742-1759	adds a His <sub>6</sub> -tag, stop codon, XbaI restriction site
PF pCDM8_2130sequ	GGCTAACTAGAGAACCAC	19	42.7	pCDM8 2130-2148	
PR pCDM8_2692sequ_b	CTCTGTAGGTAGTTGTCCAATTATG	26	50.7	pCDM8 2692-2717	
PF ICAM_Sac1_mut_1591	CCCATTGCCCGAACTCAAGTGC	23	61.3	ICAM1 1591-1613	contains a mismatch within SacI
PR ICAM_Sac1_mut_1590b	TTCCCCCAAGCCTGGC	16	53.8	ICAM1 1575-1590	
PF ICAM_Sac1_Xa_401	CTAGGAGCTCGAACAACAACAACAATA ACAATAACAACAACCTCGGATCGAGG GAAGGCAGACATCTGTGTCCTCCC	77	53	ICAM1 401-418	adds a SacI restriction site, end of MBP, Xa cleavage site
PR ICAM_D2_KpnI_898b	GATCGGTACCTTAATGATGGTGATGGT GGTGCCGAGGTCAGTTCAGTGCG	52	67.5	ICAM1 877-898	adds a His <sub>6</sub> -tag, stop codon, KpnI restriction site
PR ICAM_D5_KpnI_1759b	GATCGGTACCTTAATGATGGTGATGGT GGTGCTCATACCGGGGGAGAG	49	64.8	ICAM1 1742-1759	adds a His <sub>6</sub> -tag, stop codon, KpnI restriction site

Primers were ordered at VBC Biotech, Vienna, Austria except for \*, which was ordered at Exiqon, Vedbaek, Denmark.

## 8.3 Nucleotide sequences

### 8.3.1 Human Rhinovirus 2 with primer positions indicated

sequence source: EMBL X02316

```

1  ttaaaactgg atccaggttg ttcccacctg gatttcccac agggagtggt actctgttat
61  tacggtaact ttgtacgcc a gttttatctc cttccccca tgtaacttag aagtttttca
121 caaagaccaa tagccggtaa tcagccagat tactgaaggt caagcacttc tgtttccccg
    >> PF HRV2 5end

```

```

181 gtcaatgttg atatgctcca acagggcaaa aacaactgcg atcgttaacc gcaaagcgcc
241 tacgcaaagc ttagtagcat ctttgaaatc gtttggtcgg tcgatccgcc atttccccctg
301 gtagacctgg cagatgaggc tagaaatacc ccaactggcg cagtgttcta gcctgcgtgg
    >> PF HRV2gen LNA
    (348)

```

```

361 ctgcctgcac accctatggg tgtgaagcca aacaatggac aaggtgtgaa gagccccgtg
421 tgctcgcttt gagtcctccg gcccctgaat gtggctaacc ttaaccctgc agctagagca
481 cgtaacccaa tgtgtatcta gtcgtaatga gcaattgcgg gatgggacca actactttgg
    PR HRV2gen (553)

```

```

541 gtgtccgtgt ttcaacttttt cctttatatt tgcttatggt gacaatatat acaatatata
    << PR HRV2_5end <<

```

```

601 tattggcacc atgggtgcac aggtttcaag acaaaatggt ggaactcact ccacgcaaaa
661 ctctgtatca aatgggtcta gtttaaatta ttttaacatc aattatttca aagatgctgc
721 ttcaaatggt gcatcaaaac tggaattcac acaagatcct agtaaattta ctgaccagct
781 taaggatggt ttggaaaagg gaataccaac actacagtcc cccacagtgg aggcctgttg

```

... 841 - 5940 ...

```

5941 cttagatatt gacccaaaac ctattacact tgaggacagt gtctttggca ctgatggatt
6001 agaggctctt gatttgaaca ctagecgagg atttccatat attgcaatgg gagttaaaaa
6061 gagagattta ataaacaaca agaccaagga tataagcaaa cttaaagaag caattgacaa
6121 atacggaggt gacttaccta tggtcacctt cttgaaagat gaactcagaa agcatgaaaa
    >> PF HRV2-7A

```

```

6181 ggtaattaaa ggtaaaacta gagttattga agctagtagt gtgaatgata ccctattatt
6241 tagaacaact tttggcaacc tcttttcaaa gttccacttg aatcctggaa ttgttactgg
6301 atcagcagtt ggatgtgatc cagaggtggt ttggtcaaaa ataccagcaa tgttggatga

```

... 6361 - 6780 ...

```

6781 tagcaatggt acttttttaa aaagagggtt taagcaagat gagaagtata actttcta
6841 acatccaact ttccctgaag atgaaatatt tgaatccatc agatggacaa agaaaccatc
6901 acaaatgcat gaacatgtgt tgtctctgtg tcaacttaat tggcacaatg gacgtgacgc
6961 atacaaaaaa tttgtggaga agatacgagc tgtaagcgct ggtcgtgcac tgtacatccc
7021 tccgtatgat ttgcttttgc atgagtggta tgaaaaat taaagatata gaaatagtaa
    PR HRV2_3end <<

```

```

7081 actgatagtt tattagtttt at

```

format	explanation
tagtc	vector pCDM8
CCTA	insert ICAM1-D2 (270-898) insert ICAM1-D5 (270-1759)
TCTAGA	XbaI restriction site
TAA	stop codon
CAT	His codon
G	mutation

- 84 - diploma thesis by Nena M. Matscheko

diploma thesis by Nena M. Matscheko - 85 -

ACCAGCTCCAGACCTTTGTCCTGCCAGCGACTCCCCACAACCTTGTCAGCCCCCGGGTCC  
TAGAGGTGGACACGCAGGGGACCGTGGTCTGTTCCCTGGACGGGCTGTTCCCAGTCTCG  
GAGGCCAGGTCCACCTGGCACTGGGGGACCAGAGGTTGAACCCACAGTCACCTATGG  
CAACGACTCCTTCTCGGCCAAGGCCTCAGTCAGTGTGACCGCAGAGGACGAGGGCACCC  
AGCGGCTGACGTGTGCAGTAATACTGGGGAACCAGAGCCAGGAGACACTGCAGACAGTG  
ACCATCTACAGCTTTCCGGCGCCCAACGTGATTCTGACGAAGCCAGAGGTCTCAGAAGG  
GACCGAGGTGACAGTGAAGTGTGAGGCCACCCTAGAGCCAAGGTGACGCTGAATGGG  
GTTCCAGCCCAGCCACTGGGCCCCGAGGGCCCAGCTCCTGCTGAAGGCCACCCAGAGGA  
CAACGGGCGCAGCTTCTCCTGCTCTGCAACCCTGGAGGTGGCCGGCCAGCTTATACACA  
AGAACCAGACCCGGGAGCTTCGTGTCTGTATGGCCCCGACTGGACGAGAGGGATTGT  
CCGGGAAACTGGACGTGGCCAGAAAATTCCCAGCAGACTCCAATGTGCCAGGCTTGGGG  
GAACCCATTGCCCAGCTCAAGTGTCTAAAGGATGGCACTTTCCCACTGCCCATCGGGGA  
ATCAGTGACTGTCACTCGAGATCTTGAGGGCACCTACCTCTGTCTGGGCCAGGAGCACTCA  
AGGGGAGGTCACCCGCCAGGTGACCGTGAATGTGCTCTCCCCCGGTATGAGCACCAC  
**CATCACCATCATTAATCTAG**Aggatcttltgtaaggaaccttacttctgtggtgtgacataattggacaaactacct  
acagagatttaaagctctaaggtaaatataaaattttaagtgtataatgtgttaaactactgattctaattgttggatttttagattc  
caacctatggaacttatgaatgggagcagtggtggaatgccttaatgaggaaaacctgtttgtctcagaagaaatgccatctagt  
atgatgaggtactgtgactctcaacattctactctcaaaaaagaagagaaaggtagaagaccccaaggacttctctcagaat  
tggttaagtttttgatcatgtgtgttagtaataagaactcttgccttgccttgccttattacaccacaaagggaaaagctgcactgctat  
acaagaaaattatggaaaaatattgatgtatagtgcttgactagagatcataatcagccataccacattttagaggttttacttgc  
tttaaaaaacctccacacctccccctgaacctgaaacataaaatgaatgcaattgttgttgtaactgtttattgcagcttataatgg  
ttacaaataaagcaatagcatcacaatttcacaaataaagcattttatcactgcattctagtgtggtttgtccaaactcatcaatgt  
atcttatcatgtctggatcccgcatggtatcaacgcatatttctatttacagtagggacctcttgccttgttaggtaccgctgtattcc  
tagggaaatagtagaggcaccttgaactgtctgcatcagccatatagcccccgctgttcgacttacaacacaggcacagtactgac  
aaaccatacacctctctgaaatacccatagttgctagggctgtctccgaactcattacacctaccaagttagagctgtaatttcg  
cgatcaagggcagcgagggttctccagataaaatagcttctgccgagagtcctcgtaagggttagacacttcagctaatecctcgat  
gaggtctactagaatagtcagtgcggtctccattttgaaaattcacttacttgatcagcttcagaagatgggcgagggcctccaacac  
agtaattttctccccgactcttaaaatagaaaatgtcaagtcagttaaggaggaagtggaactaactgacgcagctggccgtgcgaca  
tctcttttaattagttgctaggaacgcctccagagggcgtgtggtttgcaagaggaagcaaaagcctctccaccaggcctaga  
atgtttccaccaatcattactatgacaacagctgttttttagtattaagcagaggccggggaccttgggcccgttactctggag  
aaaaagaagagaggcattgtagaggctccagaggcaactgtcaaaacaggactgcttctatttctgtcacactgtctgacctgt  
cacaaggtccagcacctccatacccccttaataagcagtttgggaacgggtgcgggtcttactccgccccatccccccctaactccg  
cccagttccgccccattctccgccccatggctgactaattttttattatgcagaggccgaggccgctcggcctctgagctattccag  
aagtagtgaggaggtttttggaggcctaggttttgcaaaaagctaattc



## 8.4 Acknowledgments

I owe my deepest gratitude to all my very awesome short and long term members of the lab for all their support during the production of my thesis. Dieter Blaas for giving me the opportunity to do my thesis in his lab and his guidance through it; Angela and Gerry for explaining everything to me; Victor, Abdul, Xavier, Kathi, Shushan and Mohit for being companions in all tragedies happening in a lab and for providing a great international atmosphere; Irene for sharing early mornings and knowing where to find everything.

I am also very grateful to my parents for their emotional support during difficult times and of course in material terms. I also benefitted from all the entertainment provided by my brother Michael and the challenging questions posed by my brother David.

Furthermore I would like to say thanks to all my friends. Their friendship carries me through rough times and makes the most of great moments. It's just fantastic to have you!



## 8.5 Curriculum Vitae

### PERSONAL INFORMATION

Nena Magdalena Matscheko

Address                      Hohlweggasse 17/16  
                                  1030 Wien

Phone                        +43 650 4402507

E-mail                        nenama@sms.at

Date of birth                06. October 1985

Nationality                 Austrian

### UNIVERSITY

10/2004 – 09/2010      University of Vienna, Vienna, Austria  
                                  Molecular Biology  
                                  focus on biochemistry, immunology and molecular medicine  
                                  Diploma Thesis title: RNA transfer of Human Rhinovirus through  
                                  Model Membranes  
                                  degree: Magistra rerum naturalium (Mag. rer. nat.)

01/2008 - 07/2008      Universidad de Navarra, Pamplona, Spain  
                                  semester abroad (ERASMUS programme)

### SCIENTIFIC WORK EXPERIENCE

09/2009 – 07/2010      MFPL, Department of Molecular Biochemistry, University of  
                                  Vienna/Medical University of Vienna, Laboratory Prof. D. Blaas,  
                                  Vienna, Austria  
                                  Research project on RNA transfer of Human Rhinovirus through  
                                  model membranes.

05/2009                    MFPL, Department of Molecular Biochemistry, University of  
                                  Vienna/Medical University of Vienna, Laboratory Prof. D. Blaas,  
                                  Vienna, Austria  
                                  Research practical on crosslinking of viral RNA with 4-Thiouridine.

02/2008 - 06/2008      CIMA, área terapia génica y hepatología, Universidad de Navarra,  
                                  Laboratory Dr. A. Fontanellas, Pamplona, Spain  
                                  Research project on hepatic Amphiregulin overexpression in  
                                  erythropoietic protoporphyria mouse models.

10/2007 - 11/2007      MFPL, Department of Biochemistry, University of Vienna, Laboratory  
                                  Prof. M. Teige, Vienna, Austria  
                                  Research practical on subcellular localization of CPKs.

07/2007                    FEBS Congress "Molecular Machines", Vienna, Austria  
                                  Student helper to the organizer

### EDUCATION

- 09/1996 - 06/2004      Gymnasium Rohrbach, Rohrbach, Austria  
graduation: Matura/A-levels (with distinction) in Mathematics,  
Chemistry, Latin, German, English
- 09/1992 - 07/1996      Volksschule Lembach, Lembach i.M., Austria

### PERSONAL SKILLS

- IT competence:      MS Office (Word, Excel, PowerPoint)  
Adobe Photoshop  
EndNote, BioEdit, ImageJ
- mother tongue:      German
- foreign languages:      English (excellent)  
French (good)  
Spanish (basic)

### SEMINARS

- 05/2009      Project management (University of Vienna)
- 03 - 06/2009      Introduction to French communication in economics (University of Vienna)
- 09/2008 - 06/2009      Lecture and Tutorial on Intellectual Property Rights and Patents (University of Vienna)
- 03 - 06/2007      Spanish classes: Basics (Vienna University of Economics)
- 01/2008      Intensive course (Universidad de Navarra, Pamplona, Spain)
- 09/2006 - 01/2007      Writing and speaking scientific English (University of Vienna)
- 07/2000      English course (International language school St.Julians, Malta)

### PUBLICATIONS

16. Feb 2009      Epidermal growth factor receptor ligands in murine models for erythropoietic protoporphyria: potential novel players in the progression of liver injury. Cell Mol Biol (Noisy-le-grand) 55(1):29-37
- in preparation      Liposomal Nanocontainers as Models for Viral Infection: Transfer of viral genomic RNA through lipid membranes

Vienna, September 2010